AD-A044 548 NAVAL RESEARCH LAB WASHINGTON D C F/G 3/2
NRL/ATM USER'S GUIDE TO EXPERIMENT S082A.(U)
FEB 77 I G PACKER, N P PATTERSON, S A MANGO NASA-S-60604-G
UNCLASSIFIED NRL-MR-3410 NL

1 OF 2
AD
A044548

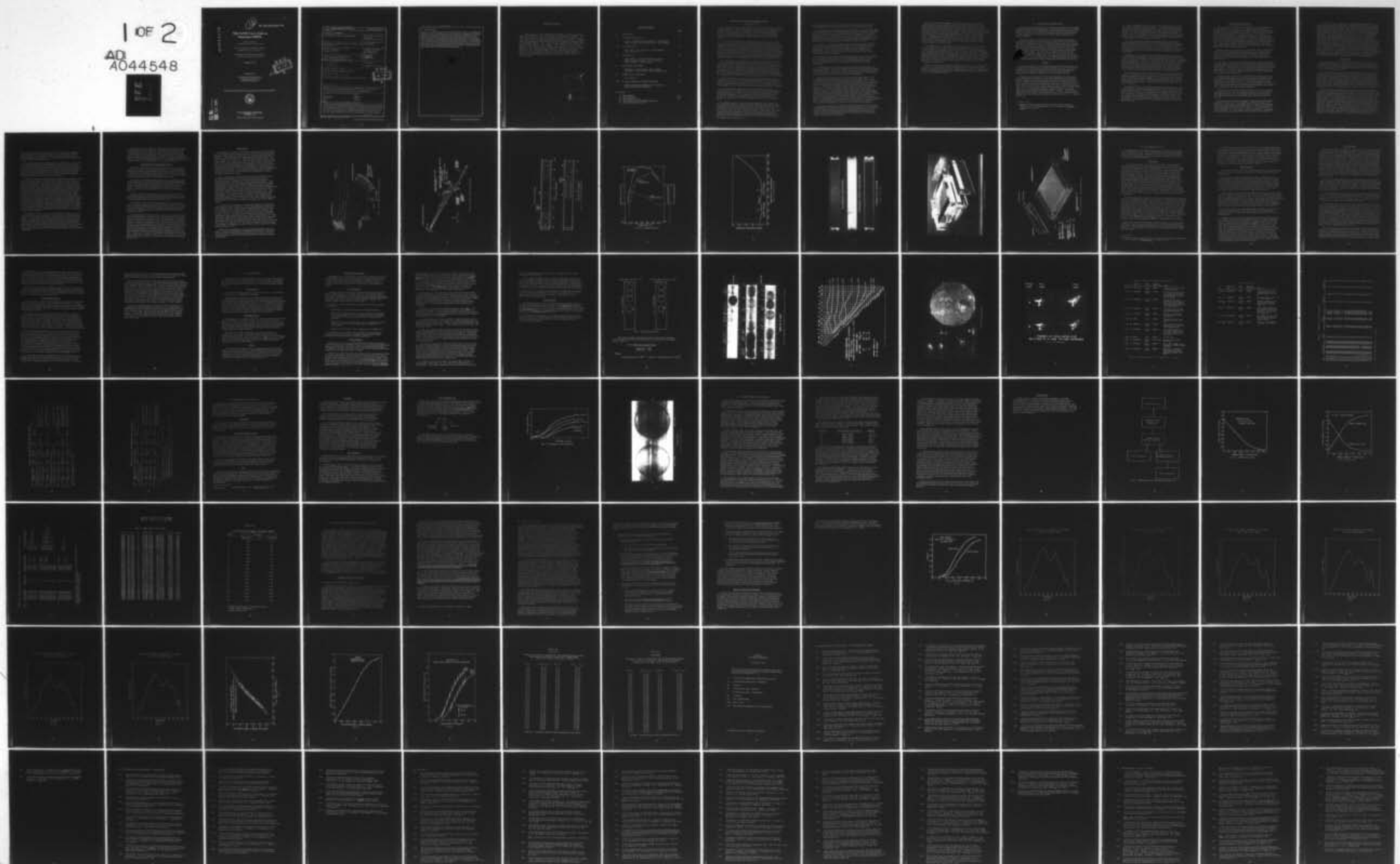

12

NRL Memorandum Report 3410

NRL/ATM User's Guide to Experiment S082A

IRENE G. PACKER
E.O. Hulburt Center for Space Research

N. PAUL PATTERSON AND STEPHEN A. MANGO
Ball Brothers Research Corporation

RICHARD TOUSEY, PRINCIPAL INVESTIGATOR
E. O. Hulburt Center for Space Research

February 1977

Prepared for the

National Space Science Data Center
Goddard Space Flight Center
Greenbelt, Maryland 20771

The preparation of this Guide was partially supported by NASA DPR S-60404-G.

DEPARTMENT OF THE NAVY
NAVAL RESEARCH LABORATORY

NAVAL RESEARCH LABORATORY
Washington, D.C.

SECURITY CLASSIFICATION OF THIS PAGE (When Data Entered)

9

REPORT DOCUMENTATION PAGE

READ INSTRUCTIONS BEFORE COMPLETING FORM

1. REPORT NUMBER: NRL Memorandum Report 3410	2. GOVT ACCESSION NO.
3. RECIPIENT'S CATALOG NUMBER	
4. TITLE (and Subtitle): 6 NRL/ATM USER'S GUIDE TO EXPERIMENT S082A	5. TYPE OF REPORT & PERIOD COVERED: Interim report on a continuing NRL problem.
	6. PERFORMING ORG. REPORT NUMBER
7. AUTHOR(s): 10 Irene G. Packer, N. Paul Patterson, Stephen A. Mango and Richard Tousey	8. CONTRACT OR GRANT NUMBER(s): 15 NASA-S-60604-G
9. PERFORMING ORGANIZATION NAME AND ADDRESS: Naval Research Laboratory, Washington, D.C. 20375	10. PROGRAM ELEMENT, PROJECT, TASK AREA & WORK UNIT NUMBERS: NRL Problem A01-24A; NASA DPR S-60604-S
11. CONTROLLING OFFICE NAME AND ADDRESS: National Aeronautics and Space Administration, George C. Marshall Space Flight Center, Marshall Space Flight Center, Alabama 35812	12. REPORT DATE: 11 February 1977
	13. NUMBER OF PAGES: 121
14. MONITORING AGENCY NAME & ADDRESS (if different from Controlling Office): 12 124p.	15. SECURITY CLASS. (of this report): UNCLASSIFIED
	15a. DECLASSIFICATION/DOWNGRADING SCHEDULE

16. DISTRIBUTION STATEMENT (of this Report)

Approved for public release; distribution unlimited.

14 NRL-MR-3410

17. DISTRIBUTION STATEMENT (of the abstract entered in Block 20, if different from Report)

18. SUPPLEMENTARY NOTES

Prepared as a User's Guide for data deposited at the National Space Science Data Center, National Aeronautics and Space Administration, Goddard Space Flight Center, Greenbelt, Maryland.

The preparation of this Guide was partially supported by NASA DPR S-60604-G.

19. KEY WORDS (Continue on reverse side if necessary and identify by block number)

Sun	Flares
Spectroheliograph	Coronal holes
Solar physics	Spectra
XUV	XUV film
Skylab	

20. ABSTRACT (Continue on reverse side if necessary and identify by block number)

Almost perfect operation of Skylab Experiment S082A resulted in the return of 1032 extreme ultraviolet solar spectroheliograms, providing an enormous wealth of new information about the sun in the wavelength range 171 Å to 630 Å. The present User's Guide was written for guest investigators and other ATM experimenters who will collaborate in interpreting the returned data. The first section is devoted to a brief overview of the Apollo Telescope Mount (ATM) as a whole and the major areas in which the data have been found to be most important. There follows a detailed

(Continues)

DD FORM 1 JAN 73 1473 EDITION OF 1 NOV 65 IS OBSOLETE

S/N 0102-014-6601

SECURITY CLASSIFICATION OF THIS PAGE (When Data Entered)

251950

LB

20. Abstract (Continued)

description of the spectroheliograph and the special Schumann film it utilized. The complementary relationship to the 5 other major instruments on ATM is explained. A large portion of the Guide is devoted to a description of the observations, the data catalogs and documentation, and listings of important events recorded during almost 9 months of nearly continuous operation of Skylab, beginning in May 1973. The main part of the Guide describes filmed copies of the data available from the National Space Science Data Center (NSSDC), Greenbelt, Maryland. A thorough discussion of how to extract data from the photographic images includes a special section on the derivation of relative intensity values. The Appendix contains an extensive bibliography of papers on the ATM results published by the Naval Research Laboratory data analysis team. A spectroheliogram overlay scaled to the NSSDC film identifies prominent spectral features.

ACKNOWLEDGEMENTS

Preparation of the NSSDC photographic material and this Guide has involved the assistance of a number of people. The NRL copy camera system was prepared by Mr. Brian Dohne, who also assisted in evaluating the photographic process. Engineering and mechanical assistance was by Mr. Robert Chaimson and Mr. William Finter. Mr. J. H. Canter prepared the flight plates and provided liaison with NSSDC. The film was processed at NSSDC by Mr. Leonard Smith under the direction of Mr. Robert Murphy. The manuscript was composed and printed by Mrs. Ruth McIntosh, Mrs. Carolyn Marks and Mrs. Margaret Williams. Illustrative assistance was provided by the NRL Graphic Arts Branch, the Photographic Branch, Mr. Brian Dohne and Mrs. Doris Stewart.

Table of Contents

NRL/ATM USER'S GUIDE TO EXPERIMENT S082A

I. INTRODUCTION

The Apollo Telescope Mount (ATM), the manned solar observatory on Skylab, provided a unique opportunity for large scale observations of the sun from above the earth's atmosphere. Supported by a coordinated program of ground-based observations, the joint observing program of its six advanced telescopes brought to bear the greatest possible observational and analytic power on fundamental problems in solar physics.

The ATM took advantage of all that had been learned from over 25 years of solar space research conducted by means of sounding rockets, Orbiting Solar Observatories (OSO's) and monitoring satellites such as SOLRAD. Each of these programs had excelled in its own particular way: rockets, for development of specialized instruments having extremely great observing power, but which were always severely limited in observing time and wavelength span, or spatial resolution or spectral resolution; OSO's, not limited in observing time, but constrained in information acquisition rate, as well as in spatial and spectral resolution; SOLRAD, having excellent time resolution, but limited to broad-band detectors.

These programs had established the need for continuous solar observation combining the specialized observing powers that each type of small instrument had provided. ATM came close to realizing this ideal. It provided almost continuous observation of the solar atmosphere for a period of 9 months. The quantity of data collected by each instrument was enormous. In addition, by fostering the simultaneous operation of the newest and most powerful ground-based observational techniques, the total resulting program represented a massive attack on the problems in solar physics, resembling that mounted during the IGY for geophysics.

Experiment S082A, an extreme ultraviolet (XUV) slitless spectroheliograph, was one of two instruments provided by the Naval Research Laboratory for ATM. It had a field of view of 1.75 solar diameters, with a spatial resolution as fine as 2 arc-sec. It covered the XUV wavelength range from 171-630 Å with a spectral resolution as fine as 0.027 Å.

A single exposure simultaneously recorded full-disk images in a multitude of XUV emission lines, showing solar features whose temperatures range from 2×10^4 K to over 2×10^7 K in relationship to their overall surroundings. The combination of high spectral and spatial resolution and broad spectral and spatial coverage added another dimension, provided by no other instrument, to the total results from ATM.

The S082A images complement the broadband X-ray images from S054 and S056, which are strictly coronal, and also tie in with the short wavelength XUV images produced by S055, which provided better time coverage, but was generally limited to a 5 arc-min by 5 arc-min raster field, with 5 arc-sec spatial resolution. In particular, the S082A images provide the intensities required for analysis of the plasma conditions in both rapidly and slowly developing solar features from the chromosphere through the corona. In the transition region, where

Note: Manuscript submitted January 7, 1977.

the temperature gradient is steepest, the height resolution provided by the multiplicity of images approaches a few hundred kilometers.

The S082A instrument operated almost perfectly. A total of 1032 XUV spectroheliograms were recorded showing a variety of features, including the chromospheric network, regions of weak emission (holes), active regions, quiescent and eruptive prominences, and flares. The enormous wealth of new information recovered was far greater than anything originally expected because of the increased length of the Skylab mission, the greater film supply, and the incredible success of ATM.

A number of scientific surprises have been uncovered in the S082A data. The results show clearly the extreme complexity of the solar atmosphere. Plane parallel models cannot be used. Hydrostatic equilibrium must be replaced by a balance of gas, magnetic, and turbulent pressures. Electric currents seem to play a major role in prominences, loops, and flares.

Among new or more fully recognized phenomena are the XUV bright points, the XUV polar plumes, the macrospicules, and the coronal holes, which the S082A results show extending below the corona to the chromospheric network, accompanied by a thickened, bright solar limb.

For the first time, eruptive prominences have been recorded not simply in relatively cool chromospheric lines, but also in higher temperature coronal lines. These spectacular eruptions vary widely in form and type. Their connection with flares, X-ray events, and terrestrial effects were well observed, but are as yet far from explained.

Of greatest importance are the new results on solar flares. The unsurpassed spatial and spectral resolution of the S082A images has provided critical views of flare structure never before seen. Monochromatic flare images and flare spectra were photographed in the emissions of ions at temperatures ranging from those in the low chromosphere to over 2×10^7 K where the flare energy is first released. Details in the structures as small as 1500 km, and velocities from a few tens to 1000 km/sec, can be distinguished and followed from one temperature region to another. A new picture of the solar flare and an understanding of the dynamic physical processes which control it are emerging. Numerical plasma codes, involving both MHD equations and kinetic plasma parameters are beginning to clarify some of the observed phenomena in flares; in particular, their relationship to the structure of magnetic arches. In the rapid changes they manifest, it is now apparent that departures from ionization equilibrium occur and must be taken into account.

The dynamic and complex nature of all these phenomena in the solar atmosphere is a challenge to previous theoretical models. More realistic models, applicable to the chromosphere and transition zone, must be devised and tested against the physical parameters derived from the results of ATM, and the S082A data are the observations to which new models will have to be compared.

Because the S082A data have such great potential for the solution of many problems in solar physics, this User's Guide has been prepared to encourage and assist collaboration in the task of interpretation. Such collaboration by ATM investigators with each other, with ground-based observers, with other space observers, and with theoreticians in both solar and plasma physics, is of vital importance. The material included is meant to be a guide to the researcher analyzing copies of S082A spectroheliograms available from the National Space Science Data Center at NASA/GSFC. An independent calibration of user film copies, employing the microdensitometry technique used in analyzing flight originals at NRL, indicates that their fidelity with respect to relative intensities can be extremely high. (See Section VII).

Two subjects are not included in this handbook: the absolute calibration of the instrument, and the extensive documentation required for a complete picture of specific events and the purposes of ATM experimenters behind particular observations. The absolute calibration of S082A is in preparation and will be made available as a supplement when completed. A brief description of selected significant events is given in Section IV, and Appendix B contains a list of documents available at NRL (and also at other ATM experimenter institutions), for more detailed cross-referencing. Otherwise, we have provided the information required to make the user essentially independent.

Requests for information about collaboration with NRL may be directed to specific members of the NRL/ATM data reduction team whose names appear on related publications in the Bibliography. Access to original flight data and supporting material may be arranged by contacting Dr. Richard Tousey, Principal Investigator.

II. INSTRUMENT DESCRIPTION+

The XUV spectroheliograph, ATM Experiment S082A, was a slitless Wadsworth grating spectrograph that employed photographic recording. This was the type of instrument first flown by NRL in an Aerobee-150 rocket on May 10, 1963. The ATM spectroheliograph was the largest of these instruments, which are still being improved and flown in rockets by NRL.

Within the XUV lie many of the emission features that are most important from the point of view of solar physics. The spectral separation is sufficient to permit obtaining images of the sun in many of these emissions by means of a slitless single-grating spectrograph. With the ATM spectroheliograph, a spatial resolution of 2 arc sec was achieved over the most important sections of the spectral range that it covered, which was 171-630 Å. Three conditions contributed to make this possible: (1) the extreme stability of the ATM, the telescope mount itself, which was well under 1 arc sec in all three axes; (2) use of a 4 m radius (2 m focal length) grating, that produced solar images 18.9 mm in diameter; (3) extreme precautions to maintain focus, by adherence to tight mechanical and thermal tolerances.

Optics

The optical diagram of the spectroheliograph is shown in Fig. 2.1. The basic components were a concave grating, a filter of 1000 Å thick aluminum, and a camera loaded with strips of Schumann-type XUV sensitive film. Parallel light from the sun formed a spectrum of solar images which were stigmatic near the grating normal.

Figure 2.2 is a schematic of the entire instrument, and Fig. 2.3 shows diagramatically the two types of photographic spectroheliogram that it produced. As will be discussed in a later section, the Wadsworth mounting provided near-perfect imagery on the grating normal. Away from the normal, the aberrations increased. Because the sun's total radiation shortward of 5000Å, the limit of sensitivity of Schumann film, is $\sim 10^5$ times greater than the XUV radiation of $\lambda < 1000$Å, it was necessary to eliminate the relatively intense, focused stray light which would have hidden completely the XUV images. The aluminum filter accomplished this, being opaque for $\lambda > 837$Å, transmiting about 10% at 630Å, and reaching a maximum of 50% at 171Å, its $L_{2,3}$ edge (cf. Fig. 2.4).

+Material for this section has been excerpted from papers by Tousey, et al. and Van Hoosier, et. al. to appear in Applied Optics, Vol. 16, 1977.

It was considered most important to cover the range 180 to 475Å with the best possible spatial resolution. To accomplish this it was necessary to divide the range and to provide a means for optimizing the direction of the grating normal for each range by rotating the grating. The positions at which the normal intersected the film were chosen to be 255Å and 400Å, the "short wavelength" and "long wavelength" ranges, respectively. The respective spectra produced in the two ranges are shown schematically in Fig. 2.3.

The short wavelength range was selected to have an effective short wavelength limit of 171Å, set by the sudden decrease of transmittance of the Al filter below its $L_{2,3}$ edge by a factor of 4 and the absence of intense solar emission. The resolution from 171Å to 335Å and from 320Å to 480Å was 2-3 arc-sec. Although the instrument recorded images to O V, 630Å, the resolution decreased at longer wavelengths.

Originally, it was hoped to obtain a grating ruled with 4800 l/mm to decrease the overlapping of the monochromatic solar images in adjacent spectral lines. However, the best grating turned out to be a Bausch and Lomb grating of 3600 l/mm and 120 by 120 mm aperture. This produced a dispersion of 1.38Å/mm, and each solar image covered 26Å. More often than not, and especially for flares, the interesting solar features were small, hence overlapping did not take place. Based on the optimum spatial resolution, 2 arc-sec, the spectral resolution was 0.027Å for the smallest features such as occur during flares.

For sun-centered pointing, as in Fig. 2.3, the coverage extended 12 arc-min beyond the limb. In this position there was minimal overlapping of images along the top and bottom edges of the spectroheliogram. By rolling the ATM canister, each solar image was caused to rotate about its own center. Therefore, any desired part of the sun's limb and the corona above it could be placed in the favorable top or bottom positions.

The field-of-view of the spectroheliograph in the direction normal to the dispersion could be extended well above the sun's limb by offset pointing the ATM. The pointing limit permitted by the ATM fine solar sensor was 24 arc-min, and the film's usable width was 33 mm, or 57 arc-min. Thus the spectroheliogram could be positioned with one solar limb beyond the top (or the bottom) of the film strip, and the opposite limb as much as 8 arc-min above (or below) the center of the strip. In this way the corona could be recorded to 36 arc-min above the limb.

Aberrations and Imagery

The focal plane of a Wadsworth mounting is best approximated by a parabola. However, the ATM instrument was designed to operate over two wavelength ranges with the grating normal located at 255Å for the one and 400Å for the other. This required a rotation of the grating through $3^{\circ}.1$, as shown in Fig. 2.2. Since the effective focal length of the grating in a Wadsworth mount depends on the angles of incidence and diffraction, the $3^{\circ}.1$ rotation resulted in a 6.6 mm change in focal length. A correction for this change was easily made by rotating the grating about a pivot position located 11.7 cm from the grating center along the tangent line, thus displacing the grating while rotating it. (This is similar to the approach used in the Johnson-Onaka mounting).

Displacement of the grating does not provide perfect registration of both the short and the long wavelength focal planes because one plane is rotated slightly with respect to the other. Consequently, the film plane was made cylindrical (R = 2000 mm) rather than parabolic to provide the best compromise resolution over the 171 - 480Å region.

In the half-size spectroheliograph on the three calibration rockets flown in support of ATM, an improved focus was achieved by using film holders of different types. The two types had different curvatures and positions, each optimized for the particular grating position. The dispersion was 4.55Å/mm because a 2400 l/mm grating was used. As a result, 4 arc-sec resolution was achieved over 171-630Å, the entire range of the instrument.

Measurements of the spatial resolution of the ATM instrument in both wavelength ranges were made at various wavelengths, using the USAF 1951 resolution test target. Resolution curves for the instrument are presented in Fig. 2.5, where the spacing between bright bars of the target, in arc- sec, is plotted against λ. The curves are means of data for bars perpendicular and parallel to the dispersion, and apply to the center of the solar disc.

At the positions of the normal, better than 2 arc-sec resolution was achieved. For the solar images, however, 2 arc-sec was the limiting resolution. This was expected, because the laboratory test target was of higher contrast than the detailed structures on the sun.

Ray tracing by computer was used to study the image sharpness and to aid in the choice of wavelengths at which the imagery was optimum. Early in the design phase this was carried out by Daryl Evans of the Marshall Space Flight Center. Further computations were made after the end of the mission by W. A. Fowler and S. T. Smith of BBRC. For the purpose of these calculations, the grating was assumed to be equally efficient at all points over its surface.

The results of ray tracing agreed only approximately with Fig. 2.5. They indicated worse resolution at $\lambda > 480\text{Å}$ than was achieved in flight. In part, the explanation is that the grating blaze moved to one edge of the grating at long wavelengths. This decreased the effective aperture of the grating and tended to sharpen the image. On the normal, the ray tracing indicated a resolution of 0.3 arc-sec, a limit set by spherical aberration. In practice this was not achieved because of insufficient resolution of the photographic emulsion, and because of distortion of the grating figure introduced by the mounting. For positions above or below the optical plane of the instrument, at least as far as the sun's limb, 32 arc-min, the ray tracing showed the change in resolution to be negligible. However, for positions in the optical plane the calculated resolution degraded from 1/3 arc-sec at the sun's center to 3 arc-sec at either limb. In the actual images, this effect was just detectable as a deterioration from the value 2 arc-sec for most of the disk that began at 20 arc-sec in the direction of dispersion, and reached 3 arc-sec at each limb. For images far from the normal, this aberration narrowed the image along the dispersion for the limb toward short wavelengths and broadened it by the same amount on the long wavelength side.

The Camera

A major problem in the design of the instrument was the camera. To achieve sharp images it was essential to develop a camera that would hold the film in the desired focal position. The tolerance, based on 1 arc-sec maximum permissible image widening, was 125 microns. This was found difficult to realize.

The emulsions used were Eastman Kodak SWR Types 101 and 104, both coated on a 175 micron Estar base. Because these emulsions are of the Schumann-type, containing almost no gelatin, and completely unprotected, the surface to be exposed could under no circumstances be touched. It was decided not to attempt to use Schumann film in roll form because of the many difficulties associated with abrasion, environment, static electrical effects, and precise registration of the film to the focal surface. Rather, 200 film strips, measuring 35 mm x 258 mm, each held in its own metal holder, were carried in a special camera.

The design of the metal holder involved the choice of a suitable metal and configuration so that, when bent into position, the film would lie precisely on the Rowland circle, within a tolerance of 0.1 mm. An equally important consideration was to choose a material for the holders that would not fog Schumann film. Holders of two types were used, as shown in Fig. 2.6. Material of extreme uniformity was required in order that the holder would bend to a perfect circular form, when pulled by 4 pairs of fingers against the Rowland circle guides along the top and bottom edges of the film, just inside retaining lips which held the film strip in the holder. The first choice was 0.25 mm stainless steel which was believed compatible with Schumann film. It was necessary, however, to increase its stiffness, by stamping five grooves lengthwise into each holder; otherwise the unsupported area would not conform properly to the Rowland circle. As will be discussed in Section V,

these grooves were a cause of fog. The edges of the metal holders were bent into lips, under which the 0.19 mm thick film could be slipped with 0.1 mm clearance. Thus formed, the stainless steel was mechanically satisfactory for the S082A cameras, for which the radius of the focal plane was 2 m.

After considerable experimentation (see Section III), it was found that completely anodized and thoroughly cleaned Al is the material least likely to fog Schumann emulsions of those found to have satisfactory mechanical properties for use in the camera. The film itself was coated with gelatin under the emulsion in such a way that when placed in a vacuum and dried out, it would attempt to press itself against the holder and conform to the curve assumed by the holder pressed against the curved rails of the camera.

Figure 2.7 shows a partially disassembled view of a camera loaded with empty film holders. The camera is shown schematically in Fig. 2.8. Upper and lower shelves each carried a stack of 100 film strips in their holders. Each camera, of which 10 were flown on Skylab, contained over 1900 parts, and was extremely complex. Reliable operation required assemblies adjusted to tolerances of a few microns. The quasi-carrousel design allowed the loaded film holders to be transferred sequentially and rapidly into and out of the focal position. A complicated mechanism opened and closed the shutter, removed the exposed film in its holder from the focal plane, and placed it in the lower stack. At the same time, a new loaded holder moved from the upper stack into the focal plane, while another transfer occurred at the back. When all the holders had made the circuit once, the camera was fully exposed. Despite the complexity of this device, only one camera malfunctioned in flight, the one in the S082A instrument during launch. All cameras not installed prior to launch, were housed in sealed canisters filled with dry nitrogen. After use, each was placed in an empty canister and sealed while still evacuated by the vacuum of space.

Recording the exact times of start and finish of each exposure on each strip of film was important, especially so with 1000 film strips involved. This was done by means of an 8 column, 5 row matrix of gallium-arsenide light-emitting diodes which were imaged on a chip of fast, panchromatic film, attached to the end of each film holder. The day of year, hour, minutes, and seconds were recorded at the start and end of each exposure, with time provided by the ATM master clock. These times were also transmitted to ground by telemetry, along with pointing and roll information, temperatures and other engineering data.

Included in each camera was a thin aluminum filter that would withstand the thermal, vibration, and acoustic environments and would remain free from pinholes. The filters were mounted on 32/cm Buckbee-Meers mesh. Each filter was located 25 mm in front of the film. The bars of the mesh were 0.02 mm in width, so that only under unusual conditions were their shadows visible in the images. The spectral transmittance of all six flight filters was measured carefully. An average for the six is plotted in Fig. 2.4.

Thermal and Contamination Control

The entire instrument measured 311.4 x 82.5 x 41.9 cm and weighed 135.5 kg. It was essential to attach it to the supporting structure with thermal-isolating, stress-free mountings, and also to stabilize the temperature at all points over the case at the temperature at which the instrument was focused. This was necessary to prevent distortions which would degrade the image.

One source of intermittent heat input was from sunlight, which entered through a door and was incident on the diffraction grating whenever the instrument was operated. A large part of this solar energy was reflected by the grating in the zero order (central) image. This beam was reflected out the entrance aperture, where it came to a focus, by means of two mirrors, as shown in Fig. 2.2.

The first mirror was actually a pair of mirrors, one used in the grating's short wavelength position, and the other in the long. The grating blank itself became heated under full sunlight, but did not change figure because it was made of Cer-vit.

To keep the case at constant temperature it was necessary to provide heating, which was controlled by means of thermistor sensors. The heat eventually found its way to the actively cooled wall of the ATM canister. Five heater panels together with insulating panels were found sufficient to maintain the temperature of the instrument at 22° C.

Contamination of the grating was, of course, a source of anxiety. When the instrument was not in use its main aperture was sealed with a flap-type door. Likewise, the sun-end aperture of the ATM canister was closed with another door. Nevertheless, the grating had been exposed to sunlight for some 500 hours by the end of the mission. Perhaps because of the extreme precautions taken to keep the instrument clean during thermal vacuum testing and during the first few days in orbit, no residues that would have polymerized under solar radiation were deposited on the grating. There is no indication that the speed of the instrument changed during the mission. Within the time period during which a particular camera was used, which was as long as one month, no change in speed was observed within the $\pm 20\%$ error range associated with photographic photometry.

The Grating

The diffraction grating for this instrument was one of the largest and most densely-ruled concave gratings, blazed for the XUV, ever produced. The blank was of Cer-vit, 4 m radius and 130 by 140 mm in size. It was ruled in gold by Bausch and Lomb with 3600 l/mm, over a surface 120 by 120 mm. The blaze was placed at 304 Å, with a blaze angle of 3°.14 degrees. Since the blaze angle changed by only ±0°.86 across its surface, there was no need to rule it in several parts. This had the advantage of eliminating the component of focused straylight that is produced at the boundaries of each segment of a multipartite grating. Several first generation, convex replicas were made from the concave master grating. Second generation replicas of gold on Cer-vit were made and were the gratings from which the flight grating was chosen.

It was important to determine the speed of the instrument as a function of wavelength in order that solar intensities could be derived from the images. This was done by measuring the grating reflectance with the NRL Optical Grating Evaluator. Measurements were made by scanning continuously across the grating perpendicular to the rulings, at three different positions along the ruling length. Figure 2.4 shows the curve of reflectance versus wavelength from measurement of the grating actually flown, and of an essentially identical grating that was kept in the laboratory. There was time to make measurements of the flight grating at only four wavelengths. The sister grating, however, was measured quite thoroughly after the mission was completed. The measurements agreed remarkably well. The degree to which they apply to the flight grating after it was placed in orbit is not known, but is still under study.

It is obvious that gratings are extremely inefficient in the XUV when used at normal incidence. The double peak is associated with the reflectance curve of gold, which caused the grating reflectance to fall rapidly from 3.5% at 400Å to 0.1% at 200Å. However, the overall speed of the instrument depended also on the transmittance of the Al filters. The final curve of speed (the product of grating reflectance and filter transmittance), is also shown in Fig. 2.4. The speed was rather uniform from 600 to 300Å. Below 300Å, the speed decreased rapidly, even though the filter transmittance was still increasing. At 200Å the instrument was slower by a factor of 10, and at 171Å by 100, than at 400Å. In spite of low speed, the instrument was capable of producing excellent results, for the quiet sun to 250Å, and for flares to 171Å.

There was no straylight of long wavelengths because of the Al filter. The focused straylight originating from the XUV solar spectrum from 300 to 630Å was minimized by proper ruling of the diffraction grating, and involved producing grooves that were uniform and smooth.

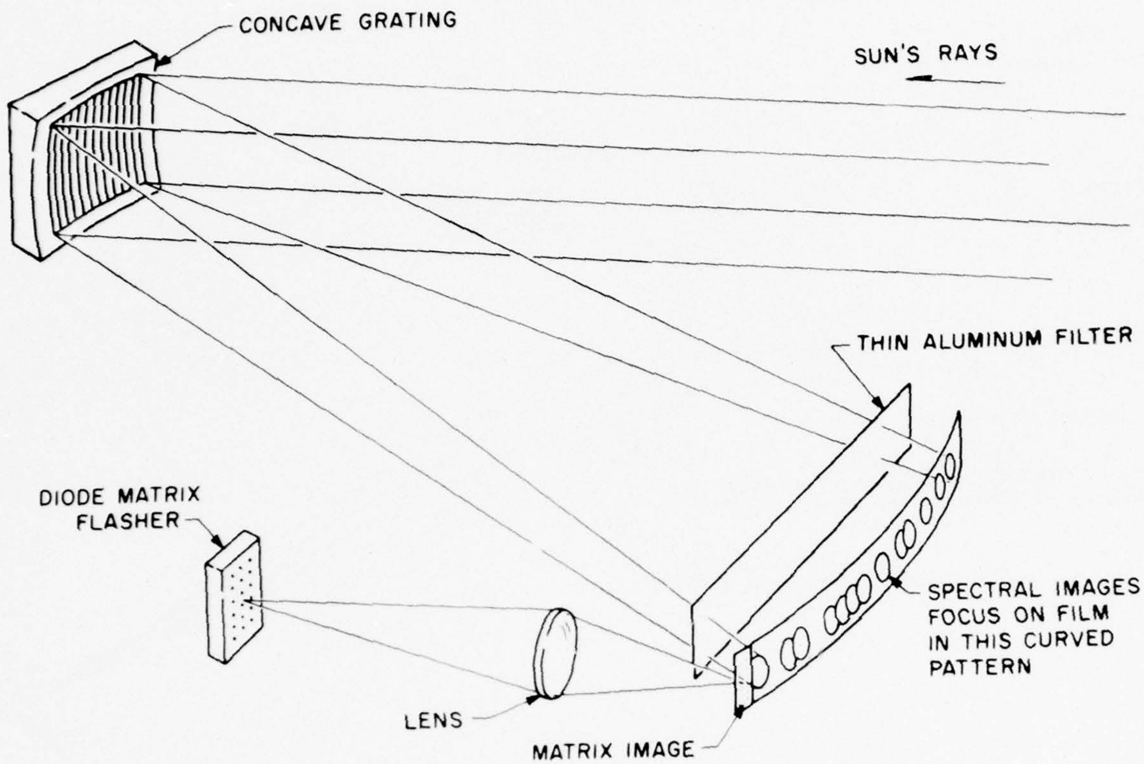

Fig. 2.1 — Optical diagram of NRL spectroheliograph

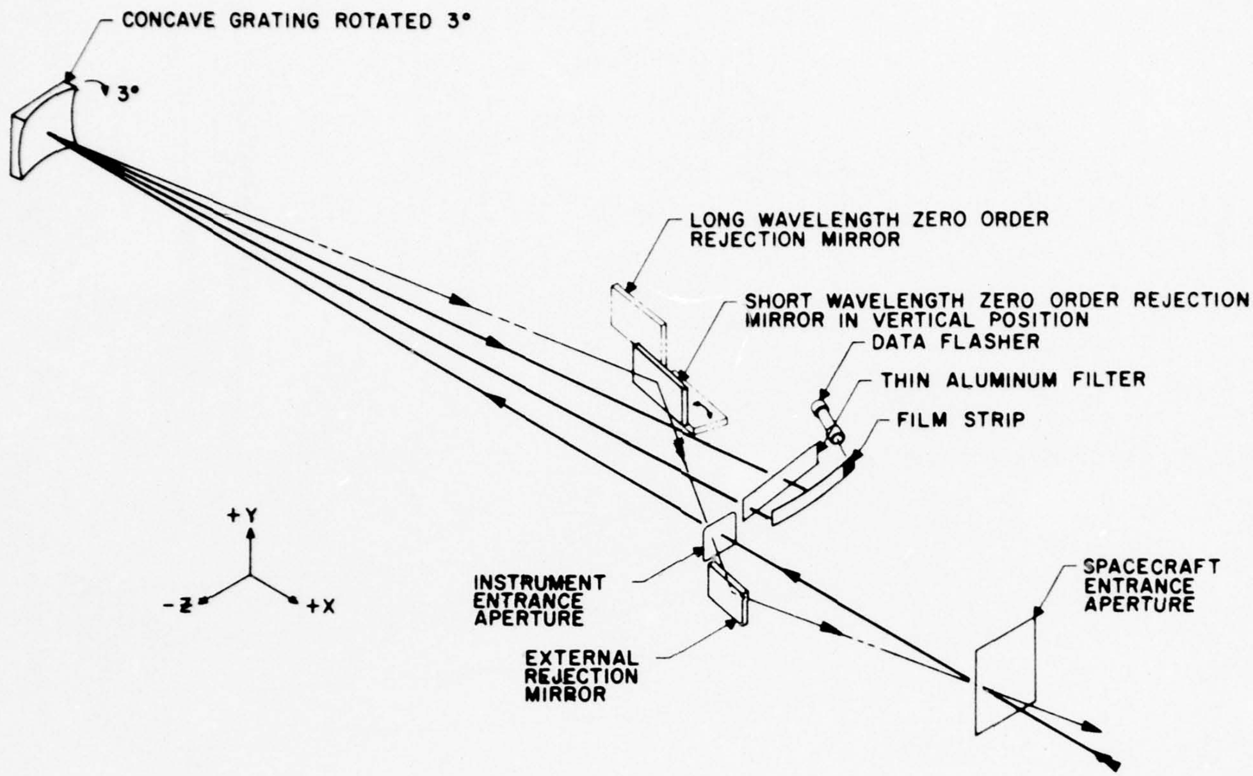

Fig. 2.2 — Schematic of NRL spectroheliograph

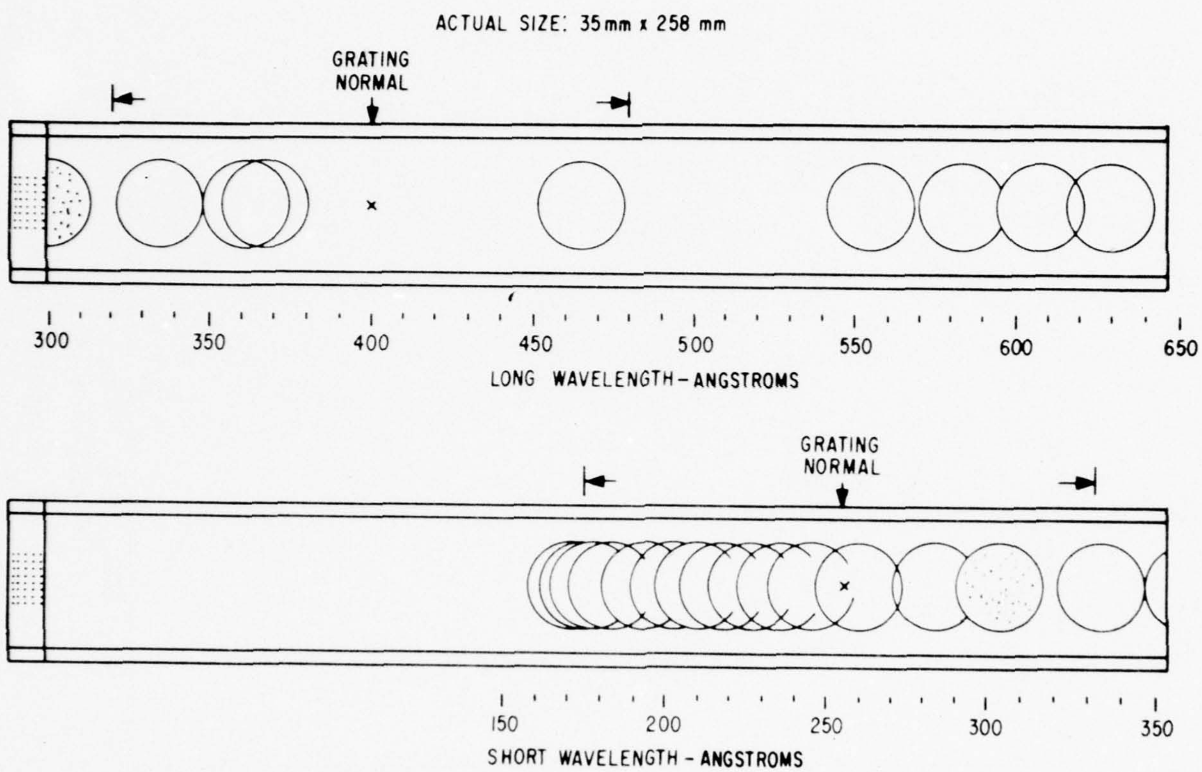

Fig. 2.3 — The two spectroheliogram ranges

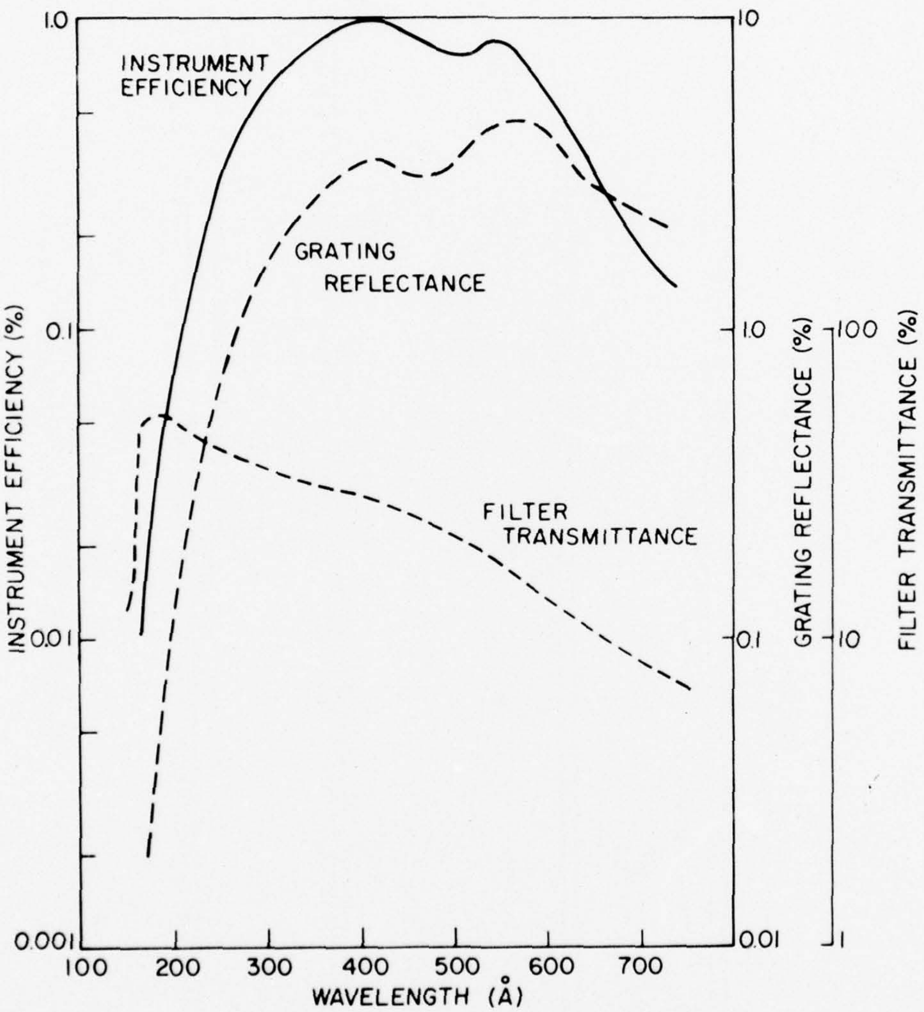

Fig. 2.4 — Instrument efficiency

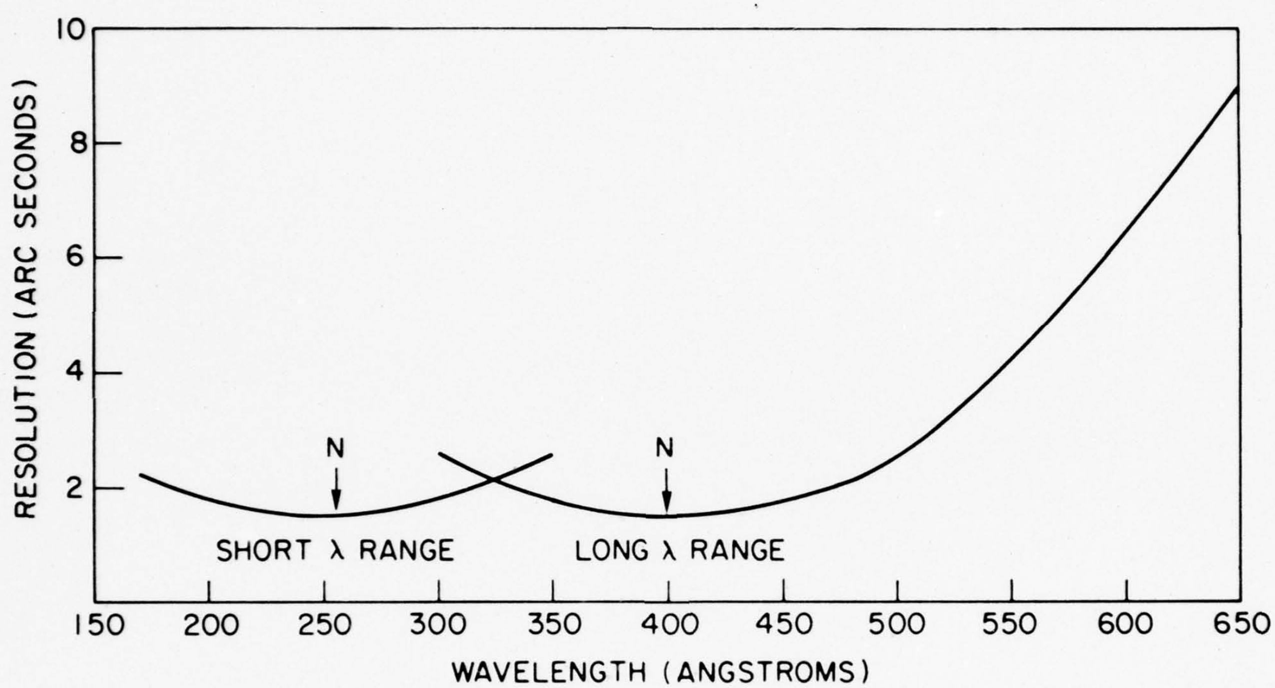

Fig. 2.5 — Resolution curves

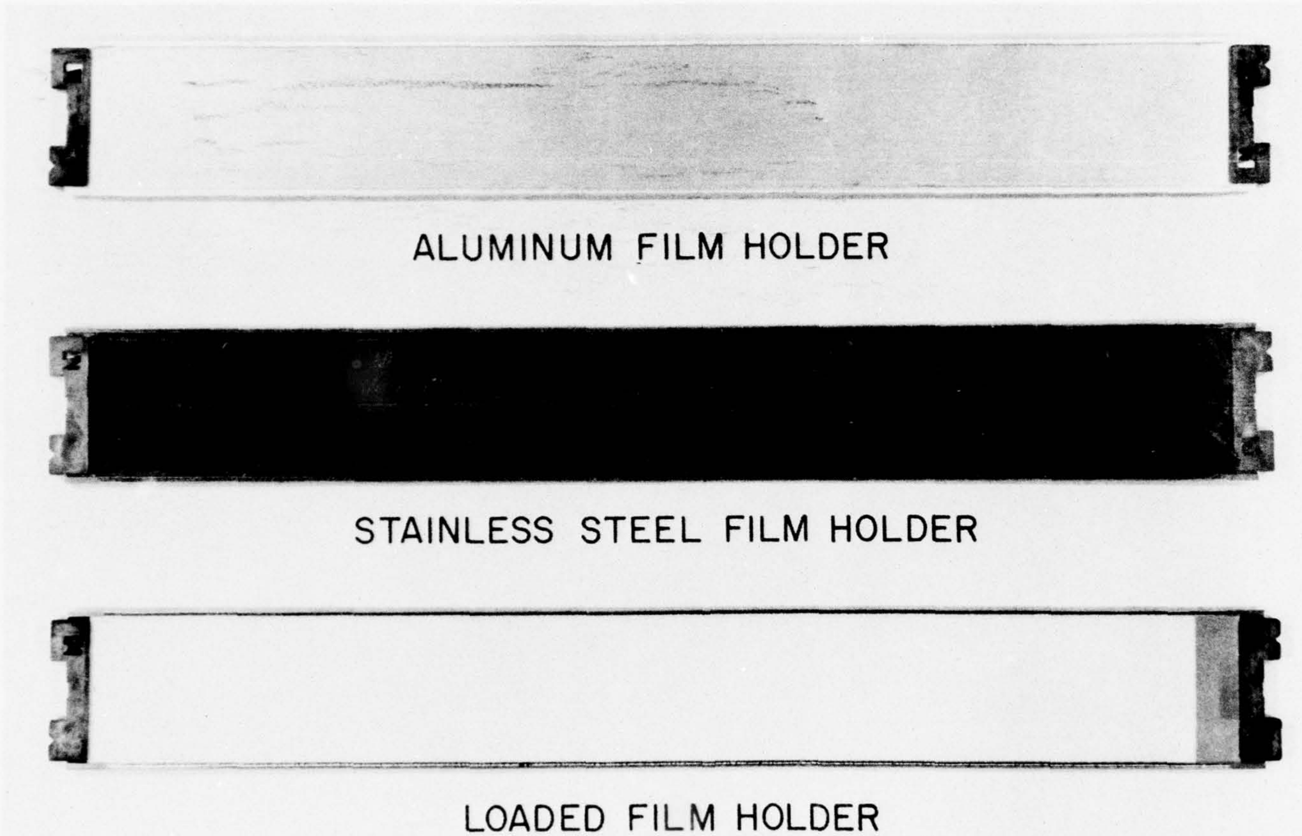

Fig. 2.6 — Film holders

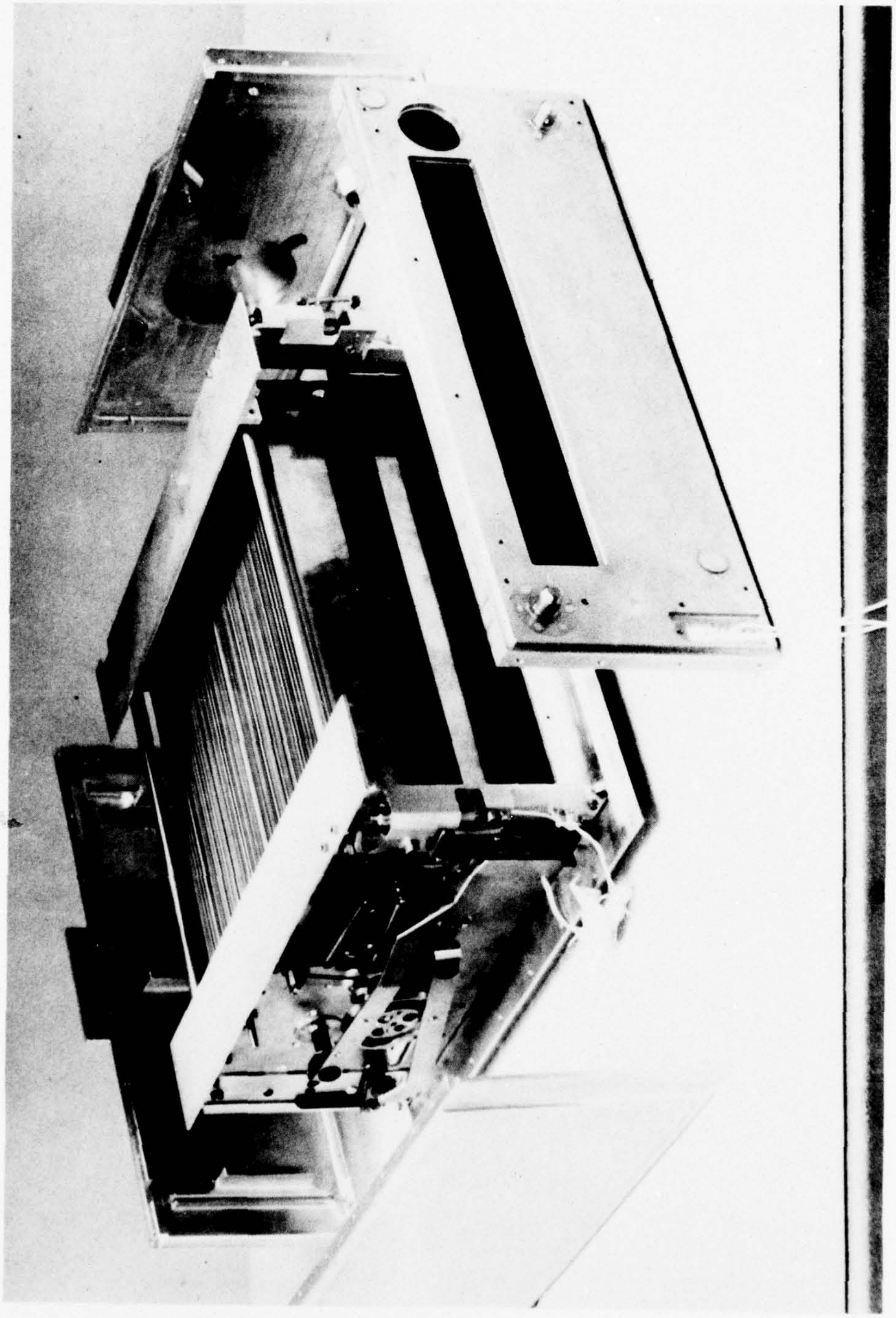

Fig. 2.7 — Spectroheliograph camera

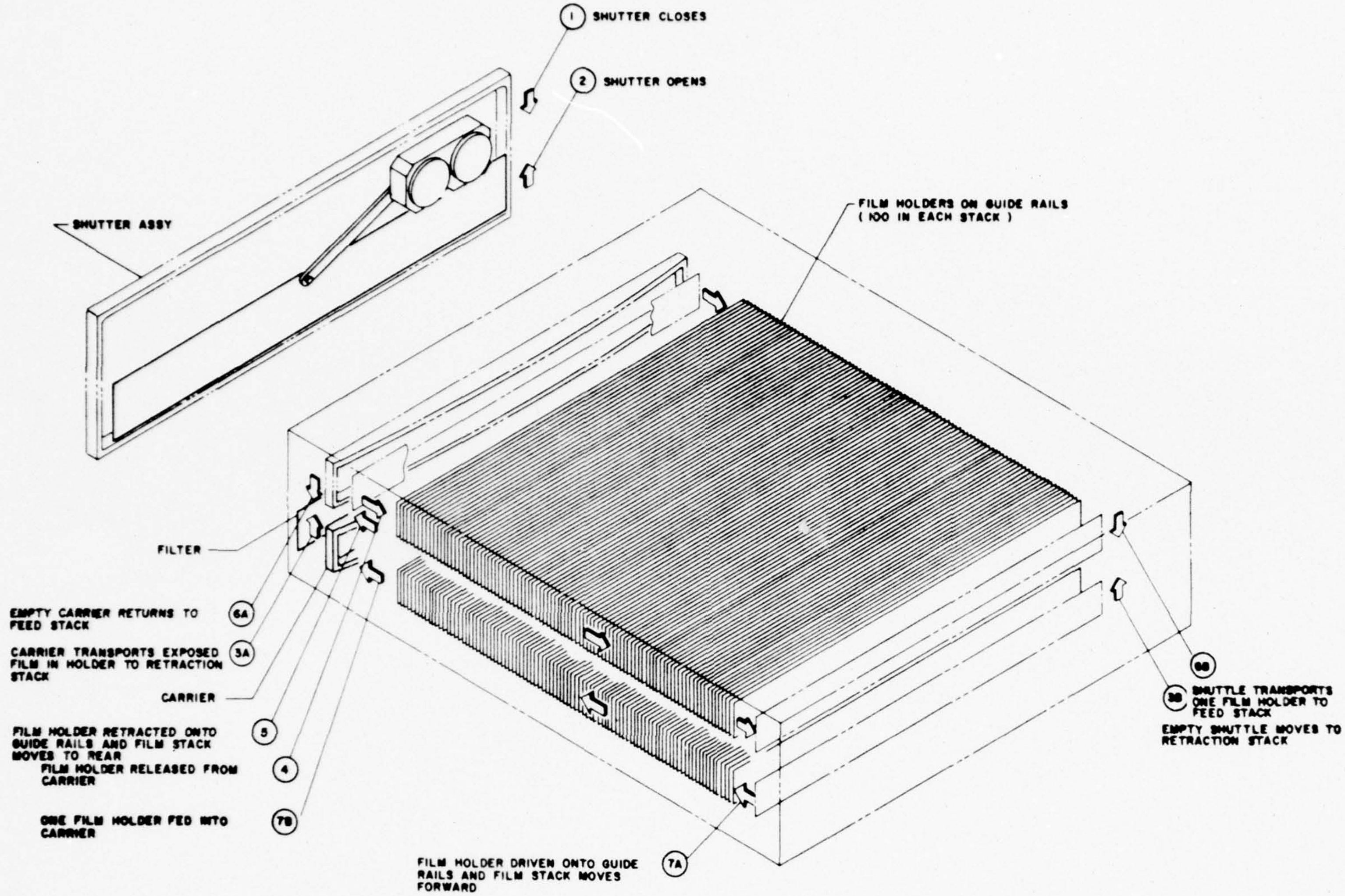

Fig. 2.8 — Schematic view of spectroheliograph camera

III. FILM DESCRIPTION+

During Skylab, 1032 spectroheliograms of the sun were recorded by the S082A instrument. This required XUV-sensitive photographic film in quantities greater than had ever before been needed. In this section, the procurement, selection, testing, handling and processing of the film is briefly described.

Film Type

The emulsion type most sensitive to the XUV was invented by Victor Schumann in 1892. Because gelatin is opaque to the XUV, he developed an emulsion with just enough gelatin to hold the silver-halide crystals on the base material, but in a layer so thin it was effectively transparent to the XUV. These emulsions were unprotected by the normal gelatin overcoat, hence extremely susceptible to abrasion. Eastman Kodak was first to produce a Schumann emulsion on a film base by machine coating, calling it SWR (for Short Wave Radiation). They also developed a method of preventing abrasion between turns of packaged rolls by coating each edge of the film with a spacer 0.2 mm thick, consisting of polystyrene beads held down with gelatin. They designated the new, fast emulsion as SWR Type 101, and produced, as SWR Type 104, a slower, but finer-grained emulsion. For use in the ATM instruments, they produced Type 101 and 104 films in special rolls, 70 mm in width and 30 m in length. The required 33 mm strips were cut from the center. Three rolls were sufficient to provide the 200 strips needed for each camera. Ten rolls were made from one batch of emulsion.

Strict controls were required to produce the many batches of emulsion needed to manufacture film that was satisfactory for the ATM experiments in the large quantity required. In the past it was not uncommon to find variations from batch to batch, and even within a single roll, on the order of a factor of 2 to 5. Eastman Kodak succeeded, however, in improving dramatically the overall quality of both Types 101 and 104 films. Large quantities of these films were produced that were uniform to a degree never previously achieved; they were remarkably free from blemishes of all kinds. Generally, the sensitivity threshold did not change significantly from batch to batch, or from place to place over a roll. The maximum density, D_{max}, and the contrast varied between batches, but not greatly. Type 104 batches having D_{max} between 1.4 and 1.6 (as measured with a Grant microdensitometer were accepted for use in ATM.

Estar was selected for the base material because of its dimensional stability. It was also exceptional in its freedom from outgassing when in vacuum. This minimized the possibility of contamination of gratings and mirrors, an important consideration in preserving the speed of XUV instrumentation.

+Material for this section has been excerpted from a paper by VanHoosier, et al. to appear in Applied Optics, Vol. 16 , 1977.

The Estar base was first coated with a 0.012 mm thick gelatin pad. The emulsion, in the form of a monolayer of silver-halide crystals, was then deposited on the gelatin pad. When dried out in vacuum, the gelatin pad shrank, whereas the Estar base did not. This produced a curl which was used to advantage in forcing the film to conform to the metal holder in which it was carried. To avoid excessive pressure, rather stiff, 0.175 mm thick Estar was used. Halation, at wavelengths above where gelatin is transparent, was reduced by adding a yellow dye to the gelatin pad, ; this reduced, by more than 100, the light reflected by the Estar base in the wavelength range 2000 - 4000 Å.

Film Selection

Schumann emulsions are not only destroyed by the slightest physical contact, they are are extremely sensitive to environmental effects of many kinds.

Various gases, such as hydrogen and oxygen, when ionized in a vacuum gauge or an open discharge used as a light source, are known to fog Schumann emulsions. At 435 km, and in the presence of solar XUV radiation, there existed the possibility that the ion density might still be sufficient to produce fogging of ATM film over the long periods of exposure to the space vacuum during Skylab. From extensive tests, it was found important to store the film in vacuum or an inert gas atmosphere, and to avoid exposure to high temperatures.

Film fogging by metals was investigated, and it was found that freshly machined aluminum did, indeed, fog Types 101 and 104 films; but aluminum, if completely anodized, did not. Therefore, the aluminum holders were thoroughly anodized after machining and bending. Similar precautions were taken with all parts of the cameras, even though they were not located close to the film. Black-anodized aluminum, made by dyeing black the anodized layer before it was dry, and found safe. Magnesium was not used because, when chemically blackened, it produced fog.

Type 101 was much more susceptible than Type 104 to fog from these sources, but neither type of film was found to be affected by the mechanical stresses induced by high acoustical and vibration levels during launch.

Another serious source of fogging in orbit was expected to be the flux of high energy protons encountered on each passage through the South Atlantic Anomoly. Predictions of fogging, based on estimated values of proton flux and shielding, although far from certain, suggested that a fog level as high as 0.5 might be produced for Type 101. Tests found that Type 104 emulsion was less sensitive than Type 101 to proton fogging, and it was therefore decided to use Type 104, even though its sensitivity to the XUV was less than that of Type 101 by a factor of 5, approximately. Because of uncertainty in the fog prediction, however, a single strip of Type 101 film was included as a test in most of the cameras on SL-2 and 3. When the fog levels expected from the proton flux did not materialize in flight, a small quantity of Type 101 film was included in the camera on SL-4 to take advantage of its greater sensitivity.

Film Handling

On the basis of the test program, and NRL's experience in previous rocket programs which used Schumann film, it was necessary to set up an elaborate protocol to safeguard the large quantities of film at every juncture, from manufacture to final mounting of the recovered and processed film. Extraordinary precautions were taken to prevent exposure to all known sources of fogging, and to treat each strip of film in exactly the same way. Strict control was exercised over the selection of materials used in film containers and the atmosphere and temperature to which the film would be exposed during handling. All the operations were conducted in a class 10 K clean room. Consultation with Eastman Kodak assisted in the selection of clean room uniforms which were free from photochemical contaminants. Chemically-treated fabrics, after-shave lotion, perfume, hair-spray, cosmetics, medicated soap and shampoos, were prohibited. Surgical latex gloves, rinsed in alcohol after donning, completed the attire approved for clean room use.

The film was shipped in dry ice from Eastman Kodak to the instrument manufacturer, Ball Brothers Research Corporation and kept near -20°C over the several month period between manufacture and loading. Loading took place in rooms that were completely dark, but illuminated by low level infrared. The entire operation was observed by quality control personnel from outside through the use of low-light-level infrared sensitive television.

To cut Estar film precisely and cleanly required the design and construction of a special vacuum-platten film cutter. With this device, 35 mm x 248 mm strips were cut from the center of the 30 m long supply roll of 70 mm film and loaded into a metal holder, all in total darkness, without ever touching the film strip.

The air in the 10 K clean room was kept at 50% RH to maintain the film's original flatness and to avoid static electrical effects. Once loaded with holders, each camera was pumped for 24 hours at 10^{-5} Torr to outgas both the film emulsions and the camera. It was then sealed in a thoroughly outgassed stainless steel canister, pumped out again and finally backfilled with dry N_2 to one atmosphere. The stainless steel canisters were designed especially to minimize thermal shock, to keep the film in a clean atmosphere, and to provide maximum physical protection of each camera. The interior of each canister was lined with 12 sheets of aluminized Mylar; this was a precaution against severe heating during EVA, when direct sunlight might fall on the canisters for up to an hour. It was also of value in reducing the heating of the film during reentry, splashdown and recovery.

Prior to installation in Skylab, and in transit to the Kennedy Space Center, the loaded canisters were kept at 2° C. During the mission, both the unexposed and exposed cameras in their canisters were stored in film vaults, made from 12.7 mm aluminum, located in the Skylab multiple docking adapter (MDA) where the temperature was 20°C. This aluminum served to shield the film against the high energy proton flux.

During EVA, when a camera change was made, canisters were carried to the sun-end of the ATM by an astronaut. He removed from the S082A instrument the camera that had been exposed, placed it in the canister and sealed the lid, which maintained the high vacuum of space. Then the new camera was removed from the other canister and installed in the instrument. The exposed camera in its canister was returned to the film vault and stored until the end of the mission, when it was returned to earth in the Command Module.

The recovery operation was highly organized. A few hours after splashdown the canisters were back in shipping containers, refrigerated to 2^{o} C. As soon as the recovery ship reached harbor they were flown direct to Johnson Space Center, then to Washington; normally reaching NRL less than 48 hours after splashdown.

Processing the Film

Over the years of using Schumann type film, and after considerable additional experimentation, it was decided that D-19 mixed 1:1 with distilled water provides the greatest uniformity, freedom from chemical fog, and minimum Eberhardt, edge and adjacency effects. The following procedure was adopted to provide maximum control and uniform quality of the flight exposures.

One flight strip was selected and processed alone at the start, to ensure that each returned flight load had not received degradation which could be corrected by different processing. The remainder of the film was developed in batches of 40 flight strips and 10 laboratory-exposed control strips. The flight strips were left in their holders, together with the Plus-X data chip. All strips were attached to a rack in a vertical position. The solutions were held in large, stainless steel tanks. Each tank contained 40 liters of solution, a quantity considered sufficient to process the entire contents of one camera without depletion.

The rack of 50 film strips, was first presoaked in a tank of distilled water for 4 minutes. This was an important step because it prevented infectious development by allowing the dried-out gelatin pad to swell. Otherwise, whiskers growing on exposed grains could touch adjacent unexposed grains, making them developable. Immersion in the water was done quickly, but smoothly; (if strips are immersed unevenly, marks are produced by the stresses of nonuniform swelling). All solutions were maintained at 20^{o} C. It was important to avoid elevated or changing temperatures, which would cause reticulation of the gelatin pad. Development was for 4 min., followed by 30 sec in acetic acid short-stop, 4 min. in Kodak acid fixer, a 20 min. wash in filtered tap water, removal to a class 10 K clean room, rinsing in distilled water, and hanging to dry.

An important part of the development process was the use of N_2 bubble agitation, introduced through an array of many small holes, roughly 3/4" apart, in a plenum at the bottom of the tank. A one second burst of N_2 was produced at 10 second intervals. In addition,

the entire film rack was moved laterally by hand, alternately parallel and perpendicular to the film, at a speed of about 1 cm per sec. This procedure had been found to produce uniform development.

The five development runs which were required for each camera could be completed in one day. The development process was controlled by including in each development the 10 control strips of film from the same batch on which a standard series of exposures had been placed 48 hours earlier. These 2 cm by 10 cm strips were exposed to the continuum spectrum of a D_2 lamp, dispersed by a McPherson normal-incidence monochromater/spectrograph. The exposure times were 1 and 10 sec. The intensity was reduced in steps of a factor of 2 by means of sectored disks, covering the range of 1:100 in transmittance. The spectral range was 1650 to 2400 Å. Use of these control strips was mainly to serve as a check that the development was the same each time it was carried out. The H - D curves of control strips developed in various runs were found to agree to $\pm$ 0.02 in log E.

Finally, the dry film strips, while still in the clean room, were mounted between high quality glass plates of 1.25 mm thickness, which had been anti-reflection coated on the inside surfaces to minimize Newton's rings. The film strip was surrounded with a brass spacer, of thickness slightly greater than the film. This, together with the normal curl, prevented the emulsion from being touched by the glass. The sandwich was then sealed with plastic tape and stored in a vault.

IV OBSERVATIONS

In this section, a brief description is given of S082A observations and a sampling of selected significant events and features. Its purpose is to convey to users an idea of solar research topics for which S082A data has been found to be well-suited. (See also Bibliography, Appendix A).

Data Catalogs

A catalog of all S082A exposures, arranged in time, is provided in microfiche form as Appendix D to this Guide.

S082A participation in the "Joint Observing Programs" (JOPs), or pre-planned ATM studies of specific solar features and events, was scheduled in such a way that it provided a continuing record of the entire disk, while supporting particular studies by the remaining ATM instruments to the maximum extent possible. For a complete record of the frame-by-frame relationship of S082A exposures to these joint studies, the user must consult catalogs containing the record of ATM observations. A simplified list of JOPs is furnished in Appendix B, together with titles of useful catalogs and outlines of their contents.

Pointing and Roll

In general, the coordinates of the ATM pointing position on the solar disk ("UP/DOWN" and "LEFT/RIGHT") are not needed when using S082A data. Since the field-of-view of the instrument was 56 arc-min, only exposures taken during pointings near the solar limb do not show the entire disk. Except during flares, S082A exposures were generally always taken at or near sun-centered pointing to avoid truncation of the image at the edge of the film.

Rotation of the ATM around its roll axis had the effect of rotating the solar image on each film strip relative to the fixed direction of dispersion. A user who wishes to determine the orientation of the image from given values of "ROLL", or "Γ_{RR}", may do so using Fig. 4.1. The ROLL value must be obtained from the appropriate catalogs referred to in Appendix B.

Flares

Tables 4.1 and 4.2 give two lists of S082A exposures associated with: (a) identified X-ray flares in SOLRAD data, and/or (b) events identified on S082A plates that caused solarization on the He II 304Å image and emission in lines of highly-ionized elements. A careful study of plates before and after those listed may reveal changes of significance in interpreting the flaring phenomenon.

Plasma Ejection Events

In addition to the many surges of all sizes that can be recognized on the S082A images, a number of large plasma ejections were recorded, both accidentally and intentionally. Table 4.3 gives a list of 11 of these events that were associated with specific flares, eruptions of previously quiescent prominences, or with an active region.

Time Sequences

S082A exposures were taken at regular intervals throughout the three manned phases of the Skylab mission. Over the last half of the second manned phase, and throughout the third phase, exposures were taken, in both the short and long wavelength bands, approximately every 12 hours. These were associated with the "synoptic" JOP program adhered to by all ATM experiments.

In addition, several other time sequences of various intervals were taken:

. during flares, in a rapid sequence of scaled exposures;

. during the "Nested Sequence", carried out on 19-20 January 1974 (every orbit for 37 orbits, with one orbit of exposures taken at time intervals progressing from 6 minutes to 30 seconds);

. during one entire orbit on 28 Nov. 1973 (a sequence of 60 sec. exposures, in the long wavelength band, at intervals of 90 seconds);

. during the "Solar Wind" JOP, conducted 16-21 August 1973;

This list is not complete. For a number of other occasions, short sequences of exposures of identical duration exist. These are readily identified in the time listing, Appendix D.

Solar Features

In Fig. 4.2, the more prominent XUV line images on the S082A spectroheliograms are identified. During a flare, hundreds of additional lines become visible. The chart in Fig. 4.3 indicates those stages of ionization for which emission lines of the various elements have been identified on the spectroheliograms to date.

Figure 4.4 is an enlargement of a section of a 10 sec exposure in the short wavelength band. At the right is the sun in He II 304 Å, and at the left in the coronal line Fe XV 284 Å. The ATM was rotated so that North is to the left and West is up. A large coronal hole covers most of the region of the South Pole, and a small hole is present at the North Pole. The quiet solar features to be seen in He II include: the chromospheric network, which covers most of the quiet sun; filament channels

and filaments, the darkest of which is the Archimedes-spiral-like feature at the bottom center of the solar image; and quiescent prominences around the limb. The activity is concentrated in the plages, of which at least seven can be seen. The plage halfway to the limb at "11 o'clock" is the one where a flare was seen in progress. Above it, on the limb, is a plage that shows strong emission in the corona and also in tight loops. Another phenomenon associated with activity is the XUV (and X-ray) bright spot. Many of these are visible in the polar holes. Although the entire solar surface is peppered with them, the bright network makes them hard to see.

The image to the left, fourteen times ionized iron (Fe XV 284Å), is completely different. In this line the emission is most intense in the plages and in the corona above them. The forms are loops, outlining magnetic field lines that arch between areas of north and south magnetic polarity. The disk emission is too faint to record with a 10 sec exposure except above the limb, where the greatly lengthened line-of-sight increases the intensity sufficiently, as is seen over the east limb.

By far the most interesting feature, however, is the flare. The image shown in Fig. 4.4 was exposed during the early stage of an X-ray Class M-2 flare. In He II 304 Å the flare shows at the center of the active region as a small angular feature, so intense that it caused the Schumann film to be solarized.

The horizontal row of images, parallel to the dispersion, shows the spectrum of the flare. It consists of a continuum background, with bright line images of the flare in almost every solar emission line ever observed in this spectral range. These images are not solarized, and show great detail.

In Fig. 4.5, images of the same flare are shown in three selected lines, enlarged about 4 times compared to Fig. 4.4, but with the same orientation. Detail of the order of 2 arc-sec is present. The upper set of images is from a 2 sec exposure made just before the exposure of Fig. 4.4; the lower set are from another 2 sec exposure which was made 3 min after the first. (Papers discussing this flare are listed in the Bibliography).

In He II 256 Å (upper left), the flare has the same form as in the first line of the He II series, λ304 Å; however this image was of sufficiently low density to show the detail. The principal feature lying East-West is interpreted as a loop. The top of the loop was heated so greatly that the material is being blown out (to the left), leaving a gap. This is really He II that is located in the gap, but moving with such a high velocity that the λ256 Å line is Doppler shifted toward short wavelength by 0.25 to 0.5 Å. To produce this Doppler shift requires a velocity of 300 to 600 km/sec.

The same is true of the image to the upper right, in Fig. 4.5 which is the λ 284 Å line of Fe XV, where the temperature is 2.6×10^6 K. The Doppler displacements of He II and Fe XV are the

same, indicating that all material at the top of the loop is moving out at the same velocity.

To the left of He II 256 Å, is the longer wavelength member of the resonance doublet of lithium-like, 23 times ionized Iron, Fe XXIV, at 255 Å. Production of this stage of ionization requires a temperature of 20×10^6 K, hence this line is seen only during the initial, hottest phase of the flare. It, too, is located at the top of the loop, and its presence is confirmation that tremendous heating has taken place at that position.

In the lower set of images, photographed 3 minutes later, the high velocity, Doppler-shifted emission is gone, and ordinary emission appears at the top of the loop. The flare is cooling, still so hot that Fe XXIV is being emitted.

Miscellaneous

Solar features that are not so apparent on these particular images, but appear prominently on others, include: the bright limb produced in a thin shell at the top of the transition region and bottom of the corona; the polar plumes that are seen to project out of bright points in the polar coronal holes; spicules; and macrospicules, giant spicules extending far above the limb in coronal holes.

Of some interest, perhaps, are exposures taken during the partial eclipse of 24 Dec. 1973. On exposures taken during perihelion passage of Comet Kohoutek in late December, 1973, no evidence of XUV emission has been found.

ROLL=0000 arc-min (0°)   ROLL=+1800 arc-min ($+30^{\circ}$)

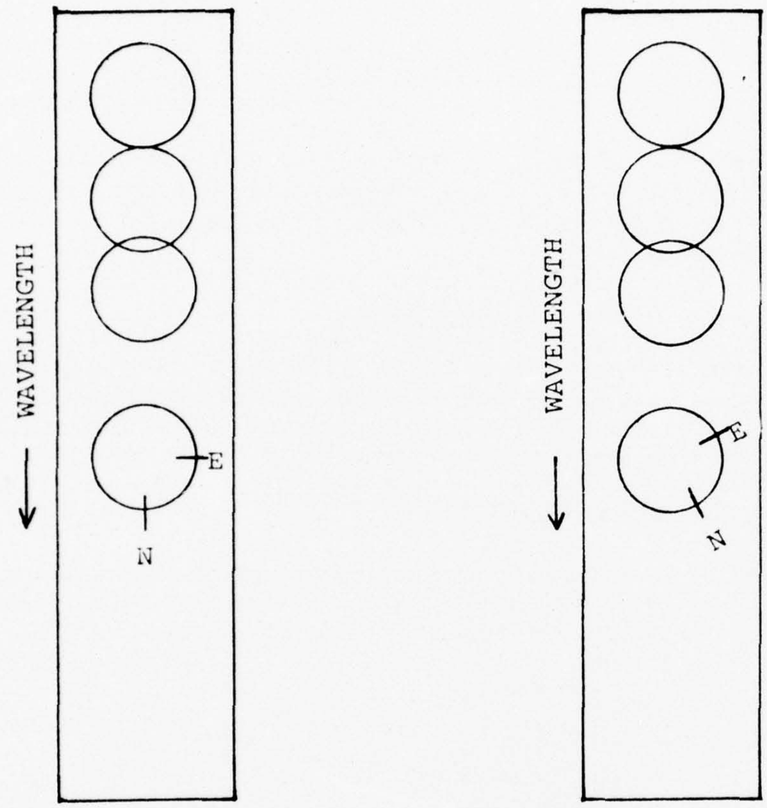

Fig. 4.1 — Roll and solar orientation

The above sketch illustrates the relationship between solar orientation and ATM roll position values and the sense of the roll :

With <u>emulsion toward viewer</u>

Positive = CCW
Negative = CW

Range:

$$-10{,}800 \text{ arc-min } (-180^{\circ}) \leq \text{ROLL} \leq +10{,}800 \text{ arc-min } (+180^{\circ})$$

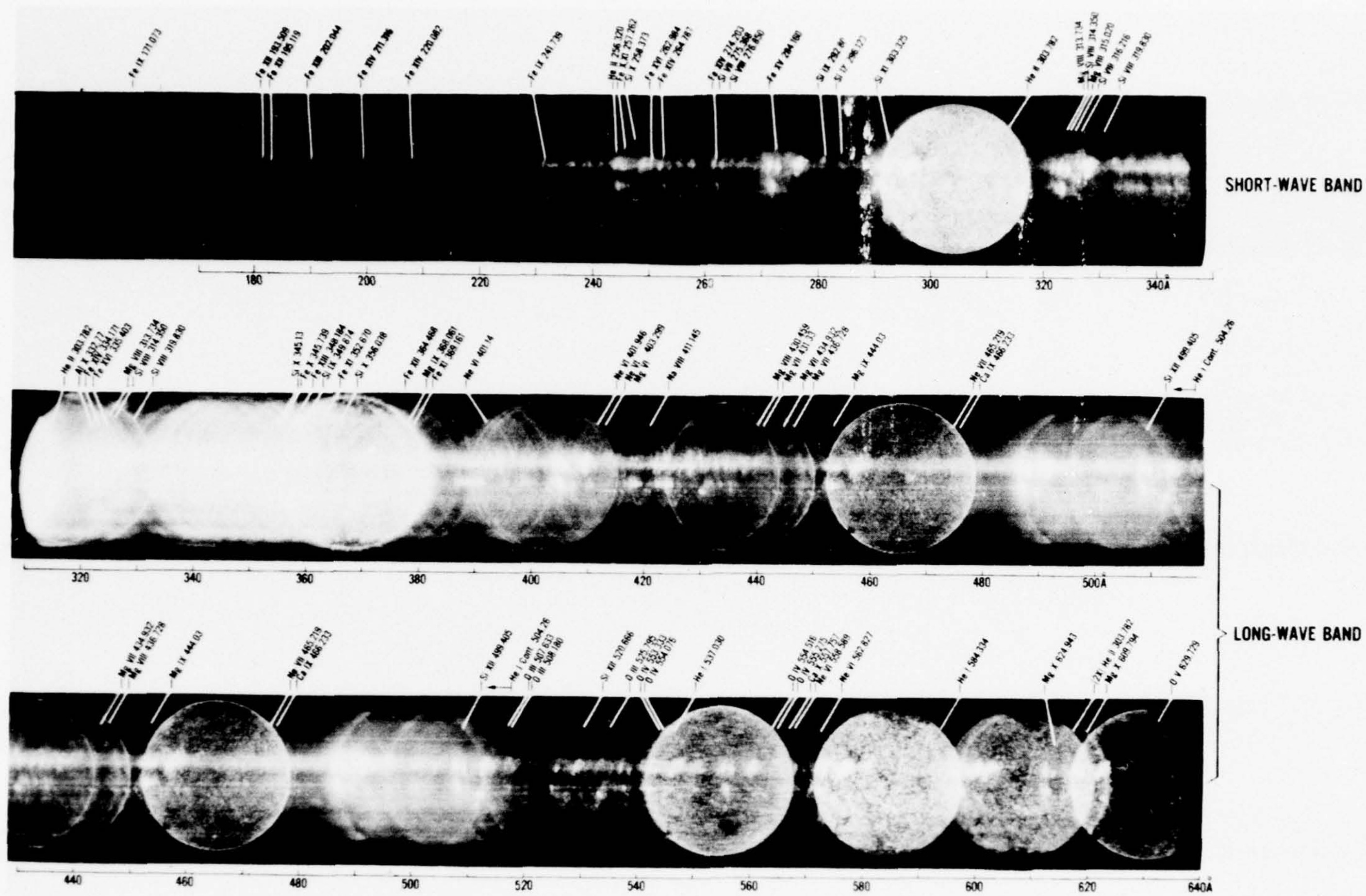

S082A λλ 171-630Å

Fig. 4.2 — Identification of prominent XUV images (prepared by J. D. Bohlin)

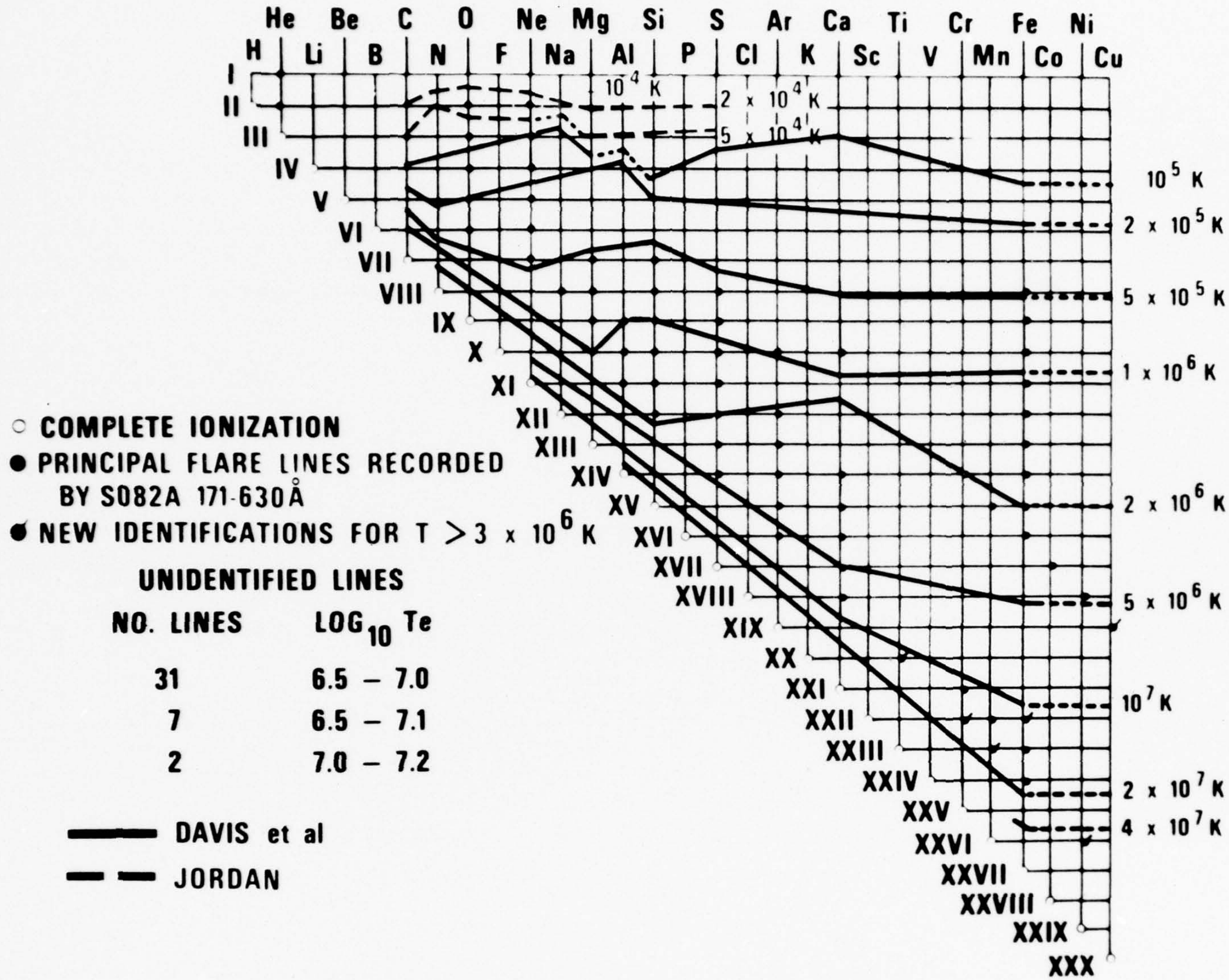

Fig. 4.3 — Stages of ionization identified in XUV (prepared by V. E. Scherrer)

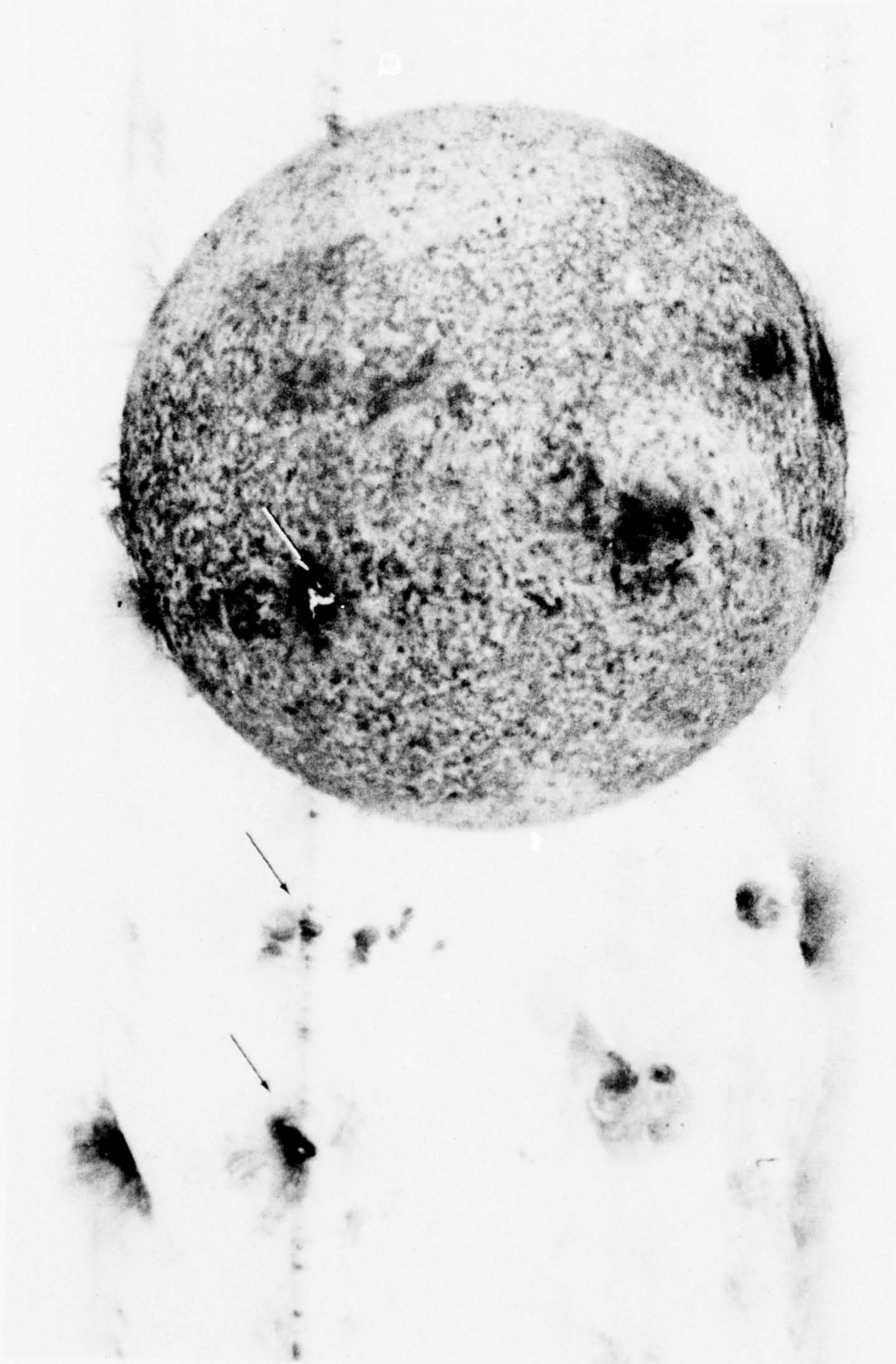

Fig. 4.4 — XUV solar features

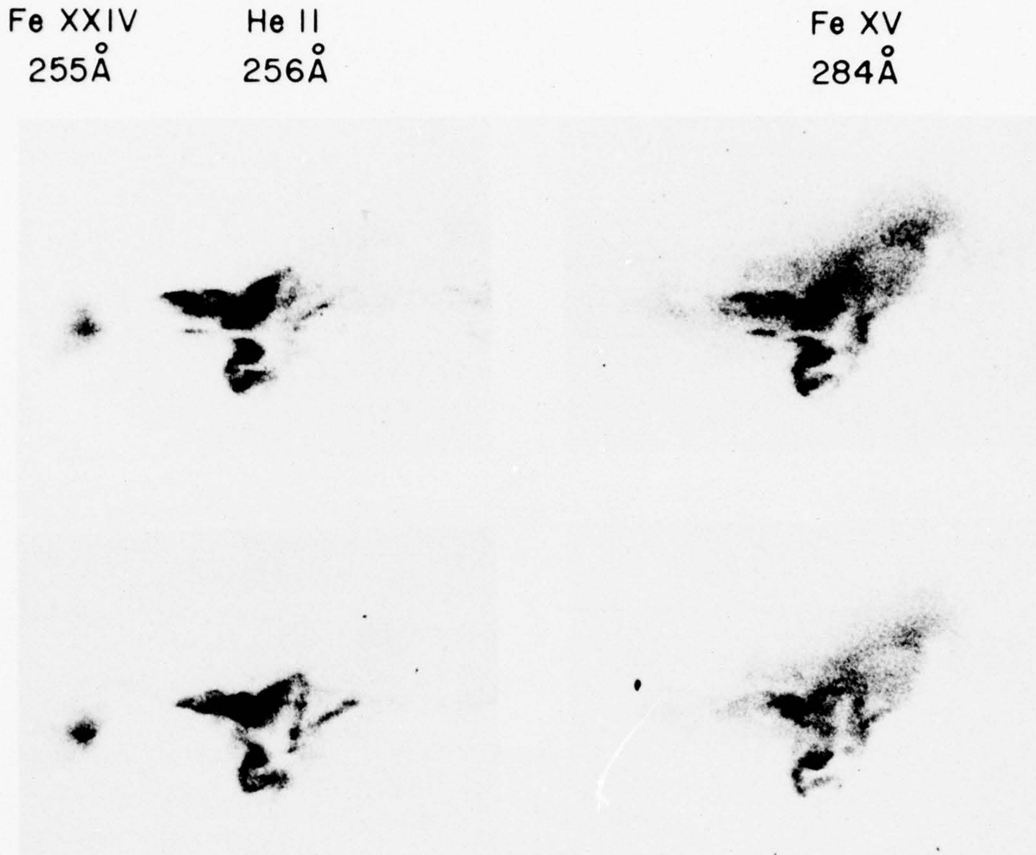

CHANGES IN 3 MIN DURING RISE
M2 FLARE OF 15 JUNE '73; 2SEC EXPOSURES

Fig. 4.5 — XUV flare images

Table 4.1 Exposures Associated with Flare Events*

Date	NRL Plate Nos.	Time (UT)	Position Angle ($\pm 5^{\circ}$)	Notes
15 June 73	1A312-347	14:11-14:38	N20W45	WV LG & ST. M2: Max. 14:14. Complete sequence.
7 Aug. 73	2A006-007	18:47-18:49	N10W30	C3: Max. 18:47. Both plates LG WV. Many flare images superposed one hour earlier and later still show AR to be very bright.
9 Aug. 73	2A022-035	15:20-15:58	N10W50	M2: Max. 15:53. May be sequence of two flares, with small limb flare on 2A022 the cause of large EPL. Many flare images superposed on film holder defect.
31 Aug. 73	2A356-357	21:57 21:59	S05W15	Two exp. (WV ST) of small flare. Emission lines well-separated and compact.
1 Sept. 73	2A371-373	21:26-21:32	N05E80	Subflare. Emission lines not distinct. LG & ST WV. Max. 21:15
2 Sept. 73	2A376	00:46	S10E70	Subflare. Emission lines not distinct. ST WV. Max. 00:43
3 Sept. 73	2A392-393	21:35-21:42	N05E30	Small flare shows "streak" emission lines in both LG & ST wavelength plates.
4 Sept. 73	2A398-399	11:29-11:32	S20E70	Twin solarized spots in He II. Bright footpoints in many highly ionized lines WV LG & ST, Synoptic pair. Max. 11:30
4 Sept. 73	2A403	16:36	N10E10	C6: Max. 16:35
5 Sept. 73	2A419-420	18:31-18:37	Disk Center	Distinct arch visible. ST WV only.
5 Sept. 73	2A421-422	20:15-20:20	S20W30	Max. @ 20:10. Small flare in NE quadrant. Complex emission structure.
7 Sept. 73	2A432-448	12:21-18:28	S20W50	X1 flare w/ 4 consecutive peaks. Post flare loops over neutral lines esp. apparent. AL1 ST WV. Max. 12:10

* Table 4.1 was compiled jointly by J. D. Bohlin and V. E. Scherrer.

Table 4.1 Continued

Date	NRL Plates Nos.	Time (UT)	Position Angle $\pm 5^{\circ}$)	Notes
10 Sept. 73	2A459-460	02:32	S20W60	Synoptic pair may have caught small flare. He II barely solarized. LG & ST WV.
2 Dec. 73	3A037-045	15:04-15:17	S10W80	M1 flare. Max. 15:18 LG & ST WV. Good sequence.
16-17 Dec. 73	3A097-143	19:00-02:00	S20E85	Complete sequence on C2 & M1 (Max. 00:32 & 00:41) limb flares. 47 plates total.
22 Dec. 73	3A176-178	00:22-01:20	S10E05	Small flare on 3A176 (ST WV); emission lines still apparent on synoptic pair 177 & 178. May only be a very bright AR.
15 Jan. 74	3A375-376	14:25-14:28	N10W85	Limb flare (C6: Max. 14:25) with sheet-like surge. ST WV only. Surge seen hour earlier as well.
21-22 Jan. 74	3A452-472	23:15-00:49	N30W50	C8 flare, full sequence of 21 plates. Max. 23:23.

TABLE 4.2 - SUMMARY OF NRL FLARE OBSERVATIONS *

	X-Ray U. T.			X-Ray	LOCATION			S082B OBS.		S082A OBS.	
Date	Begin	Peak	End	Class.	ATM Region	McMath	Coordinates	Preflare	Flare	Preflare	Flare
6/13/73	1757	1806	1841	C4	137	387	N12E50	0	0	2	6
6/15/73	1405	1413	1455	M3	131	379	N17W32	0	136	5	45
8/7/73	1838	1847	1853	C2	185	474	N6W24	58	12	4	2
8/9/73	1551	1553	1600	M1	185	474	N8W49	9	29	3	11
8/21/73	1334	1500	1800	C1		497	N12E90	0	0	5	7
8/31/73	1220	1228	1245	C1	212			0	2	0	2
8/31/73	1410	1415	1423	C1	209	507	S12E44	0	1	2	0
8/31/73	2155	2208	2230	C1	213	511	N4W19	0	2	2	4
9/1/73	2122	2126	2130	C4	215	512	S17E65	0	9	4	3
9/1/73	2303	2311	2317	C1	215	511	N06W33	34	8	5	0
9/2/73	0042	0045	0050	C4	215	512	S16E57	0	8	6	1
9/2/73	0241	0245	0320	C3	215	512		9	1	3	0
9/2/73	1904	1904	1925	C2	215	512	S18E47	0	11	0	1
9/2/73	2140	2150	2220	C9				0	0	1	3
9/3/73	1610	1618	1650	C7	210	508	N23W4	0	0	0	3
9/4/73	1123	1125	1130	C3	219	513	S10E57	0	5	0	2
9/4/73	1627	1635	1652	C7	212	510	W14E16	0	16	1	1
9/5/73	1828	1832	1850	M1	212	510	N11E4	2	17	4	2
9/5/73	2003	2021	2054	C8	209	507	S13W25	0	38	2	2
9/6/73	1250	1255	1400	C4	209	507	S18W33	0	0	0	1
9/6/73	1816	1832	1920	C2	215	512	S19W8	0	0	0	1
9/7/73	1141	1212	1342	X1	209	507	S18W46	0	96	0	15
9/9/73	2143	2150	2210	C1	224	520	S10W37	2	3	0	0
9/10/73	0223	0232	0251	M1	224	520	S11W41	0	8	0	2
9/10/73	1140	1149	1216	C3	224	520	S10W46	0	0	0	2
12/2/73	1459	1505	1514	C2	287	628	S11W64	0	0	0	3
12/2/73	1505	1518	1537	M1	292	628	S13W64	0	14	1	8
12/2/73	2010		2020	C5	292	628	S14W67	4	41	0	0
12/16/73	1954	1956	2023	C2	300	664	S17E74	10	31	2	12
12/17/73	0029	0032	0057	M1	300	664	S17E77	1	79	2	25
12/20/73	1321	1326	1340	C2	300	664	S17E26	0	0	0	2
12/22/73	0112	0112	0210	C1	300	664	S19E3	4	12	2	2
1/11/74	2010	2025	2040	C1	320			0	6	0	1
1/13/74	1609	1611	1628	C1	314	686	N5W57	0	0	2	1
1/15/74	1422	1422	1450	C6	314	686	N7W84	0	7	4	2
1/21/74	2313	2316	2345	C7	331	708	N6W51	13	53	0	19

* Table 4.2 was compiled by V. E. Scherrer.

Table 4.3 — SKYLAB/NRL Solar Plasma Ejection Events

	DATE	TIME(S) OF NRL OBS. (UT) & PLATE NOS.	COORD. OF FEATURE[1]	ASSOC. AR (McMATH NO.) & COORD.[2]	HAO CORONAL TRANSIENT[3] (P.A. & TIMES)	SOLRAD X-RAY EVENT[4] (8-20 Å)	ASSOC. FLARE TIMES-POSITION-CLASSIFICATION-	COMMENTS
	I. EVENTS ASSOCIATED W/ERUPTION OF (PREVIOUSLY) QUIESCENT PROMINENCE							
1	26 Aug. 73	13:16 - 23:50 2A315-321	P.A. 45-60° East Limb	12504 (N10 E80)	"Massive, Slow" P.A. 70°; 23:02-	Very faint GRF 14:00 - 18:00	None	Massive erupting prom., identical w/Hα seen from Mauna Loa.
2	19 Dec. 73	06:32 - 06:37 3A149-154	P.A. 45-80° East Limb	None	"Spectacular loops" P.A. 80° 07:00 -	None	None	Eruption of one of largest prominences in last decade
3	18 Jan. 74	18:52 only 3A394-395	(N15 E10) On disk	12706 (S08 E10)	None expected due to location on disk	Classic GRF 18:30 - 23:30	None	Hα disappearing filament, coincides w/He II absorp. feature near disk center.
	II. EVENTS ASSOCIATED W/ACTIVE REGIONS, BUT NOT W/REPORTED Hα FLARE							
4	10 June 73	01:46 only 1A215	P.A. 80° East Limb	12387 (N14 E90)	"Bright, turbulent" P.A. 80°; 01:50-	None	None	Coincident w/Imp. 1 Hα spray (N15 E90) 00:55 - 01:40. Large spray @ ~30° to limb.
5	9 Aug. 73	15:20 -15:58 2A022-035	P.A. 270-300° West limb	12471 (N15 W90)	"Diffuse loop" P.A. 280° 15:30-	IS @ 15:50; no GRF	14:27 & 15:51 (N07 W48) -F & -N ?	Extended "elbow" or "fig. 7"; resembles eruptive prom.; may have been triggered by disk flares.
6	12 Sept. 73	01:08 2A469-470	P.A. 250-270° West limb	12510, 12512, 12520 (N15 - (S16 W70-80)	"Fast loop" P.A. 300° @ 17:44 on 11 Sept.	Classic GRF 17:45 on 11 Sept to - 05:00 on 12th	None	Almost certainly the remains of an event occurring ~6 hrs earlier, based on transient, X-ray GRF, & post-event loops observed @ 01:08 on 12th.
7	17 Jan. 74	19:44 - 20:46 3A387-391	P.A. 277° West Limb	12686 (N07,W~110)	"Diffuse loops & bright tongue" P.A. 280° 19:43-	Very small GRF 19:00 - 24:00	Region over west limb by ~20°	Most energetic & bright of all ejections; almost certainly assoc. w/AR 12686 just over limb.

Table 4.3 was compiled by J. D. Bohlin

Table 4.3 (Continued) — SKYLAB/NRL Plasma Ejection Events

	DATE	TIME(S) OF NRL OBS. (UT) & PLATE NOS.	COORD. OF FEATURE[1]	ASSOC. AR (McMATH NO.) & COORD.[2]	HAO CORONAL TRANSIENT[3] (P.A. & TIMES)	SOLRAD X-RAY EVENT (8-20 Å)	ASSOC. FLARE TIMES-POSITION-CLASSIFICATION-	COMMENTS
	III. EVENTS COINCIDING W/OBSERVED FLARE							
8	21 Aug. 73	14:42 - 15:33 2A183-187	P.A. 80° East limb	12497 (N12 E90)	"Bright loop" P.A. 50° 14:41 -	Classic GRF 13:55 - 19:00	13:44 - 14:30 (N12 E90) 1F or 2N	Bright & massive "horn" spray; extreme filament coincides w/bright thread of coronal transient.
9	3 Sept. 73	21:35 - 21:42 2A392-393	(N10 E30) on Disk	12510 (N15 E28)	None expected due to location on disk	Night pass may obscure small IS; no GRF	21:24 - 21:39 (N13 E28) --F	Surge seen in emission from small disk flare; only one like it in the mission.
10	16 Dec. 73	20:09 - 20:14 3A099-110	P.A. 110° East limb	12664 (S16 E70)	None reported	I.S. @ 20:10 & 20:20 No GRF	19:54 - 20:73 (S17 E74) --N	Spectacular "dog leg" ejection from limb flare.
11	15 Jan. 74	13:19 - 14:28 3A374-376	P.A. 280° West limb	12686 (N07 W88)	"Rapid bright loops" P.A. 270° 11:32 -	I.S. @ 09:00, 10:50, 14:20 No GRF	14:22 - 14:29 (N07 W84) --N	A sheet-like ejecta from limb AR having complex flare activity. The coronal transient preceeded the NRL event & may have been assoc. w/ 1N flare @ 10:56.

NOTES:

(1) Coordinates given as position angle (P.A.) if limb event, or as heliographic (Latitude, Longitude) if disk event.

(2) Active region (AR) closest to event, if not source of event.

(3) Lists "comment", P.A., & time of first observation from HAO transient log.

(4) SOLRAD event distinguished as impulsive spikes (I.S.), i.e., fast rise and fall; or as gradual rise and fall (GRF) which occurred just before or during the NRL observations.

(5) Flare must have occurred directly before or during the NRL observations, & be in same AR as in Col. 4.

V. DESCRIPTION OF THE DATA

The S082A spectroheliograph performed almost perfectly throughout the Skylab mission. Except for the jamming of the first camera, no other failures were encountered. Although the time coverage was limited by the film supply, a total of 1032 XUV spectroheliograms were recorded, showing a wide variety of solar phenomena in exceptional detail. This section contains a number of brief notes on the photographic quality of the S082A flight film, the glass-mounted negatives stored at NRL, from which user film copies originate.

Resolution

In Section II of this Guide, a discussion is given of the spectral and spatial resolution of the S082A instrument. The best resolution attained on the flight film corresponds to 2 arc-sec on the sun (20μ on the film), a limit set by the emulsion. Away from the grating normal the resolution decreases.

Loss of D_{max} and Contrast

An unexpected film effect was a reduction in D_{max} and contrast on all of the flight film, apparently due to prolonged exposure to the hard vacuum in space. *Figure* 5.1 **shows* a comparison between the characteristic curves for Types 101 and 104 flight film and those for film samples from the same emulsion batch kept at 2° C in the laboratory. Especially conspicuous is the long, flat maximum on the flight film. This is followed by a sudden turn-down caused by solarization, for extremely high exposures (typical of solar flares). These curves show that there was no loss in threshold sensitivity. Film stored for an extended period under vacuum in the laboratory did not show this effect. That the loss was due to a cause other than degradation of the latent image was shown by sensitometric tests made post-flight on unexposed strips of flight film.

When working with the flight film, one notices that some He II 304Å images seem perceptibly less "sharp" than usual, causing the viewer to readjust the focus of the microscope or enlarger. No systematic study has been made of the strips on which this effect occurs.

Fog

It turned out that the proton fogging of the Type 104 film was negligible, and for Type 101 only 0.02. The explanation appears to be that the proton flux from the South Atlantic anomaly was much less than was expected, and also that the shielding provided by the Skylab was more effective than calculated. Furthermore, high temperatures were never experienced. No fogging of the film occurred, due to ions, metallic surfaces, or contamination.

---

*From paper by Van Hoosier et. al., Applied Optics 16, 1977.

Artifacts

On occasional film strips, tiny pressure-fog marks, film imperfections, and dust spots appear. Many film strips exhibit very fine lines or scratches parallel to their length. Despite the great care exercised at all stages of handling, small abrasions and finger smudges can be found on several plates. Bits of detached emulsion, specks of dust and hair are found here and there between film strips and the glass mounting plates.

On long exposures, the shadow pattern of the aluminum filter support mesh can sometimes be detected. On the very longest exposures (e.g. those taken of Comet Kohoutek), localized fogging by light leaking through microscopic pinholes begins to appear.

A more serious artifact is found on film strips from the camera loads exposed during the first and second manned phases of the mission. Contact on the back of the Estar film base, at the edges of the stiffening grooves stamped in the stainless steel holders, resulted in narrow stripes of fog extending the full length of the film. An example of this unexpected photographic effect is shown in Fig. 5.2, running across the center of two solar images on a film strip exposed on 13 August 1973. The effect is most pronounced along the central groove, and most noticeable on film strips exposed from 6 August to 24 August, 1973 (in a camera load of relatively high contrast film launched on the Saturn IB used for Skylab 3). In the two camera loads exposed during the third manned phase, anodized aluminum holders were used to preclude the possibility of reoccurrence of this effect. A possible cause of the fogging may have been light emission induced by vibration of the film base against the edges of the grooves during launch.

Miscellaneous

Several film strips were doubly-exposed, presumably on rare occasions when the instrument inexplicably failed to advance the camera. A few are blank or extremely underexposed due to accidental termination of the exposure.

A small number of film strips are mounted with the emulsion facing the wrong side of the glass plates. (A strip is mounted properly when the emulsion is toward the viewer, the short wavelength end is on the left, and the plate number is in the upper left corner reading properly.) In preparing the master copy for NSSDC, plates were always positioned in the enlarger as if they were properly mounted. On a user's negative copies, therefore, the solar image may be reversed, with the sense of the north, east, south and west limbs moving clockwise instead of counter-clockwise. Therefore, the solar orientation should always be verified by comparison of S082A XUV images with $H\alpha$ or other solar images known to be oriented properly.

Film Sequence Log

Each of the six cameras exposed during Skylab contained film strips cut from several different rolls, and each camera load of strips was developed in several different runs. A record was kept of the roll of film from which each film strip was cut, the emulsion batch in which that roll was manufactured, and the development run in which the film strip was developed. This record is known as the Film Sequence Log, and it is reproduced in Appendix C. The emulsion batch appears as the second suffix in the film type number of each roll, i.e.

Film Type

104	-	06	-	05
(Type 104 emulsion)		(7 mil Estar base)		(batch 5)

It should be noted, due to the malfunction of the first S082A camera, only 21 of its 203 film strips were returned exposed (1A001 to 1A021). The full complement of film strips (approximately 200) was exposed in all subsequent cameras. Development runs A and B were made as tests prior to the full tank runs.

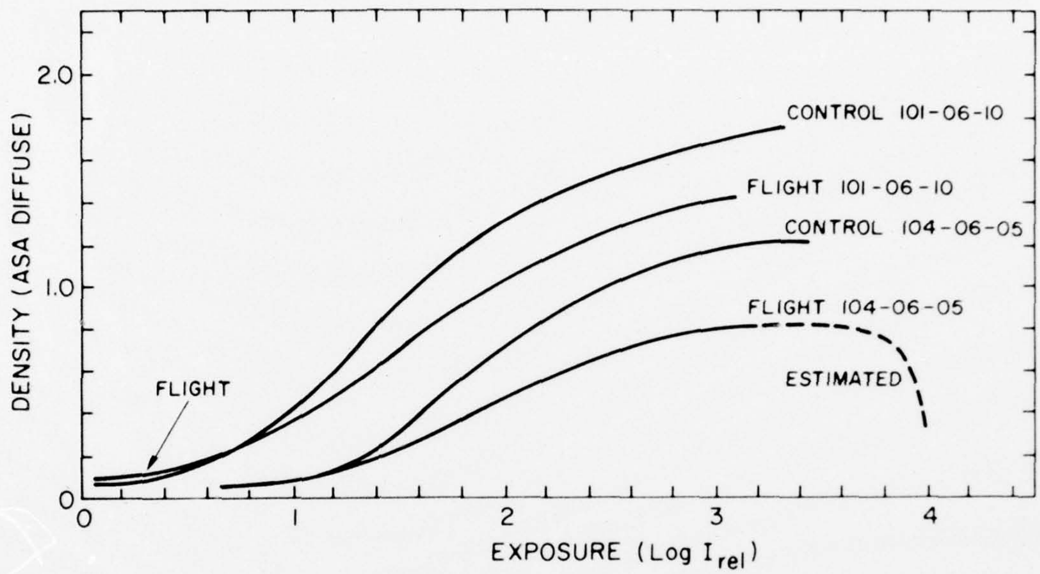

Fig. 5.1 — Characteristic curves for flight film

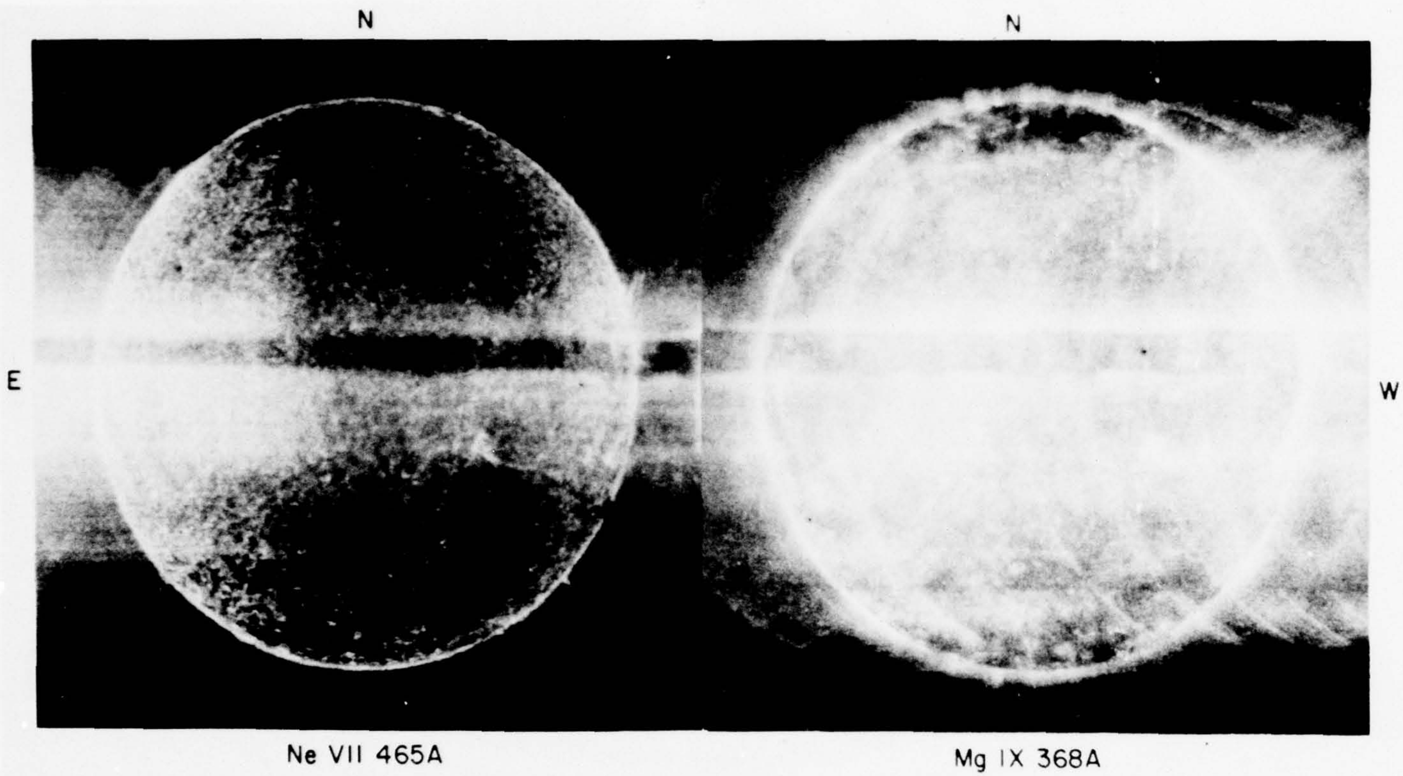

Fig. 5.2 — Example of fog defect

VI. NSSDC COPIES OF THE DATA

The S082A flight film is kept in a secure area at the Naval Research Laboratory, Washington, D. C. Anyone who needs to perform an analysis from the original film should contact Dr. Richard Tousey, Code 7140, Principal Investigator, or Mr. Richard Schumacher, Code 7149, Program Manager.

An enlarged, positive copy of each of the S082A film strips has been made onto 70 mm roll film and deposited at the National Space Science Data Center. Figure 6.1 illustrates the photographic history of copies available for distribution to interested users. The master positive copy, produced at NRL, was used to make a contact working negative at NSSDC, and a working positive was then printed from the working negative. A user may therefore request data in either positive or negative form. These subsequent generation copies are made from the NSSDC working copies, and are indicated in the figure as "User's Positive" and "User's Negative."

All film shown on this "film tree," except for the flight film, was processed at NSSDC under good quality control. It was intended that the film would be useful primarily as an intermediate negative or positive from which prints could be made, or it could be used in various qualitative or survey-type investigations. During the entire photographic procedure, however, care was taken to produce a high quality uniform product. The degree to which the film can be used for photometric purposes was tested by measuring six user's negatives and associated step wedge on NRL's precision microdensitometer. The results derived from these data compared with results derived from the flight film are described in Section VII, Calibration.

The individual flight film strips are 35 x 258 mm, and have been mounted for protection between 2 x 12 inch glass plates separated by a thin brass spacer. In the duplication process, the images were enlarged approximately 1.8 times onto 70 mm Kodak 2421 Aerial Duplicating roll film (Estar Base). The "plates", as the flight exposures are now called, were copied in groups of 50 to 100, with all film in the process bearing the same batch number. At the beginning and end of each photographic session, the film was given a sensitometric exposure using a Kodak Process Control Sensitometer, Model 101. These frames reside on the film at NSSDC, and were used primarily to check the uniformity of film development from beginning to end of a particular group. A great amount of credit is due NSSDC in maintaining its processor control to such a degree that no significant differences could be measured from end to end in the various development runs.

The processor was a Kodak Model 11 Versamat with one rack, employing Hunt E. R. Aeroflo (Regular) developer at 85° F. The film was processed at a speed of 12 ft. per min to a gamma of 1.0. Sensitometric strips at NSSDC developed at intervals during the runs verified the gamma to a tolerance of about 0.02 as derived from measurements with a Macbeth Model TD 504 densitometer (diffuse density).

Of more importance to a user who would attempt rough photometric use of the film, is the 21 step Kodak calibrated wedge which was photographed with the copy camera at least once during each copy session at NRL. The film in the wedge conforms closely to the dimensions and and granularity of the flight film (except for the scratches), and was mounted identically between glass plates of the same size and thickness as the S082A mounting plates. Table 6.1 is a listing of the various exposures, giving the location of a particular wedge whose exposure and general history matches any particular frame number. The symbols in front of the plate numbers indicate a wedge image just prior to or just after that plate. For example, a wedge exposed and processed with plate number 3A020 will be found just before plate 3A001 and another just after plate 3A350 on the roll film.

The S082A plates are listed in Table 6.1 by Skylab mission number and in order by camera number. It will be noted that 6 cameras were used to supply the film for the 3 manned phases. The cameras carried film strips of the following numbers:

Camera	Film Strip No. or Plate No.	Mission
1.	1A001-1A021	SL-1/2
2.	1A201-1A402	SL-1/2
3.	2A001-2A202	SL-3
4.	2A301-2A503	SL-3
5.	3A001-3A202	SL-4
6.	3A301-3A502	SL-4

Table 6.1, for completeness, identifies a roll number assigned to each 350 ft. roll of the 2421 film. Although all batch numbers were the same, and each roll was stored and processed under the same conditions as every other roll, number 9 differs in density readings by as much as about 0.25 density units (diffuse) from the average. Otherwise, a remarkable consistency of wedge step density variations from roll to roll of less than 0.10 density units was obtained. During the editing process, some frames were remade to eliminate extraneous marks, scratches, or dirt, and are listed under "spliced frames" in the table. A wedge was photographed with this set of plates and is identified in the footnote.

A complete listing of the Skylab exposures is contained in a microfiche catalog listed as Appendix D. Table 6.2 is a sample sheet showing the film or plate number, calendar and day of year dates of exposure, time of shutter opening and closing, the total exposure time, and identification of "long" or "short" wavelength band selected for exposure. The information listed is a corrected table based on diode array coded data photographed on the data film chip during the XUV exposure. Other listings of the data are contained in documents described in the Appendix B.

Typical transfer curves derived from the wedge images are shown in Figs. 6.2 and 6.3. Figure 6.2 characterizes the master positive film archived at NSSDC. The diffuse densities on the copy were measured on a Macbeth Model TD504 densitometer, and are plotted against a specular measurement of the wedge itself, as measured on the NRL precision Grant microdensitometer. Both specular and diffuse step densities of the wedge are given in Table 6.3. The specular reference was used in order to relate to the various phenomena studied on the flight film by the NRL data analysis team. Since most data of value fall between about 0.10 and 0.80 specular density units on the flight film (see Section VII), a copy of the data was deemed useful when the transfer curve was straight in that density range. As shown in Fig. 6.3, a good curve was also maintained for the user's generations of film, with D_{max} (diffuse) of 1.6 for the User's Positive and 1.8 for the User's Negative. D_{min} values for the Positives and Negatives are 0.12 and 0.10, respectively.

Image degradation from the copy process was evaluated by making enlargements from each copy generation and the flight film. Prints were made from selected wavelength regions onto Kodak Polycontrast RC paper without filtration. Exposures were adjusted slightly to achieve approximately equal densities from each copy. No image degradation was apparent, and the acutance and resolution of the copy material were significantly improved, compared with the conventional enlargements from the original plates. The effect is similar to that obtained using enhancement techniques with the LogEtronic instrument and probably resulted from the use of a highly specular light source in the enlarger. Contrast was also improved by minimizing both internal and external stray light.

To obtain the high quality results in the duplication of the flight film it was necessary to develop photographic equipment for the purpose. This equipment, the duplicating film, and the processing conformed to criteria established to obtain optimum resolution, moderate grain compression on the copy film, and the retention of the full density range of the data. In the enlarger, a 600W quartz lamp was used to obtain maximum resolution, acutance, and image contrast. This point light source was adjusted in position to minimize color fringing and parallax and to achieve best uniformity of illumination. The latter adjustment was checked photometrically and was found to be within $\pm$ 6% over the entire film plane. The lens was selected to minimize distortions and curvature of field. Alignment of the system was achieved with of a helium-neon autocollimating laser, using three-point control at the lens board and at the carrier for the film magazine. A vacuum back was used to hold the film flat at the enlarging surface.

The film was stored at 55° F until 24 hours prior to exposure, and was refrigerated after exposure until time to be processed. These pre-precautions were taken to minimize latent image loss and fogging of the film.

Film Overlay

A three-section overlay is provided in Appendix E. It is scaled to the NSSDC User's copies and identifies prominent spectral lines and wavelengths. The copies are correctly viewed when the plate numbers can be read properly. The film emulsion will be down. One section of the overlay is to be used with the short wavelength exposures, where the 304 Å, He II image is the most conspicious feature. The long wavelength overlay is in 2 sections, which overlap at the 465 Å, Ne VII image. A portion of the 304 Å image also can be readily identified at the short wavelength end.

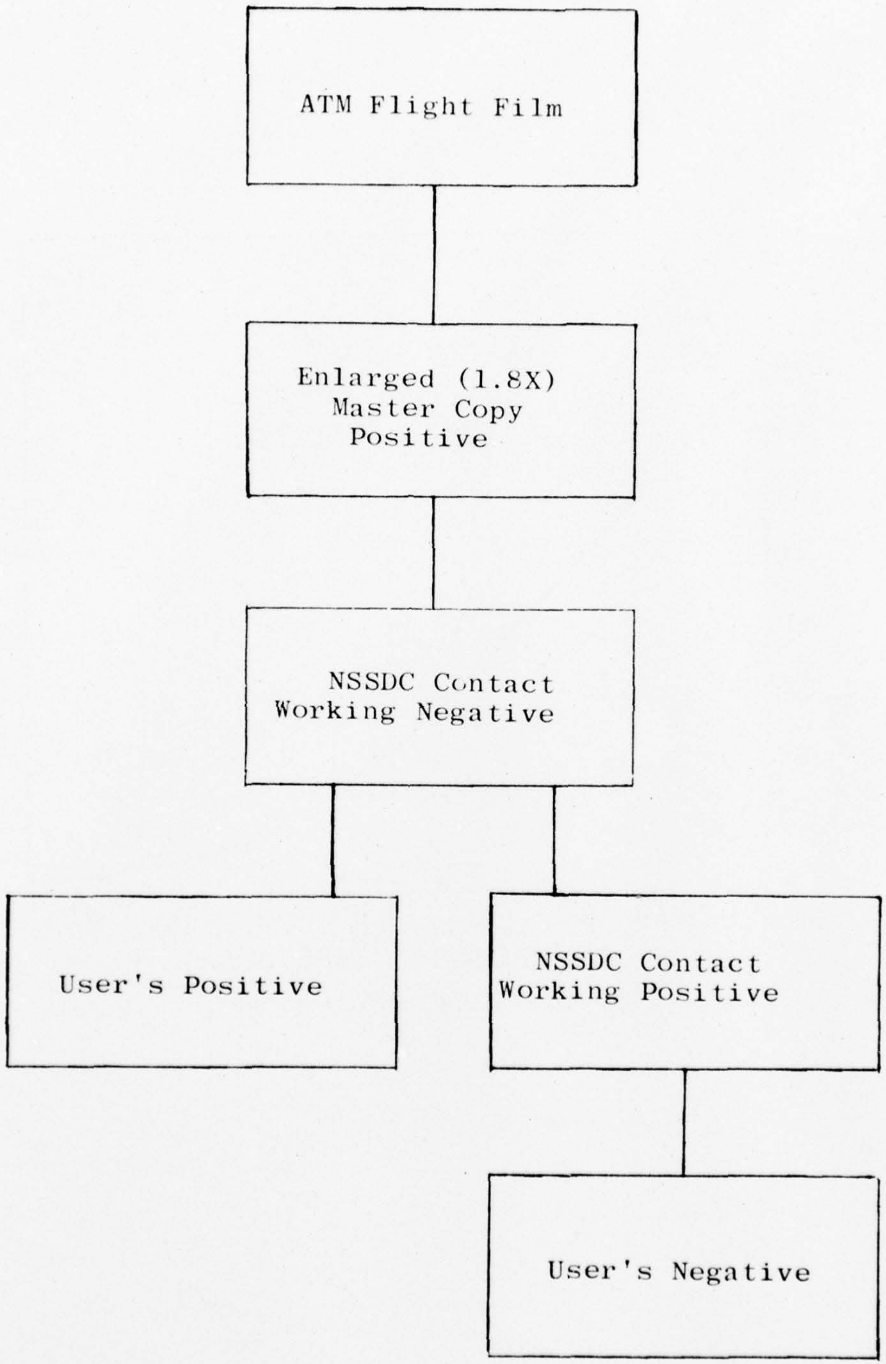

Fig. 6.1 — Duplication process for NRL/ATM photographic data

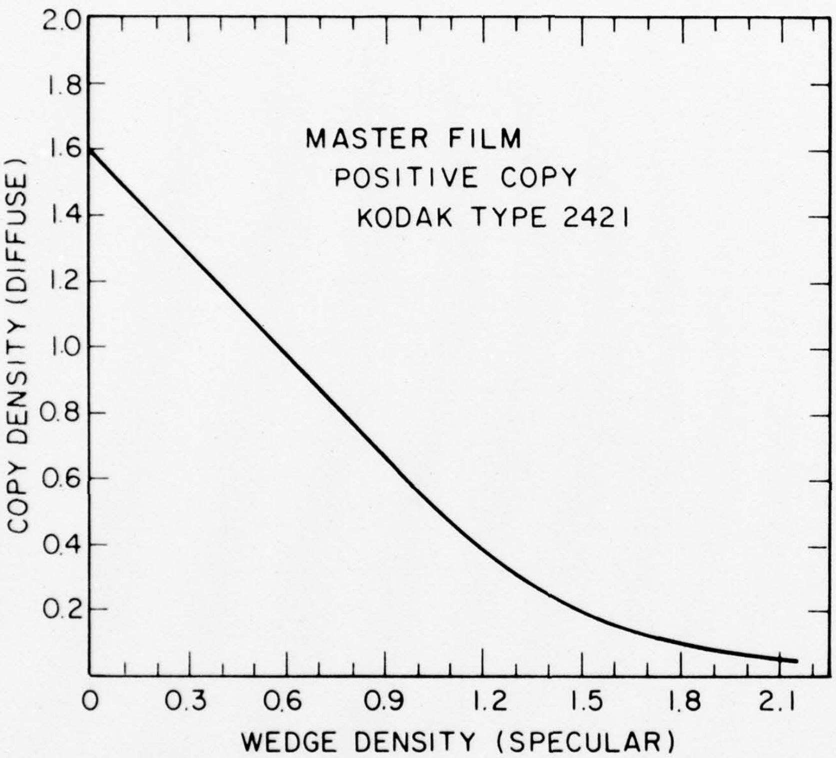

Fig. 6.2 — NSSDC archived master

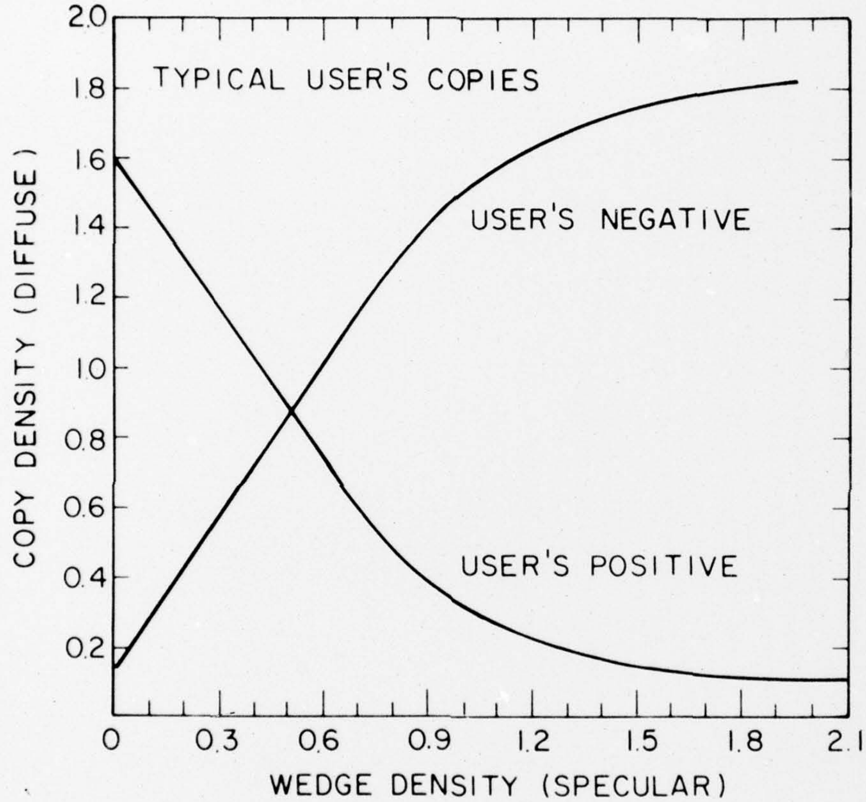

Fig. 6.3 — Transfer curves

Table 6.1 - IDENTIFICATION OF WEDGES FILMED WITH GROUPS OF PLATES

SL	PLATE NO'S.	ROLL NO.	WEDGE LOCATION	SPLICED FRAMES *
1/2	1A001-021	3	<1A001	1A009, 019
	1A201-250	3	<1A201, >1A250	1A217, 226
	1A251-300	4	<1A251	1A263, 282, 285, 286
	1A301-350	4	<1A301, >1A350	1A301, 306, 308, 315, 323
	1A351-375	5	<1A351, >1A375	1A367
	1A376-402	5	<1A376	1A382
3	2A001-015	5	<1A376, >2A015	
	2A016-050	5	<2A016, >2A050	2A022
	2A051-100	6	<2A051	2A054, 084, 085, 087
	2A101-150	6	<2A101, >2A150	2A102, 116, 120, 128
	2A151-202	6	<2A151, >2A202	2A165, 168, 172, 175, 185, 189
	2A301-350	7	<2A301	2A313, 315, 327, 342, 348
	2A351-400	7	<2A351	2A378
	2A401-450	7	<2A401	2A402, 418, 429
	2A451-500	11	<2A451	
	2A500-503	7	>2A503	
4	3A001-050	10	<3A001, >3A050	
	3A051-100	10	<3A051	
	3A101-150	11	<3A101	3A110
	3A151-202	9	<3A151	3A163, 164, 181
	3A301-350	9	<3A151, >3A350	
	3A351-400	11	<3A351	
	3A401-450	9	>3A450	
	3A451-502	10	<3A451	

* Use wedge just before plate 2A451 for all spliced frames (Roll 11)
< Exposure just prior to XAXXX plate
> Exposure just after XAXXX plate

Table 6.2 Sample Sheet of Film Catalog

FILM NR	DATE	DOY	SHUTTER OPEN	CLOSE	EXP TIME	WAVELENGTH
3A351	JAN 10.74	10	14H 45M 15.00S	46M 34.00S	79.00S	LONG
3A352	JAN 10.74	10	19H 25M 31.75S	25M 51.25S	19.50S	SHORT
3A353	JAN 10.74	10	22H 23M 49.50S	24M 48.75S	59.25S	LONG
3A354	JAN 10.74	10	22H 25M 1.00S	25M 19.75S	18.75S	SHORT
3A355	JAN 11.74	11	13H 57M 28.75S	58M 28.25S	59.50S	LONG
3A356	JAN 11.74	11	13H 59M 5.75S	59M 25.25S	19.50S	SHORT
3A357	JAN 11.74	11	16H 16M 42.75S	17M 1.75S	19.00S	SHORT
3A358	JAN 11.74	11	20H 26M 8.00S	26M 27.75S	19.75S	SHORT
3A359	JAN 12.74	12	0H 49M 34.25S	50M 33.25S	59.00S	LONG
3A360	JAN 12.74	12	0H 50M 59.25S	51M 18.25S	19.00S	SHORT
3A361	JAN 12.74	12	19H 29M 20.75S	30M 0.25S	39.50S	SHORT
3A362	JAN 13.74	13	0H 8M 4.75S	9M 3.50S	58.75S	LONG
3A363	JAN 13.74	13	0H 10M 17.75S	10M 37.50S	19.75S	SHORT
3A364	JAN 13.74	13	14H 6M 39.75S	7M 39.00S	59.25S	LONG
3A365	JAN 13.74	13	14H 7M 51.00S	8M 10.00S	19.00S	SHORT
3A366	JAN 13.74	13	16H 20M 31.50S	20M 50.75S	19.25S	SHORT
3A367	JAN 13.74	13	20H 35M 27.50S	36M 7.50S	40.00S	SHORT
3A368	JAN 13.74	13	20H 46M 4.25S	48M 44.25S	160.00S	LONG
3A369	JAN 14.74	14	13H 25M 14.50S	26M 13.25S	58.75S	LONG
3A370	JAN 14.74	14	13H 26M 25.75S	26M 45.25S	19.50S	SHORT
3A371	JAN 15.74	15	12H 47M 24.25S	48M 23.25S	59.00S	LONG
3A372	JAN 15.74	15	12H 48M 44.50S	49M 3.25S	18.75S	SHORT
3A373	JAN 15.74	15	13H 17M 53.50S	18M 52.25S	58.75S	LONG
3A374	JAN 15.74	15	13H 19M 1.50S	19M 20.25S	18.75S	SHORT
3A375	JAN 15.74	15	14H 25M 25.75S	27M 16.50S	110.75S	SHORT
3A376	JAN 15.74	15	14H 28M 28.50S	28M 48.00S	19.50S	SHORT
3A377	JAN 15.74	15	22H 19M 9.75S	19M 18.75S	9.00S	SHORT
3A378	JAN 15.74	15	22H 19M 28.25S	19M 47.75S	19.50S	SHORT
3A379	JAN 15.74	15	22H 19M 55.25S	20M 34.75S	39.50S	SHORT
3A380	JAN 15.74	15	22H 21M 6.50S	21M 35.75S	29.25S	LONG
3A381	JAN 15.74	15	22H 21M 51.50S	22M 50.75S	59.25S	LONG
3A382	JAN 15.74	15	22H 23M 5.00S	25M 4.75S	119.75S	LONG
3A383	JAN 16.74	16	12H 7M 23.50S	8M 23.00S	59.50S	LONG
3A384	JAN 16.74	16	12H 8M 39.75S	8M 59.00S	19.25S	SHORT
3A385	JAN 17.74	17	14H 34M 40.50S	35M 40.00S	59.50S	LONG
3A386	JAN 17.74	17	14H 36M 4.50S	36M 24.00S	19.50S	SHORT
3A387	JAN 17.74	17	19H 44M 20.00S	44M 59.00S	39.00S	SHORT
3A388	JAN 17.74	17	19H 45M 27.75S	48M 7.00S	159.25S	LONG
3A389	JAN 17.74	17	19H 58M 15.00S	58M 54.00S	39.00S	SHORT
3A390	JAN 17.74	17	20H 10M 39.50S	11M 19.00S	39.50S	SHORT
3A391	JAN 17.74	17	20H 46M 17.25S	47M 36.00S	78.75S	SHORT
3A392	JAN 18.74	18	14H 5M 30.75S	6M 29.50S	58.75S	LONG
3A393	JAN 18.74	18	14H 6M 59.00S	7M 17.50S	18.50S	SHORT
3A394	JAN 18.74	18	18H 52M 27.25S	52M 46.75S	19.50S	SHORT
3A395	JAN 18.74	18	18H 53M 33.00S	56M 11.75S	158.75S	SHORT
3A396	JAN 19.74	19	11H 43M 41.50S	44M 40.25S	58.75S	LONG
3A397	JAN 19.74	19	11H 46M 2.75S	46M 22.25S	19.50S	SHORT
3A398	JAN 19.74	19	13H 24M 13.75S	24M 33.00S	19.25S	SHORT
3A399	JAN 19.74	19	14H 55M 11.75S	56M 10.75S	59.00S	LONG
3A400	JAN 19.74	19	16H 29M 35.00S	29M 54.50S	19.50S	SHORT

Table 6.3

STEP DENSITIES OF KODAK CALIBRATED WEDGE

Step	Density	
	Specular*	Diffuse+
1	.135	.12
2	.275	.22
3	.400	.32
4	.535	.42
5	.660	.51
6	.795	.61
7	.935	.71
8	1.06	.81
9	1.19	.91
10	1.32	1.00
11	1.44	1.10
12	1.58	1.20
13	1.72	1.30
14	1.84	1.39
15	1.99	1.50
16	2.09	1.58
17	2.21	1.68
18	2.35	1.78

* Measured with Grant Microdensitometer
(above clear film step)

+ Kodak Calibration

VII. INTENSITY CALIBRATION OF NRL/S082A Data

The quantitative study of any solar data such as the NRL/S082A spectroheliograph films requires some form of intensity calibration; that is, the derivation of the relationship between the measurable photographic density or degree of blackening on the film and the intensity of the source of illumnination. For many purposes a relative intensity calibration will suffice, whereas in other cases an absolute intensity calibration in terms of flux received from the sun (in photons-cm^{-2}-sec^{-1}), or specific solar intensity (ergs-cm^{-2}-sec^{-1}-steradian^{-1}) is required. In studies using the original spectroheliograms these procedures are relatively straightforward and well-known, although very often difficult to execute. In using photographic copies (negatives or positives) of the original NRL S082A materials, such as the multiple-generation user copies received from NSSDC, any difficulties of extracting an intensity calibration for the original solar source may be compounded, for the quality of the results depends upon the quality control of the photographic duplication processes as well as the user's ability to derive a transfer characteristic between the original material and the user's copies.

This section will discuss the relative intensity calibration of both the original NRL/S082A spectroheliograms and typical NSSDC user's copies (including an example of the derivation of the needed transfer characteristic between the user's copies and the original material), and a summary of the general procedure for the relative intensity calibration of user's negatives (or positives). Some comments are also given on the absolute intensity calibration of the NRL/ S082A spectroheliograms.

Relative Intensity Calibration

A. Original NRL/S082A Spectroheliograms

An example of the typical relative intensity calibration of the NRL/S082A original spectroheliograms is displayed in the H-D curves in Fig. 7.1, for both the short wavelength (Sλ) and the long wavelength (Lλ) regions. The figure is a plot of the specular density above the fog level measured with the NRL Grant microdensitometer vs. the common logarithm of the relative solar intensity. The Sλ curve was derived from the solar images at the wavelengths of the Lyman-alpha and Lyman-beta type transitions of singly ionized helium, He II 304 Å and 256 Å, respectively, on three closely spaced plates of different exposure times (3A377-3A379), taken January 15, 1974. Similarly, the Lλ curve was derived from the solar images produced by He I 584Å and the less intense second line in the series, 537Å, again on three closely spaced plates of different exposure times (3A380-3A382) taken on the same date (see NRL/S082A Diode Array Data Listing, Supplement A).

At each of the four wavelengths an H-D intensity calibration curve was derived from a microdensitometer scan across the solar disk image through sun center and in a direction perpendicular to the dispersion. This was done for each of the three different exposure lengths. This scan direction was selected to minimize the effects of overlapping of other wavelength solar images. Each of the three scans across the sun recorded densities for many solar features which covered a wide range of intensities. It was important to match precisely the scans of the three different exposures; this was done by shifting the microdensitometer traces until corresponding features on the solar disk were in coincidence.

Thus a set of three points on the H-D curve was determined for each solar feature from the three exposures; some 1000 sets of points were derived from a single scan of each of the three exposures. The resulting 1000 groups of three points on the H-D curve were shifted along the scale of log (relative exposure) in a least squares fashion to obtain one continuous calibration curve at that wavelength. The RMS deviation of the data points with respect to a least squares curve was typically in the range 10-15% in intensity. The curves for 584Å and 537Å were nearly identical and were combined into the single curve in Fig. 7.1 whose abscissa is really a relative exposure. Similarly, for the Sλ region, the curves for 304Å and 256Å were of the same shape and were combined. The Sλ and Lλ curves have been separated by an arbitrary amount in order to avoid confusion. The data from which the curves were plotted are tabulated for the two wavelengths in Tables 7.1 and 7.2. Note, however, that these curves represent the reponse of ONLY the specific emulsion batch of the filmstrips involved (batch 7).

The user should note that the curves for the two wavelength regions show a different contrast value or slope of the H-D curve even though the six films used were from the same emulsion batch and the same development run. This seems to be a real wavelength effect which is is not completely understood at this time. It is recommended that the user determine an H-D curve for each wavelength of interest using films of the same emulsion batch and development run as the exposure(s) of interest.

To apply this relative intensity calibration in any study comparing solar images of different wavelengths, the user must take into account the relative wavelength response of the NRL/S082A instrument. This is shown as a function of wavelength in Figs. 7.2 through 7.7.* Each curve applies only to the plate numbers listed at the top of each figure. The instrument efficiency plotted in these figures is the product of the first-order efficiency of the grating and the percentage transmission of the aluminum filter in each of the six cameras.

* Based on measurements by William R. Hunter at NRL

B. NSSDC User's Copies

The derivation of a relative intensity calibration for the S082A solar images, using photographic copies (negatives or positives) of the original plates, depends upon the quality control of the photographic duplication process as well as the user's ability to derive a transfer characteristic between the original plates and the user's copies. It was decided to test this procedure with actual user's copies. Copy negatives of the six Sλ and Lλ plates (3A377-3A382) used for the intensity calibration discussed in part A above were requested from NSSDC. A user's copy of the appropriate step wedge was also requested. The test was conducted at NRL, using the Grant microdensitometer. An H-D curve of user's negative specular density vs. logarithm of relative exposure was generated for each of the two test wavelengths, He I 584 Å and He II 304 Å, using the three exposure technique described in part A. Figure 7.8 presents the resulting H-D curve at He I 584 Å. The RMS deviation of the data points with respect to a least squares fit corresponds to approximately $\pm 10\%$ in relative intensity. The user should note the much larger density range of the user's negatives compared to the original materials in part A. Similar results were obtained for the Sλ region at He II 304 Å.

The next step in the procedure was to obtain a transfer characteristic between the user's negatives and the original negatives. The transfer characteristic is derived from a comparison of the specular densities of the NRL step wedge and the densities of the user's copy of the step wedge, measured by the user. For the purposes of this test the user's copy of the step wedge was measured with the NRL Grant microdensitometer. In order for a user to effect the transfer he must measure his copy of the step wedge with the same microdensitometer that he plans to use in the measurement of his copies of the plates. The original NRL step wedge was a Kodak step wedge with 21 individual light steps and a relatively larger clear film step at one end of the wedge. The specular densities above clear film of the original wedge are presented in Section VI. Plotting the specular densities above the clear film step of the user's wedge against the specular densities above clear film of the original wedge produced the density transfer curve in Fig. 7.9.

The application of the density transfer curve to the user's negative H-D curve in each wavelength range should independently reproduce the original H-D curve or actual relative intensity calibration. Fig. 7.10 portrays the results for the original H-D curve derived from the user's negatives in both wavelength regions. The open and closed circles represent the values of density derived by a least squares curve derived from the user's negatives at He II 304 Å and He I 584 Å respectively. Error bars reflect the RMS scatter in the data from the user's negatives.

These data, after adjustment to form the best H-D curve for the user's negatives are compared with the solid curves for the original negatives, which were redrawn from Fig. 7.1. Even though there may be a slight systematic difference between the original and the "derived original" results, the agreement is considered excellent

with a mean absolute deviation of approximately 8% in relative intensity. Therefore, with the accuracy stated, the original relative distribution can be obtained from the user's copies and his derived density transfer curve.

C. Summary of the General Procedure for the Relative Intensity Calibration of User's Negatives (Positives)

1. Select S082A exposure(s) of interest from Catalog of S082A Exposures, Appendix D.

   a. Note time and date of exposure(s) using Appendix D.

   b. Note the camera, emulsion batch and development run of the exposure(s) of interest, Appendix C.

2. Select S082A exposures for the generation of an H-D calibration curve. Search the Catalog of S082A Exposures for a series of at least 2 or, preferably, 3 different exposure times that are closely spaced in time (an interval less than about 30 min) for the wavelength region. Select exposures of the same emulsion batch and development run as that of the exposure(s) of interest in step 1. above from Appendix C.

3. Generate an H-D curve for user's negatives (or positives) using the series of images selected in step 2 above. Ideally, a separate H-D curve should be derived for each wavelength. Recommended procedure: select the same position on the solar disk on each of the selected user's negatives (or positives) and plot density above fog vs. log (Relative Exposure); repeat this procedure for a sufficient number of points on the solar disk to generate a single H-D curve for each wavelength.

4. Generate a density transfer curve using measurements of the photographic step wedge using the same microdensitometer as in step 3.

   a. Select the photographic step wedge on the user's negative (or positive) appropriate for the exposure(s) of interest (See Table 6.1 - Identification of Wedges Filmed with Groups of Plates).

   b. Measure the density above the clear film step of each step of the wedge(s) on the user's negative (positive).

   c. Generate a density transfer curve using the measured densities above the clear film step of the wedge on the user's material vs. the specular densities above clear film on the original step wedge provided in Table 6.3 which were measured at NRL using a Grant microdensitometer.

5. Generate a derived H-D curve for each wavelength by applying the density transfer characteristic from step 4. to the user's H-D curve determined in step 3. The abscissa of this curve is now the log (Relative Intensity) on the original S082A negatives.

6. Relative intensity calibration of the images of interest - in order to derive relative intensities of the exposure(s) of interest on the user's negative (positive) perform the following steps:

   a. Measure the density above fog of the solar features of interest on the user's negative (or positive) with the same microdensitometer used in steps 4. and 5.

   b. For each user's density, apply the density transfer curve from step 4. to determine the specular density on the original S082A negatives.

   c. Use the specular density value determined in b. above to determine a relative intensity value from the H-D curve derived in step 5.

7. In applications comparing solar features at different wavelengths the user should take into account the effect of the S082A instrument efficiency as a function of wavelength presented in Figs. 7.2 through 7.7.

If a user desires to measure several exposures on the user's negative (positive) spread throughout the Skylab mission(s), the generation of a Density Transfer Curve from a single step wedge may be sufficient, with exception of data copied on roll 9 (See Section VI). This statement is based on measurements at NRL of the densities of all the step wedges on the master positives and negatives on file at NSSDC. These measurements indicate that, for every step on the wedge, the difference in density between any of the wedges is less than 0.1 density units (a testament to the quality control used by the NSSDC in the photographic duplication of the original NRL materials).

Absolute Intensity Calibration

The absolute intensity calibration consists of three major parts: (i) Determination of the absolute intensity response of a small-scale version (CALROC) of the S082A instrument using the continuous spectrum from the NBS synchrotron as a standard laboratory source: (ii) Calibration of the solar images from the same rocket-borne CALROC instrument flown during each Skylab mission using results from step (i); and (iii) Transfer of the absolute intensities from the CALROC images to the ATM S082A solar images exposed at the same time. In essence there are two transfers, CALROC-Synchrotron to CALROC-Sun and CALROC-Sun to S082A-Sun.

Since the end of the Skylab missions a large effort has been made at NRL to execute this absolute intensity calibration program. An NRL report on this subject is in preparation. Users having a need for absolute intensity calibration may contact Dr. Stephen A. Mango, c/o Code 7149M, Naval Research Laboratory, Washington, D. C. 20375.

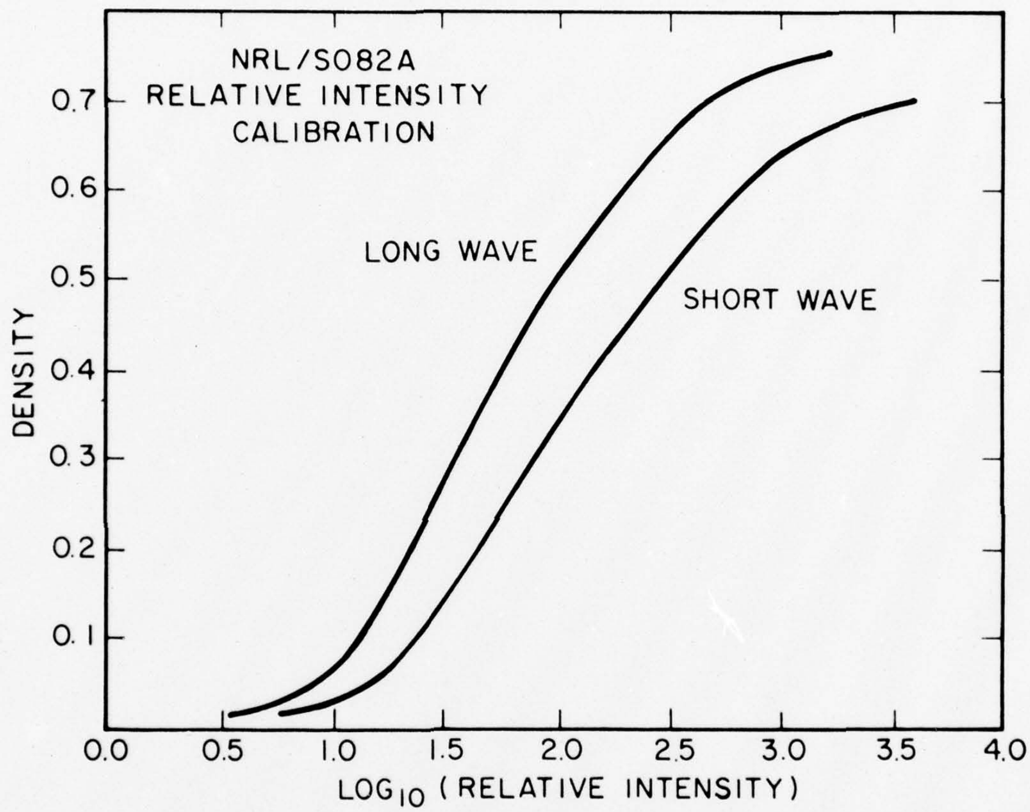
NRL/S082A
RELATIVE INTENSITY
CALIBRATION
LONG WAVE
SHORT WAVE
DENSITY
0.1
0.2
0.3
0.4
0.5
0.6
0.7
0.0
0.5
1.0
1.5
2.0
2.5
3.0
3.5
4.0
LOG10 (RELATIVE INTENSITY)

Fig. 7.1

S082A FIRST ORDER INSTRUMENT EFFICIENCY
FOR FILMS 1A001-1A019

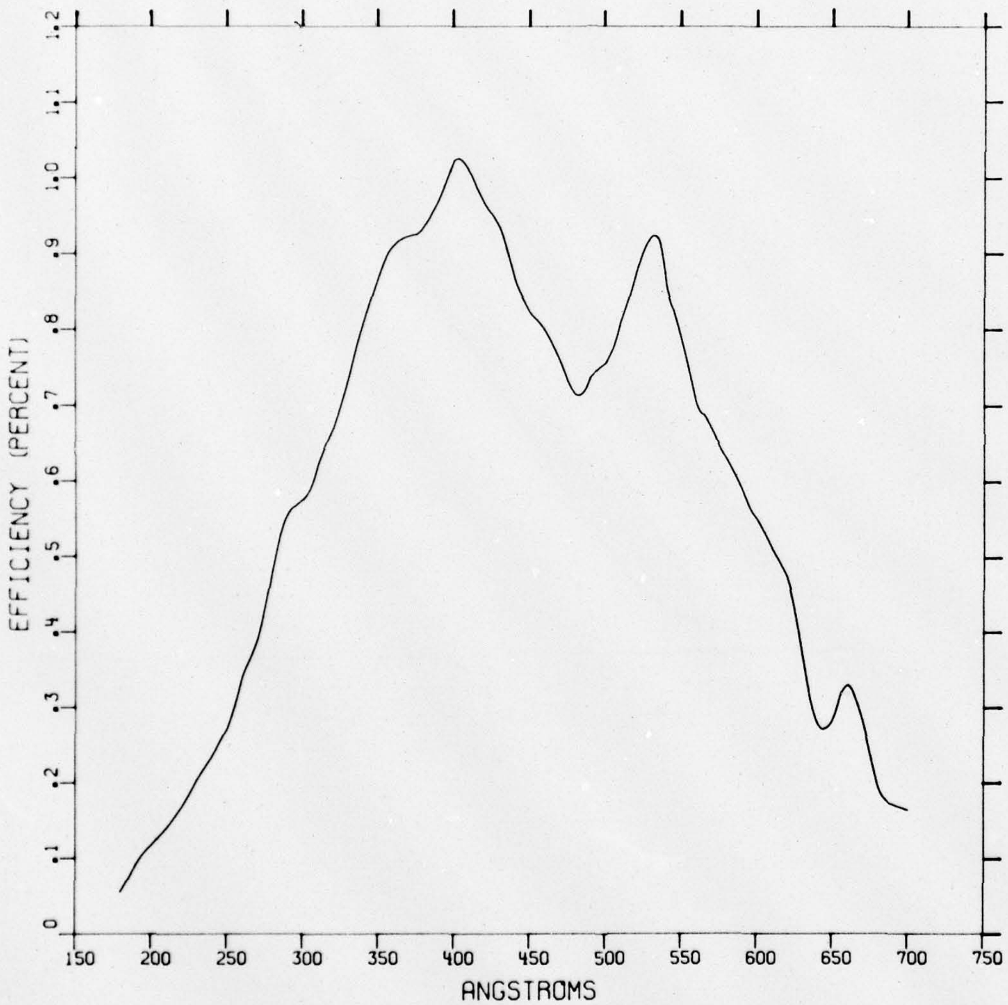

Fig. 7.2

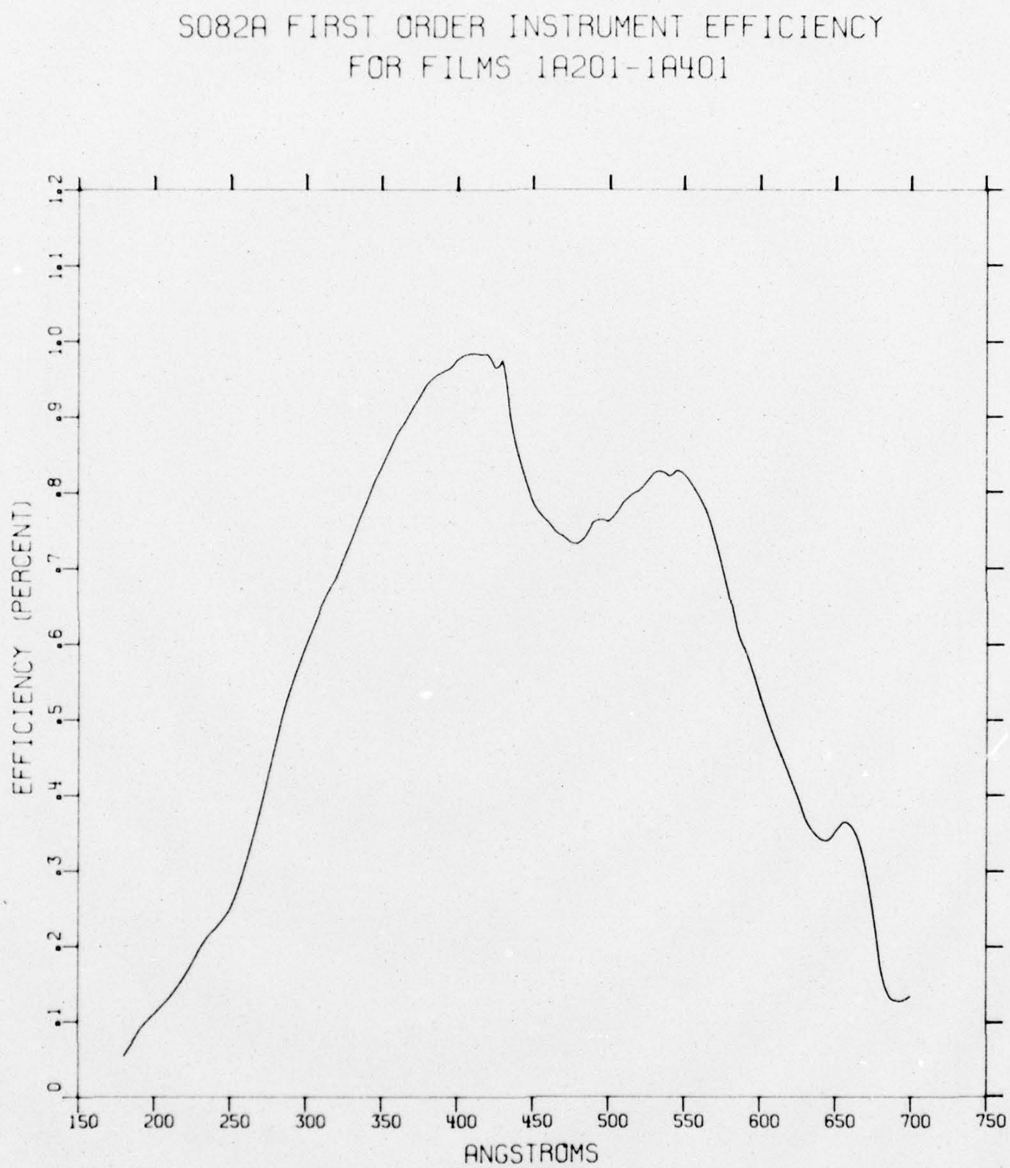

S082A FIRST ORDER INSTRUMENT EFFICIENCY
FOR FILMS 1A201-1A401
EFFICIENCY (PERCENT)
0
.1
.2
.3
.4
.5
.6
.7
.8
.9
1.0
1.1
1.2
150
200
250
300
350
400
450
500
550
600
650
700
750
ANGSTROMS

Fig. 7.3

S082A FIRST ORDER INSTRUMENT EFFICIENCY
FOR FILMS 2A001-2A201

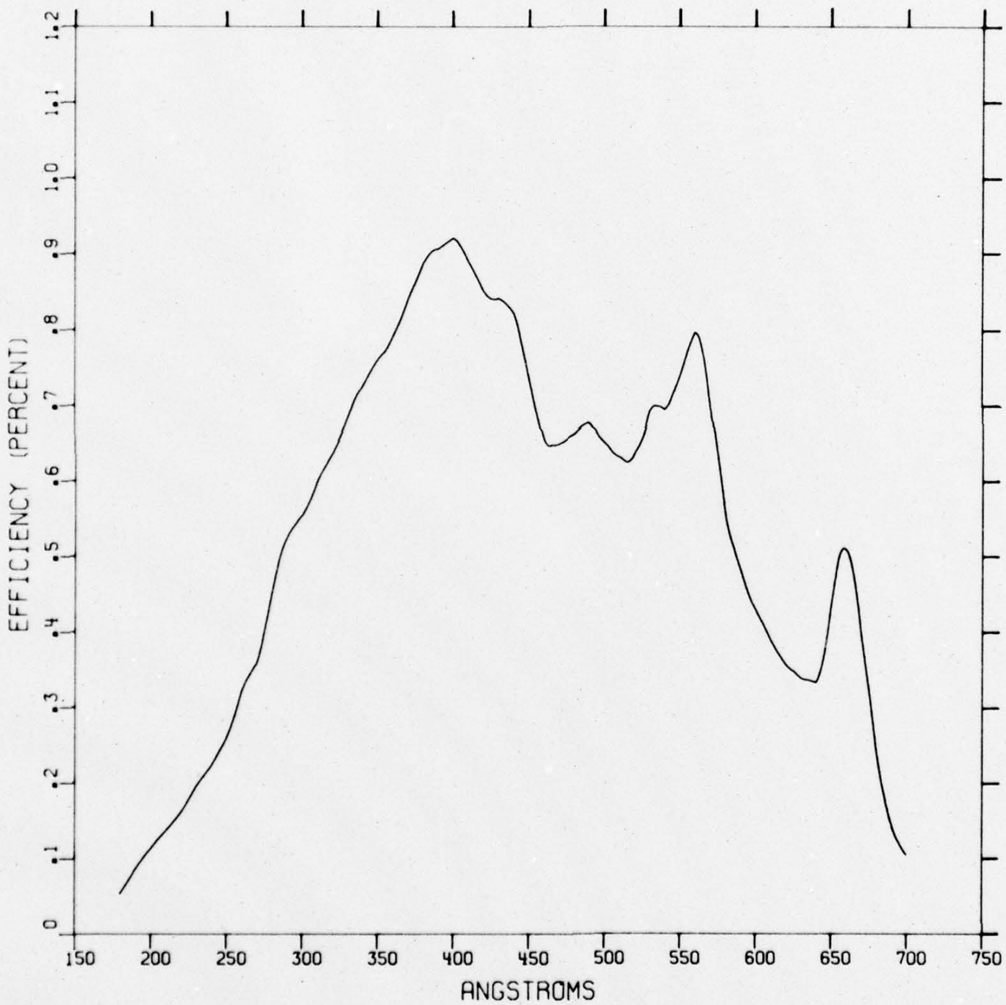

Fig. 7.4

S082A FIRST ORDER INSTRUMENT EFFICIENCY
FOR FILMS 2A301-2A501

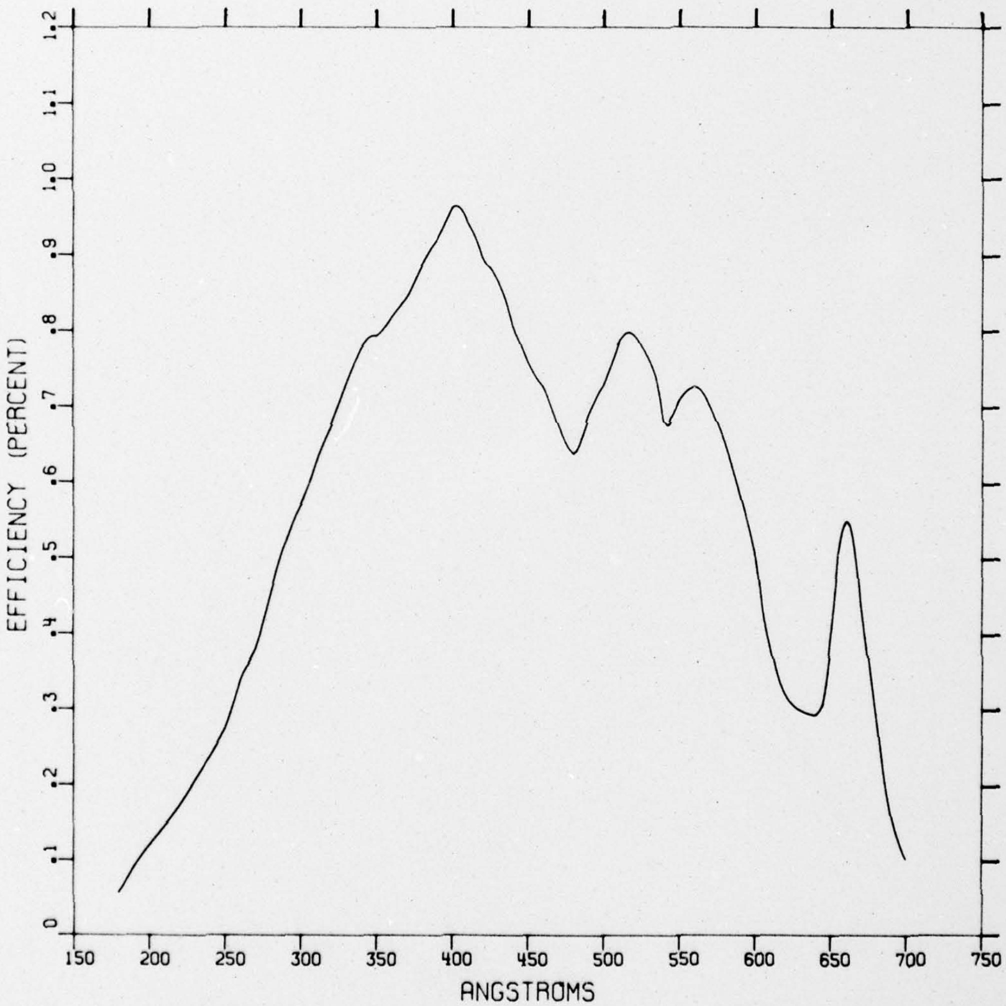

Fig. 7.5

S082A FIRST ORDER INSTRUMENT EFFICIENCY
FOR FILMS 3A001-3A201

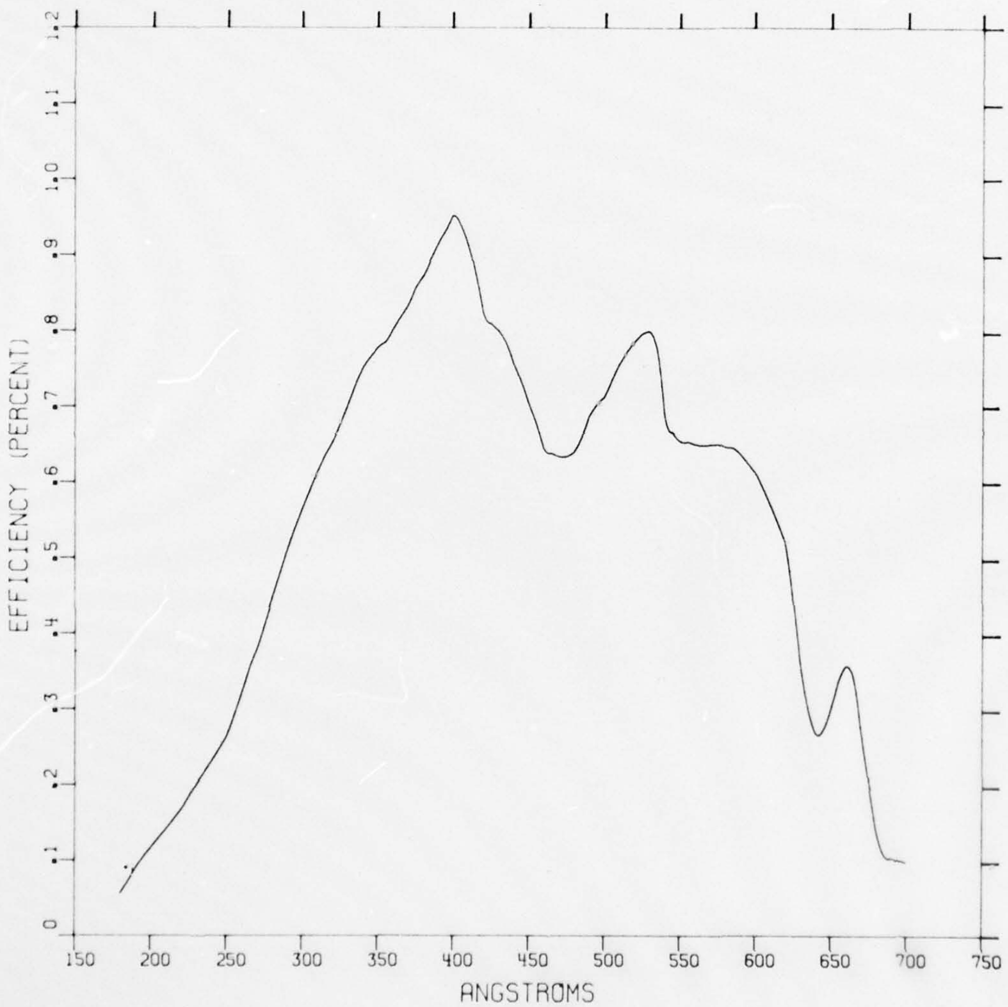

Fig. 7.6

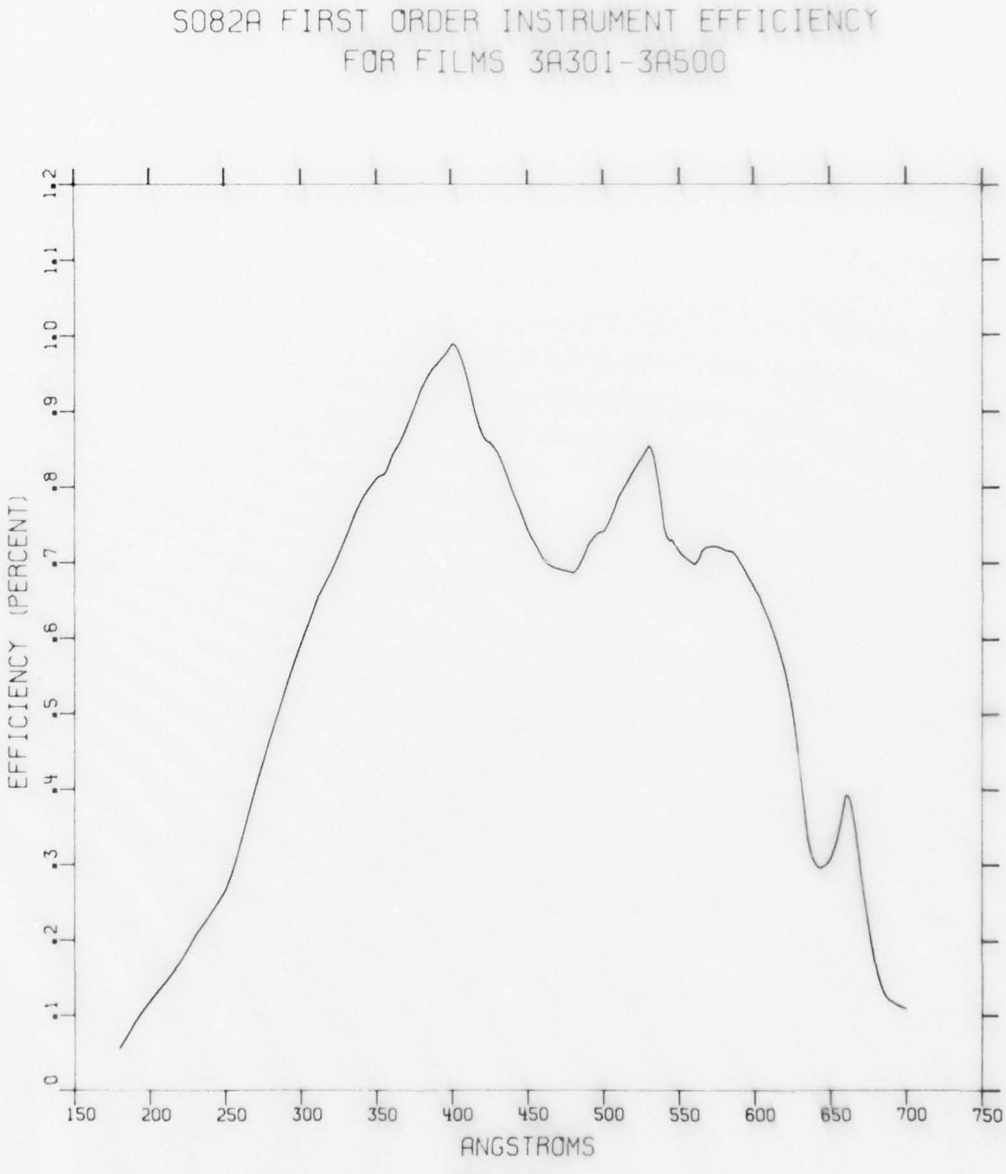
S082A FIRST ORDER INSTRUMENT EFFICIENCY
FOR FILMS 3A301-3A500
EFFICIENCY (PERCENT)
ANGSTROMS
0
.1
.2
.3
.4
.5
.6
.7
.8
.9
1.0
1.1
1.2
150
200
250
300
350
400
450
500
550
600
650
700
750

Fig. 7.7

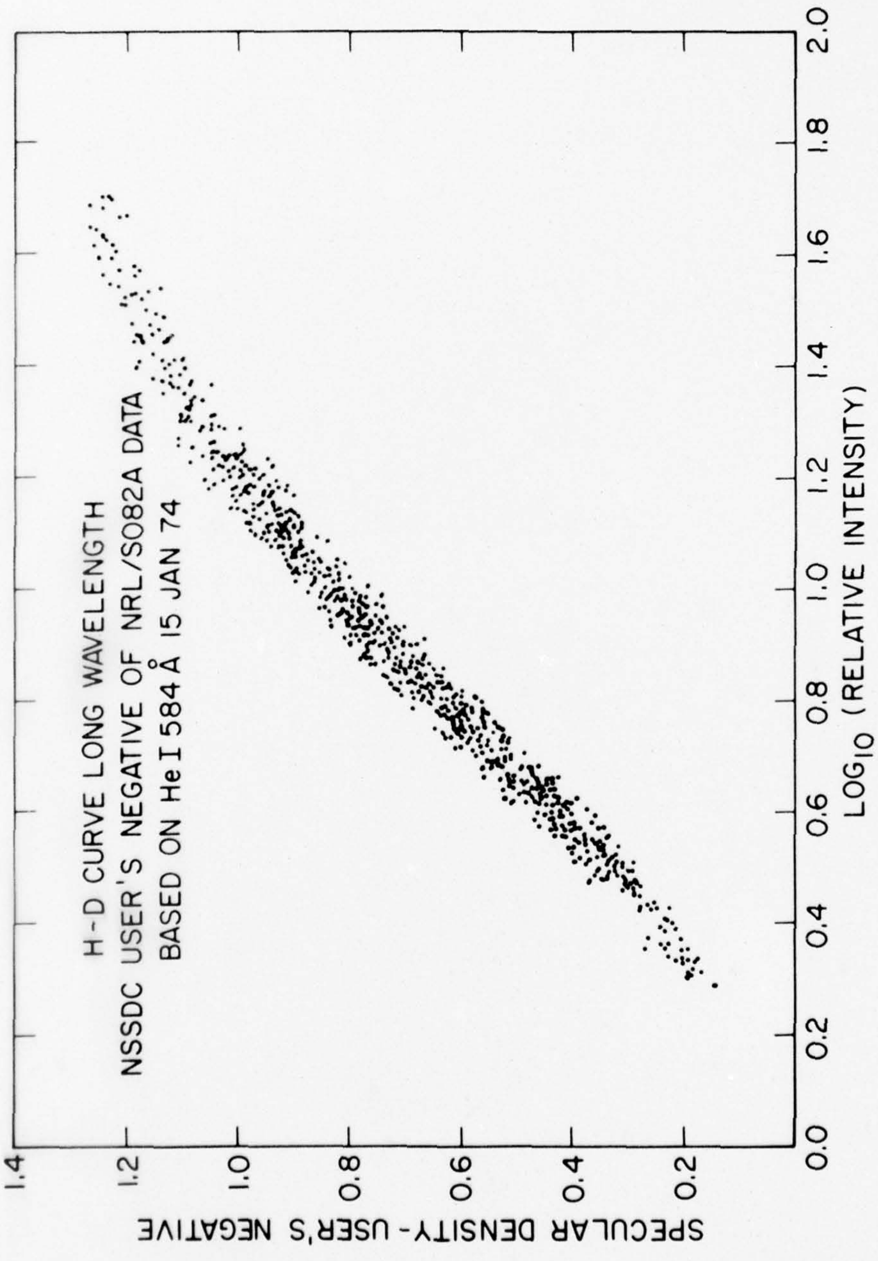

H-D CURVE LONG WAVELENGTH
NSSDC USER'S NEGATIVE OF NRL/S082A DATA
BASED ON He I 584 Å 15 JAN 74
SPECULAR DENSITY - USER'S NEGATIVE
1.4
1.2
1.0
0.8
0.6
0.4
0.2
0.0
0.2
0.4
0.6
0.8
1.0
1.2
1.4
1.6
1.8
2.0
LOG10 (RELATIVE INTENSITY)

Fig. 7.8

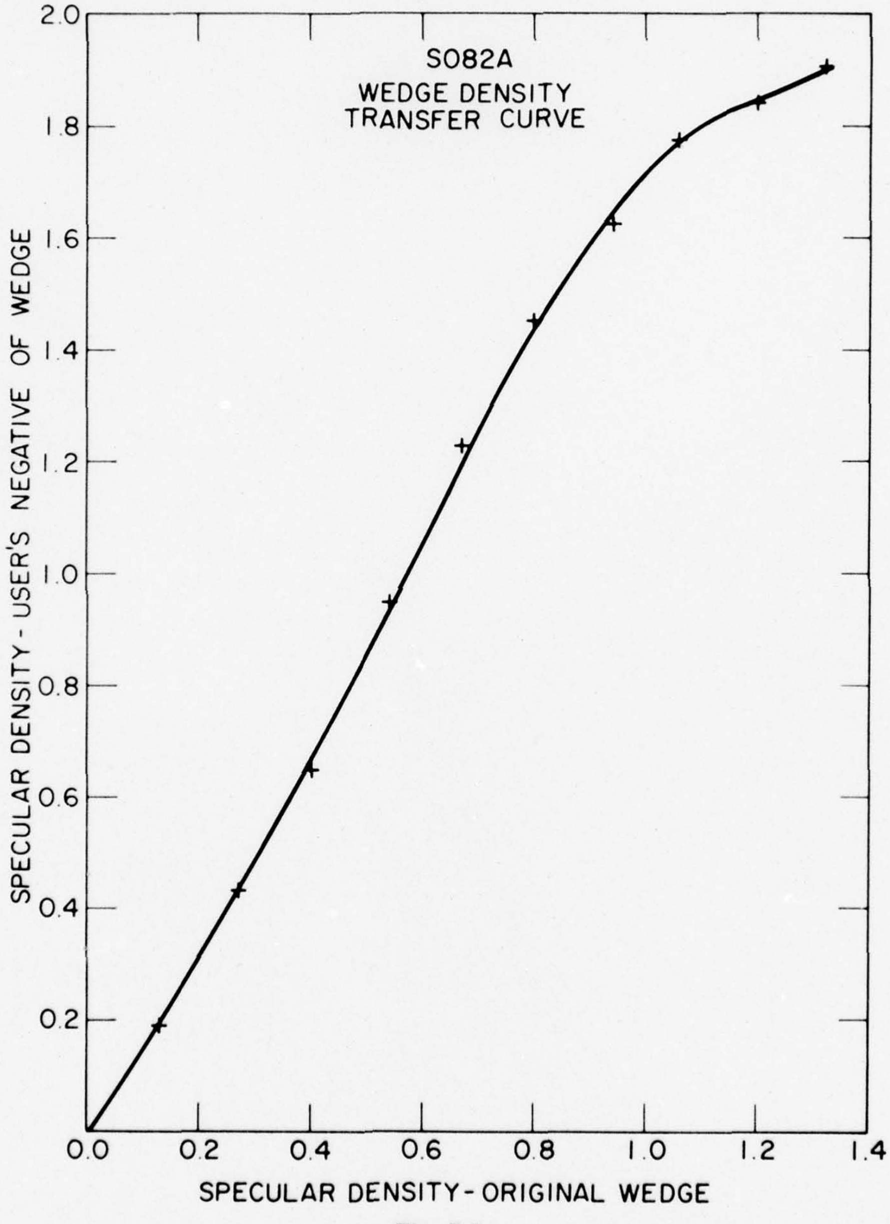

S082A
WEDGE DENSITY
TRANSFER CURVE
2.0
1.8
1.6
1.4
1.2
1.0
0.8
0.6
0.4
0.2
0.0
0.2
0.4
0.6
0.8
1.0
1.2
1.4
SPECULAR DENSITY - USER'S NEGATIVE OF WEDGE
SPECULAR DENSITY - ORIGINAL WEDGE

Fig. 7.9

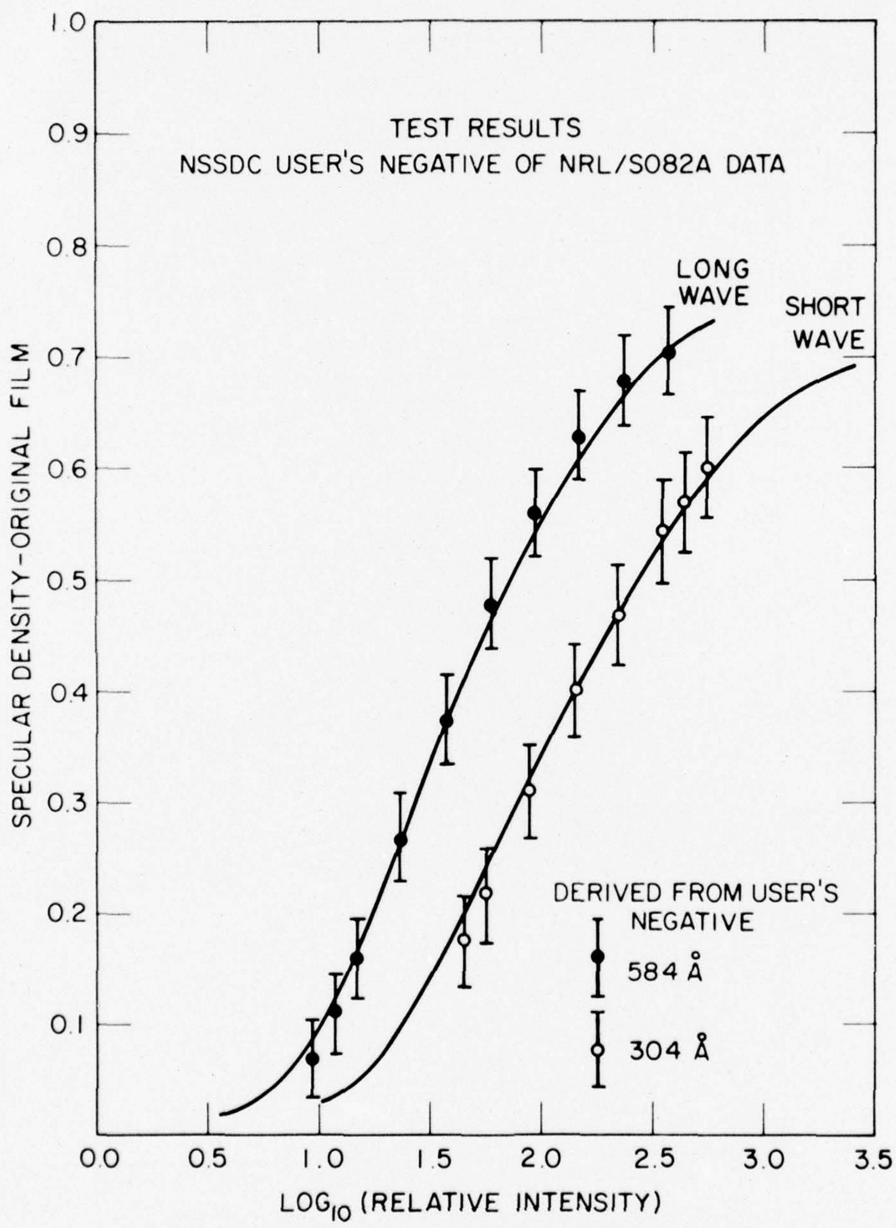

TEST RESULTS
NSSDC USER'S NEGATIVE OF NRL/S082A DATA
LONG WAVE
SHORT WAVE
DERIVED FROM USER'S NEGATIVE
584 Å
304 Å
SPECULAR DENSITY-ORIGINAL FILM
LOG10 (RELATIVE INTENSITY)
1.0
0.9
0.8
0.7
0.6
0.5
0.4
0.3
0.2
0.1
0.0
0.5
1.0
1.5
2.0
2.5
3.0
3.5

Fig. 7.10

Table 7.1

NRL/S082A

Relative Intensity Calibration for Emulsion Batch 7 Only
Long Wavelength Region from Plates 3A380-3A382
(Based on He I 584 Å and He I 537 Å Data)

Density	$Log_{10}(I_{rel})$	Density	$Log_{10}(I_{rel})$
0.02	-0.940	0.38	+0.089
0.03	-0.780	0.39	+0.110
0.04	-0.717	0.40	+0.131
0.05	-0.670	0.41	+0.153
0.06	-0.632	0.42	+0.175
0.07	-0.596	0.43	+0.197
0.08	-0.562	0.44	+0.220
0.09	-0.529	0.45	+0.244
0.10	-0.501	0.46	+0.269
0.11	-0.472	0.47	+0.295
0.12	-0.447	0.48	+0.320
0.13	-0.413	0.49	+0.347
0.14	-0.394	0.50	+0.374
0.15	-0.372	0.51	+0.401
0.16	-0.349	0.52	+0.429
0.17	-0.327	0.53	+0.456
0.18	-0.305	0.54	+0.484
0.19	-0.282	0.55	+0.512
0.20	-0.260	0.56	+0.541
0.21	-0.240	0.57	+0.571
0.22	-0.218	0.58	+0.601
0.23	-0.199	0.59	+0.632
0.24	-0.179	0.60	+0.662
0.25	-0.159	0.61	+0.694
0.26	-0.139	0.62	+0.727
0.27	-0.120	0.63	+0.762
0.28	-0.100	0.64	+0.796
0.29	-0.082	0.65	+0.831
0.30	-0.063	0.66	+0.870
0.31	-0.045	0.67	+0.910
0.32	-0.026	0.68	+0.953
0.33	-0.010	0.69	+0.997
0.34	+0.008	0.70	+1.043
0.35	+0.030	0.71	+1.100
0.36	+0.049	0.72	+1.163
0.37	+0.069	0.73	+1.270

Density = Specular Density Above Background Fog Level

Table 7.2

NRL/S082A

Relative Intensity Calibration for Emulsion Batch 7 Only
Short Wavelength Region from Plates 3A377-3A379
(Based on He II 304 Å & He II 256 Å Data)

Density	$Log_{10}(I_{rel})$	Density	$Log_{10}(I_{rel})$
0.03	-0.968	0.37	+0.064
0.04	-0.880	0.38	+0.091
0.05	-0.812	0.39	+0.119
0.06	-0.770	0.40	+0.147
0.07	-0.726	0.41	+0.175
0.08	-0.692	0.42	+0.204
0.09	-0.654	0.43	+0.233
0.10	-0.626	0.44	+0.262
0.11	-0.592	0.45	+0.291
0.12	-0.563	0.46	+0.320
0.13	-0.535	0.47	+0.349
0.14	-0.507	0.48	+0.375
0.15	-0.478	0.49	+0.407
0.16	-0.452	0.50	+0.440
0.17	-0.426	0.51	+0.470
0.18	-0.400	0.52	+0.505
0.19	-0.375	0.53	+0.540
0.20	-0.350	0.54	+0.572
0.21	-0.327	0.55	+0.607
0.22	-0.305	0.56	+0.643
0.23	-0.279	0.57	+0.679
0.24	-0.253	0.58	+0.715
0.25	-0.231	0.59	+0.755
0.26	-0.210	0.60	+0.795
0.27	-0.189	0.61	+0.836
0.28	-0.166	0.62	+0.882
0.29	-0.143	0.63	+0.931
0.30	-0.118	0.64	+0.980
0.31	-0.091	0.65	+1.032
0.32	-0.066	0.66	+1.095
0.33	-0.040	0.67	+1.166
0.34	-0.012	0.68	+1.262
0.35	+0.013	0.69	+1.400
0.36	+0.039		

Density = Specular Density Above Background Fog Level

Appendix A

ATM BIBLIOGRAPHY*

15 October 1976

(Commences with the initiation of the ATM Project and includes all publications and papers based on S082A and B material up to the present.)

I. Professional Publications Published or in Press

II. Professional Publications - Submitted

III. Abstracts

IV. Professional Talks - Invited

V. Professional Talks - Contributed

VI. Colloquia

VII. Other Publications

VIII. Other Talks

IX. Miscellaneous Appearances of NRL Material

* Compiled by Mrs. Margaret Williams

I. PROFESSIONAL PUBLICATIONS - PUBLISHED OR IN PRESS

1457 "Apollo Solar Experiments - Paving the Way for Advanced Space Observatories", Winter, T. C., Jr. 1969, Astronautics and Aeronautics, March, p. 64.

1481 "Observations of the Extreme Ultraviolet Solar Spectrum", Tousey, R. 1971, in 'A Discussion on Solar Studies with Special Reference to Space Observations', Phil. Trans. Roy. Soc. Lond. A 270, 59. (Invited)

1489 "Semi-Automatic Acquisition of Extreme Ultraviolet Reflectance Data for Calculating Optical Constants", Hunter, W. R. 1970, Rev. Sci. Instr. 41, 1419.

1502 "Spectral Radiance of the Carbon Arc Between 2500 Å and 1900 Å", Pitz, E. E. 1971, Appl. Opt. 10, 813.

1515 "Survey of New Solar Results", Tousey, R. 1971, in 'New Techniques in Space Astronomy', IAU Symp. 41, 223, ed. F. Labuhn and R. Lust, Reidel, Dordrecht.

1517 "High Angular Resolution Absolute Intensity of the Solar Continuum from 1400 Å to 1790 Å", Brueckner, G. E., and Moe, O. K. 1972, Space Research XII, Vol. 2, 1595, ed. S. A. Bowhill, L. D. Jaffe, and M. J. Rycroft, Akademie-Verlag, Berlin.

1518 "Solar Spectroscopy from Space Vehicles", Tousey, R. 1972, in 'Developments in Applied Spectroscopy', Vol. 10, 191, ed. A. J. Perkins, E. L. Grove, E. F. Kaelble and J. E. Westermeyer, Plenum, New York. (Invited)

1522 "High Angular Resolution Observations from Rockets: Solar XUV Observations", Tousey, R. 1972, Space Research XII, Vol. 2, 1719, ed. S. A. Bowhill, L. D. Jaffe, and M. J. Rycroft, Akademie-Verlag, Berlin. (Invited)

1529 "On the Classification of Some Highly Ionized Iron and Nickel Lines in the 200-400 Å Region of the Solar Spectrum", Widing, K. G., Sandlin, G. D., and Cowan, R. D. 1971, Astrophys. J. 169, 405.

1548 "Simultaneous Optical Monitoring of Angular and Translational Alignment", Bohlin, J. D. 1972, Appl. Opt. 11, 961.

1549 "Extreme Ultraviolet Solar Images Televised In-Flight with a Rocket-Borne SEC Vidicon System", Tousey, R. and Limansky, I. 1972, Appl. Opt. 11, 1025.

1566 "Rocket Observation of Ar XII-XVI and Ca XIV-XVIII in the XUV Spectrum of a Solar Flare", Purcell, J. D. and Widing, K. G. 1972, Astrophys. J. 176, 239.

1570 "Cleaning of Contaminated Channel Electron Multiplier Arrays", Harlow, F. E. and Hunter, W. R. 1972, Appl. Opt. 11, 2719.

1573 "Comparison of an Aluminum-Coated Phosphor Layer and a Channeltron Electron Multiplier Array as Extreme Ultraviolet-to-Visible Image Converters for Use in Space Applications", Hunter, W. R., and Harlow, F. E. 1973, Appl. Opt. 12, 968.

1579 "The Extreme-Ultraviolet Spectrum of Fe XV in a Solar Flare", Cowan, R. D. and Widing, K. G. 1973, Astrophys. J. 180, 285.

1606 "The Increase in Transmittance of Unbacked Aluminum Filters Exposed to RF and DC Discharge in Oxygen", Hunter, W. R., Steele, G. N. and Gillette, R. B. 1973, Appl. Opt. 12, 2800.

1620 "A Preliminary Study of the Extreme Ultraviolet Spectroheliograms from Skylab", Tousey, R., Bartoe, J.-D. F., Bohlin, J. D., Brueckner, G. E., Purcell, J. D., Scherrer, V. E., Sheeley, N. R., Jr., Schumacher, R. J. and Van Hoosier, M. E. 1973, Solar Phys. 33, 265.

1642 "The Extreme Ultraviolet Spectrograph", Bartoe, J.-D. F., Brueckner, G. E., Purcell, J. D., and Tousey, R. 1974, SPIE 44, 153. (Invited)

1647 "On the Fe XXIV Emission in the Solar Flare on June 15, 1973", Widing, K. G. and Cheng, C. C. 1974, Astrophys. J. Lett. 194, L111.

1650 "Structure of the Sun's Polar Cap in the Wavelengths 240-600 Å", Bohlin, J. D., Sheeley, N. R., Jr., and Tousey, R., 1975 Space Research XV, 651, ed. Akademie-Verlag, Berlin.

1652 "Preliminary Results from the NRL/ATM Instruments from Skylab 2", Tousey, R., Bartoe, J.-D. F., Bohlin, J. D., Brueckner, G. E., Purcell, J. D., Scherrer, V. E., Schumacher, R. J., Sheeley, N. R., Jr., and Van Hoosier, M. E. 1974, in 'Coronal Disturbances', p. 491, ed. G. Newkirk, Jr., Reidel, Dordrecht. (Invited)

1655 "Implications of NRL/ATM Solar Flare Observations on Flare Theories", Cheng, C. C. and Spicer, D. S. 1975, in 'Solar Gamma-, X-, and EUV Radiation', p. 423, ed. S. R. Kane, Reidel, Dordrecht.

1666 "Some Reflections on the Use of Conventional and Holographic Diffraction Gratings in the Vacuum Ultraviolet Spectral Region", Hunter, W. R. 1974, Proc. IV International Conf. on Vacuum-Ultraviolet Radiation Physics, p. 683.

1671 "Diffraction Gratings for the XUV - Conventional vs. Holographic", Hunter, W. R. 1974, Japanese J. of Spectroscopical Soc. 23, 37. (Invited)

1673 "Flare-Like Ultraviolet Spectra of Active Regions", Brueckner, G.E. 1975, in 'Solar Gamma-, X-, and EUV Radiation', 105, ed. S. R. Kane, Reidel, Dordrecht.

1675 "Ultraviolet Emission Line Profiles of Flares and Active Regions", Brueckner, G. E. 1975, in 'Solar Gamma-, X-, and EUV Radiation', 135, ed. S. R. Kane, Reidel, Dordrecht. (Invited)

1676 "The Fine Structure of the Solar Atmosphere in the Far Ultraviolet", Brueckner, G. E., and Bartoe, J.-D. F. 1974, Solar Phys. 38, 133.

1677 "Fe XXIV Emission in Solar Flares Observed with the NRL/ATM XUV Slitless Spectrograph", Widing, K. G. 1975, 'Solar Gamma-, X-, and EUV Radiation', 153, ed. S. R. Kane, Reidel, Dordrecht. (Invited)

1678 "Flares Observed by the NRL/ATM Spectrograph and Spectroheliogram During the Skylab Missions", Scherrer, V. E. and Tousey, R. 1975, Proc. International Conf. on 'X-rays in Space', Vol. II, 986, Univ. of Calgary.

1683 "Observations of the Hydrogen Ly-α (1216 Å) Emission Line of Comet Kohoutek (1973f) by the Skylab/ATM S082B Spectrograph", Keller, H. U., Bohlin, J. D., and Tousey, R. 1975, Proc. Comet Kohoutek Workshop, NASA SP-355, ed. G. A. Gary, in press. (Invited)

1684 "High Resolution Ly-α Observations of Comet Kohoutek by Skylab and Copernicus", Bohlin, J. D., Drake, J. F., Jenkins, E. B., and Keller, H. U., Proc. IAU Colloq. 25, in press.

1686 "XUV Observations of Coronal Magnetic Fields", Sheeley, N. R., Jr., Bohlin, J. D., Brueckner, G. E., Purcell, J. D., Scherrer, V. E., and Tousey, R. 1975, Solar Phys. 40, 103.

1688 "Selected Tables of Atomic Spectra; Atomic Energy Levels and Multiplet Tables; NI, NII, NIII", Moore-Sitterly, C. E. 1975, NSRDS-NBS 3, Section 5.

1687 "Observed Heights of EUV Lines Formed in the Transition Zone and Corona", Simon, G. W., Seagraves, P. H., Tousey, R., Purcell, J. D., Noyes, R. W. 1974, Solar Phys. 39, 121.

1689 "Ultraviolet Solar Identifications Based on Extended Absorption Series Observed in the Laboratory Spectra of Si I", Moore, C. E., Tousey, R., Sandlin, G. D., Brown, C. M., Ginter, M. L., and Tilford, S. G., 1975, Astrophys. and Sp. Sci., 38, 359.

1691 "Eruptive Prominences Recorded by the XUV Spectroheliograph on Skylab", Tousey, R. 1976, 'A Discussion on the Physics of the Solar Atmosphere', Phil. Trans. Roy. Soc. Lond. A 281, 359.

1692 "High Resolution Ly α Observations of Comet Kohoutek Near Perihelion", Keller, H. U., Bohlin, J. D., and Tousey, R. 1975, Astron. and Astrophys. 38, 413.

1695 "A Comparison of Spicules in the Hα and He II (304 Å) Lines", Moe, O. K., Engvold, E. and Beckers, J. 1975, Solar Phys. 40, 65.

1709 "The Reconnection of Magnetic Field Lines in the Solar Corona", Sheeley, N.R., Jr., Bohlin, J. D., Brueckner, G. E., Purcell, J. D., Scherrer, V. E., and Tousey, R. 1975, Astrophys. J. Lett. 196, L129.

1713 "Forbidden Lines of Highly Ionized Iron in Solar Flare Spectra", Doschek, G. A., Feldman, U., Dere, K. P., Sandlin, G. D., Van Hoosier, M. E., Brueckner, G. E., Purcell, J. D., and Tousey, R. 1975, Astrophys. J. Lett. 196, L83.

1715 "XUV Results from Skylab", Tousey, R. 1975, Proc. International Conf. on 'X-Rays in Space', Vol. I, 472, Univ. of Calgary. (Invited)

1716 "The XUV Sun as Observed by ATM S082", Tousey, R., Proc. of AIAA/AGU Space Science Conf. on 'Scientific Experiments of Project Skylab', in press.

1718 "Classification of Flares and Flare-Like Events Observed by the ATM XUV Spectroheliograph S082A and Spectrograph S082B During the Skylab Missions", Scherrer, V. E. and Tousey, R., Proc. of AIAA/AGU Space Science Conf. on 'Scientific Experiments of Project Skylab', in press.

1720 "The Stark Broadening Mechanism in an Unstable Plasma", Spicer, D. S. and Davis, J. 1975, Solar Phys. 43, 107.

1721 "On the Fe XXIV Emission in the Solar Flare of 1973 June 15", Widing, K. G. and Cheng, C. C. 1974, Astrophys. J. Lett. 194, L115.

1724 "Fe XXIII 263 Å and Fe XXIV 255 Å Emission in Solar Flares", Widing, K. G. 1975, Astrophys. J. Lett. 197, L133.

1727 "A Newly Observed Solar Feature: Macro-Spicules in He II 304 Å", Bohlin, J. D., Vogel, S. N., Purcell, J. D., Sheeley, N. R., Jr., Tousey, R., and Van Hoosier, M. E. 1975, Astrophys. J. Lett. 197, L133.

1729 "The 1640.4 Å Hα Line of He II Observed from Skylab", Feldman, U., Doschek, G. A., Van Hoosier, M. E., and Tousey, R. 1975, Astrophys. J. Lett. 199, L67.

1733 "XUV Emission from Above the West Limb Near 20:00 U.T., January 17, 1974", Tousey, R. 1975, Astrophys. and Sp. Sci., Vol. 38, 327.

1741 "ATM Observations of the XUV Emission from Solar Flares," Brueckner, G. E. 1976, 'A Discussion on the Physics of the Solar Atmosphere', Phil. Trans. Roy. Soc. Lond. A 281, 443.

1745 "Spatial Distribution of XUV Emission in Solar Flares", Cheng, C.C. and Widing, K. G. 1975, Astrophys. J. 201, p. 735.

1748 "The Interpretation of Ultraviolet Solar Spectra", Moore-Sitterly, C. E., Proc. Twentieth Liege International Astrophysical Symp., 1975, Mem. de la Societe Royale de Liege 9, p. 59.

1749 "Coronal Changes Associated with a Disappearing Filament," Sheeley, N. R., Jr., Bohlin, J. D., Brueckner, G. E., Purcell, J. D., Scherer, V. E., Tousey, R., Smith, J. B., Jr., Speich, D. M., Tandberg-Hanssen, E., Wilson, R. M., de Loach, A. C., Hoover, R. B., and McGuire, J. P., Solar Physics 45, p. 377.

1760 "Absolute Solar Intensities 1750 Å-2100 Å and their Variations with Solar Activity", Brueckner, G. E., Bartoe, J.-D. F., Moe, O. K., Van Hoosier, M. E. 1975, Proc. of the Workshop: The Solar Constant and the Earth's Atmosphere, p. 71. (Invited)

1762 "Selected Tables of Atomic Spectra, Atomic Energy Levels and Multiplet Tables OI", Moore-Sitterly, C. E. 1976, NSRDS-NBS 3, Sec. 7.

1765 "Limb Brightening Curves of XUV Transition Zone Lines in the Quiet Sun and in a Polar Coronal Hole Observed from Skylab", Doschek, G. A., Feldman, U. and Tousey, R. Astrophys. J. Lett. 202, L147.

1766 "The Intensities and Profiles of XUV Transition Lines in a Quiet Sun Region Compared to a Polar Coronal Hole", Feldman, U., Doschek, G. A. and Tousey, R. Astrophys. J. Lett. 202, L151.

1773 "Advances in X-Ray and EUV Spectroscopy of Solar Flares and Laboratory Plasmas", Doschek, G. A. 1975, Proc. International Conf. on 'X-Rays in Space', Vol. I, p. 306.

1783 "The Calculation of Force-Free Fields from Discrete Flux Distributions," Sheeley, N. R., Jr., and Harvey, J. W., Solar Physics 45, p. 275.

1795 "Synoptic Maps of Coronal Hole Boundaries Derived from He II 304 Å Spectroheliograms from the Manned Skylab Missions," Bohlin, J. D. and Rubenstein, D. M. 1975, World Center A for Solar-Terrestrial Physics, NOAA, Report UAG-51.

1796 "The Emission Line Spectrum Above the Limb of the Quiet Sun: 1100-1940 Angstroms," Doschek, G. A., Feldman, U., Van Hoosier, M. E. and Bartoe, J.-D. F. 1976, Astrophys. J. Supp. Series 31, 417.

1797 "The Emission Line Spectrum Above the Limb of a Solar Coronal Hole: 1100-1940 Angstroms," Feldman, U., Doscheck, G. A., Van Hoosier, M. E. and Purcell, J. D. 1976, Astrophys. J. Supp. Series 31, 445.

1799 "The Lithium-Like $2s\ ^2S-2p\ ^2P$ Transition in Solar Flares," Widing, K. G. and Purcell, J. D. 1976, Astrophys. J. Lett. 204, L151.

1800 "High Temperature Flare Lines in the Solar Spectrum 171-630Å," Sandlin, G. D., Brueckner, G. E., Tousey, R. and Scherrer, V. E. 1976, Astrophys. J. Lett. 205, L47.

1804 "Space-Resolved Spectra of Laser-Produced Plasmas in the XUV," Feldman, U., Doschek, G. A., Prinz, D. K. and Nagel, D. J. 1976, J. of Appl. Phys. 47, No. 4, 1341.

1806 "The Profile of the Solar Lyman Beta Line of Hydrogen," Nicolas, K. R., Moe, O. K., Bartoe, J.-D. F. and Tousey, R. 1976, J. of Geophys. Res. - Space Physics 81, 3465.

1807 "Effects of Plasma Microfields on Radiative Transients from Atomic Levels Above the Ionization Threshold," Davis, J. and Jacobs, V. L., Phys. Rev. A 12, 2017.

1808 "High Latitude Observations of Solar Wind Streams and Coronal Holes," Rickett, B. J., Sime, D. G., Sheeley, N. R., Jr., Crockett, W. R. and Tousey, R. 1976, J. of Geophys. Res. 81, 3845.

1810 "The Sources of Material Comprising a Mass Ejection Coronal Transient," Hildner, E., Gosling, J. T., Hansen, R. T. and Bohlin, J. D. 1975, Solar Physics 45, 363.

1812 "Doppler Wavelength Shifts of Transition Zone Lines Measured in Skylab Solar Spectra," Doscheck, G. A., Feldman, U. and Bohlin, J. D. 1976, Astrophys. J. Lett. 205, L177.

1813 "Polar Faculae During the Interval 1906-1975," Sheeley, N. R., Jr. 1976, J. of Geophys. Res. 81, 3462.

1824 "Density Sensitive Lines of Highly Ionized Iron," Doschek, G. A., Feldman, U., Davis, J. and Cowan, R. D., Phys. Rev. A 12, 980.

1826 "Transitions of Zn XXII, Zn XXIII, Zn XXIV, Ge XXIV and Ge XXV Observed in Laser-Produced Plasmas," Behring, W. E., Cohen, Leonard, Doschek, G. A., Feldman, U., J. Opt. Soc. Am. 66, 376.

1844 "The XUV Spectrum of C I Observed from Skylab During a Solar Flare," Feldman, U., Brown, C. M., Doschek, G. A. Moore, C. E. and Rosenberg, F. D. 1976, J. Opt. Soc. Am. 66, 853.

1851 "The Quiet Sun Chromospheric Network Observed from Skylab," Feldman, U., Doschek, G. A. and Patterson, N. P. 1976, Astrophys. J. 209, 270.

II. PROFESSIONAL PUBLICATIONS - SUBMITTED

1789 "Energy Released by the Interaction of Coronal Magnetic Fields", Sheeley, N. R., Jr. Submitted to Solar Physics (Supplements).

1814 "Spectroscopic Far Ultraviolet Observations of Transition Zone Instabilities and Their Possible Role in a Pre-Flare Energy Build-up," Brueckner, G. E., Patterson, N. P. and Scherrer, V. E. Submitted to Solar Physics.

1817 "Absolute Solar Ultraviolet Intensities and Their Variations with Solar Activity Part I: The Wavelength Region 1750Å - 2100Å," Brueckner, G. E., Bartoe, J.-D. F., Moe, O. K., and Van Hoosier, M. E. Submitted to Astrophys. J.

1820 "Observation of a Kink Instability in a Solar Flare," Cheng, C. C. Submitted to Astrophys. J.

1822 "Thin Aluminum Filters for Use on the Apollo Telescope Mount Extreme Ultraviolet Spectrograph," Schumacher, R. J. and Hunter, W. R. Submitted to Appl. Opt.

1827 "NRL/ATM Extreme Ultraviolet Solar Image Television Monitor Flown on Skylab," Crockett, W. R., Patterson, N. P., Purcell, J. D., Schumacher, R. J. and Tousey, R. Submitted to Appl. Opt.

1837 "The Emission Line Spectrum of a Sunspot in the Far Ultraviolet," Cheng, C. C., Doschek, G. A., and Feldman, U. Submitted to Astrophys. J.

1846 "Coronal Holes, Solar Wind Streams and Recurrent Geomagnetic Disturbances: 1973-1976," Sheeley, N. R., Jr., Harvey, J. W. and Feldman, W. C. Submitted to Solar Physics.

1850 "Emission Measures, Electron Densities and Nonthermal Velocities from Optically Thin UV-Lines Near a Quiet Solar Limb," Kjeldseth Moe, O. and Nicolas, K. R. Submitted to Astrophys. J.

1866 "The Influence of Autoionization Accompanied by Excitation on Dielectronic Recombination and Ionization Equilibrium," Jacobs, V. L., Davis, J., Kepple, P. C. and Blaha, M. Submitted to Astrophys. J.

1869 "The Emission Spectrum of the Hydrogen Balmer Seriesd Observed Above the Solar Limb from Skylab I. A Quiet-Sun and Polar Coronal Hole," Rosenberg, F. D., Feldman, U. and Doschek, G..A. Submitted to Astrophys. J.

1872 "The Profile of the 977 Å Line of C III," Moe, O. K., Nicolas, K. R. and Bartoe, J.-D. F. Contribution to the NASA Workshop on the Physical Output of the Sun, 1976.

1873 "A Comment on the Acceleration of Charged Particles in the Presence of Micro-Turbulence as Related to Solar Flares," Spicer, D. S. Research Note submitted to Solar Physics.

1875 "The Apollo Telescope Mount of Skylab - An Overview," Tousey, R. Submitted to Appl. Opt.

1876 "The Solar XUV Grazing Incidence Spectrograph on Skylab," Garrett, D. L. and Tousey, R. Submitted to Appl. Opt.

1880 "The Emission Spectrum of the Hydrogen Balmer Series Observed Above the Solar Limb from Skylab II. Active Regions," Feldman, U. and Doschek, G. A. Submitted to Astrophys. J.

1882 "Extreme-Ultraviolet Observations of Coronal Holes: I. Locations, Sizes and Evolution of Coronal Holes June 1973 - January 1974," Bohlin, J. D. Submitted to Solar Physics.

1883 "Exploring the Earth's Atmosphere by Photography from Skylab," Packer, D. M. and Packer, I. G. Submitted to Appl. Opt.

1884 "Emission Measures and Structure of the Transition Region of a Sunspot from Emission Lines in the Far Ultraviolet," Cheng, C. C. and Moe, O. K. Submitted to Solar Physics.

1885 "The Naval Research Laboratory's Extreme Ultraviolet Solar Spectrograph on Skylab," Bartoe, J.-D. F., Brueckner, G. E., Purcell, J. D. and Tousey, R. Submitted to Applied Optics.

1886 "Observations of the O_2 Column Density Between 120 km and 70 km and Absorption Cross Sectrion in the Vicinity of H-Lyman Alpha," Prinz, D. K. and Brueckner, G. E. Submitted to J. of Geophys. Res.

1887 "Multiple Loop Activations and Continuous Energy Release in the Solar Flare of 1973 June 15," Widing, K. G. and Dere, K. P. Submitted to Solar Physics.

1894 "Solar XUV Emission Line Profiles of Si II and Si III and Their Center to Limb Variations," Nicolas, K. R., Brueckner, G. E., Tousey, R., Tripp, D. A., White, O. R. and Athay, R. G. Submitted to Solar Physics.

1897 "The 3s-3p and 3p-3d Lines of Mg II Observed Above the Solar Limb from Skylab," Feldman, U. and Doschek, G. A. Submitted to Astrophys. J. Lett.

1898 "Comparison of Flare Bremsstrahlung Resulting from Energetic Thermal and Non-Thermal Electrons," Davis, J. and Rogerson, J. E. Submitted to Solar Physics.

1899 "Observing and Recording Instanteous Images on ATM Television Monitors," Patterson, N. P., Tousey, R. and Delamere, W. A. Submitted to Appl. Opt.

1900 "Experience with Schumann-Type XUV Film on Skylab," Van Hoosier, M. E., Bartoe, J.-D. F., Brueckner, G. E., Patterson, N. P. and Tousey, R. Submitted to Appl. Opt.

1901 "The Naval Research Laboratory's Extreme Ultraviolet Spectroheliograph on Skylab," Tousey, R, Bartoe, J.-D. F., Brueckner, G. E., and Purcell, J. D. Submitted to Appl. Opt.

1902 "The Thermal and Non-Thermal Flare: A Result of Non-Linear Threshold Phenomena During Magnetic Field Line Reconnection," Spicer, D. S. Submitted to Solar Physics.

1904 "Chromospheric Limb Spectra from Skylab: 2000 to 3200 Å," Doschek, G. A. and Feldman, U. Submitted to Astrophys. J.

1905 "Forbidden Lines of the Solar Corona and Transition Zone $\lambda\lambda$955 Å - 3000 Å," Sandlin, G. D., Brueckner, G. E. and Tousey, R. Submitted to Astrophys. J.

1906 "Enhancement of Dielectronic Recombination by Plasma Electric Microfields," Jacobs, V. L., Davis, J. and Kepple, P. C. Submitted to Physical Rev. Lett.

III. ABSTRACTS

1509 "Absolute Intensity of the Continuum in the Ultraviolet Spectrum of the Sun Between 1650-1800 Å", Brueckner, G. E., Moe, O. K., and Pitz, E., BAAS 3, 260 (1971).

1510 "High Spectral and Spatial Resolution Ultraviolet Spectroscopy of the Sun in the Region 1170-1800 Å", Brueckner, G. E., BAAS 3, 259 (1971).

1529 "On the Classification of Some Highly Ionized Iron and Nickel Lines in the 200-400 Å Region of the Solar Spectrum", Widing, K. G. and Sandlin, G. D., Cowan, R. D., Sp. Sci. Rev. 13, 665 (1972).

1544 "Extreme Ultraviolet Spectroheliograms of a Solar Flare", Purcell, J. D. and Tousey, R., BAAS 3, 448 (1971).

1545 "Preliminary Results of Identifications in the XUV Spectrum of a Solar Flare", Purcell, J. D., Tousey, R., and Widing, K. G., BAAS 3, 448 (1971).

1565 "The Coronal Origin of a Solar Flare", Brueckner, G. E., BAAS 4, 378 (1972).

1572 "A Recalibration of Spectral Radiance of Mercury and Deuterium Arc Standard Lamps in the Near UV", Bartoe, J.-D. F. and Ott, W. R., J. Opt. Soc. Am. 62, 1372 (1972).

1623 "The 1175 Å to 1900 Å Ultraviolet Spectrum of Solar Flares", Brueckner, G. E., Bohlin, J. D., Moe, O. K., Nicolas, K. R., Purcell, J. D., Scherrer, V. E., Sheeley, N. R., Jr., and Tousey, R., BAAS 6, 285 (1974).

1624 "Electron Density from Line Ratios in the XUV Spectrum of a Solar Flare", Widing, K. G., Purcell, J. D., and Tousey R., BAAS 6, 297 (1974).

1625 "The Screw Pinch and the Solar Flare", Spicer, D. S. and Cheng, C. C., BAAS 6, 294 (1974).

1626 "A Preliminary Study of Coronal Structures by Means of Time-Lapse Photography", Sheeley, N. R., Jr., Bohlin, J. D., Brueckner, G. E., Purcell, J. D., Scherrer, V. E., and Tousey, R., BAAS 6, 294 (1974).

1628 "Rocket Spectroheliogram Observations of the Heights of Formation and Sizes of Bright Features in the Transition Zone", Simon, G. W., Seagraves, P. H., and Tousey, R., BAAS 6, 294 (1974).

1629 "Cinematographic Observations for ATM and Their Comparison with Some ATM Results", Zirin, H., Holt, J., Brueckner, G. E., Bohlin, J. D., Purcell, J. D., Scherrer, V. E., Sheeley, N. R., Jr., and Tousey, R., BAAS 6, 298 (1974).

1637 "Studies of Atmospheric Extinction from Skylab", Brown, C. M., Tousey, R., Tilford, S. G., and Prinz, D. K., EOS <u>55</u>, 371 (1974).

1640 "Coronal Extreme Ultraviolet Spectroheliograph and Chromospheric Extreme Ultraviolet Spectrograph", Tousey., BAAS <u>6</u>, 297 (1974).

1642 "The Extreme Ultraviolet Spectrograph", Bartoe, J.-D. F., Brueckner, G. E., Purcell, J. D., and Tousey, R., SPIE, 'Instrumentation in Astronomy - II', 1974, SPIE <u>44</u>, 153.

1657 "Skylab Observation of the White Light Corona and the He II 304 Å Chromosphere During the Eruptive Prominence Event of August 21, 1973", Bohlin, J. D., Brueckner, G. E., Purcell, J. D., Scherrer, V. E., Sheeley, N. R., Jr., Tousey, R., Poland, A. I., EOS <u>55</u>, 409 (1974).

1657 "The Eruptive Prominence of August 21, 1973, Observed from Skylab in the White Light Corona and in the He II 304 Å Chromosphere", Poland, A. I., Bohlin, J. D., Brueckner, G. E., Purcell, J. D., Scherrer, V. E., Sheeley, N. R., Jr., and Tousey, R., BAAS <u>6</u> 219 (1974).

1658 "Preliminary Results from the Extreme Ultraviolet Spectroheliograph and Ultraviolet Spectrograph on ATM", Tousey, R., EOS <u>55</u>, 408 (1974).

1668 "Skylab Observations of the Sun (170-630 Å) with the NRL Objective Grating Spectroheliograph", Widing, K. G., J. Opt. Soc. Am. <u>64</u>, 1375 (1974).

1674 "Spectrophotometry of the Solar Ultraviolet Line Spectrum with the NRL Spectrograph onboard Skylab", Brueckner, G. E., J. Opt. Soc. Am. <u>64</u>, 1375 (1974).

1685 "ATM Observations on the XUV Emission from Flares", Brueckner, G. E., Astrophys. and Sp. Sci., in press.

<u>Ibid</u>., Stanford Univ. Inst. for Plasma Res. Report No. 594 (1974).

1696 "A Catalog and Classification of Flares and Flare-Like Events Observed by the ATM XUV Spectrograph S082A and Spectroheliograph S082B", Scherrer, V. E., Tousey, R., and Sandlin, G. D., BAAS <u>7</u>, 356 (1975).

1697 "Polar Plumes in XUV Emission-Line Corona", Bohlin, J. D., Purcell, J. D., Sheeley, N. R., Jr., and Tousey, R., BAAS <u>7</u>, 356 (1975).

1698 "Macro-Spicules in He II 304 Å Over the Sun's Polar Cap", Bohlin, J. D., Vogel, S. N., Purcell, J. D., Sheeley, N. R., Jr., Tousey, R. and Van Hoosier, M. E., BAAS <u>7</u>, 354 (1975).

1699 "Flare Mechanisms Based on the Current Limitation Concept", Spicer, D. S., BAAS 7, 352 (1975).

1700 "Absolute Solar UV Intensities 1680 Å to 2100 Å", Moe, O. K., Brueckner, G. E., Bartoe, J.-D. F., and Van Hoosier, M. E., BAAS 7, 360 (1975).

1701 "On the XUV Emissions in Solar Flares Observed with the ATM/NRL Spectroheliograph", Cheng, C. C. and Widing, K. G., BAAS 7, 356 (1975).

1703 "Observations from Skylab of the Density Dependent C III Multiplet at 1175 Å in Active and Quiet Regions and Above the Limb", Nicolas, K. and Brueckner, G. E., BAAS 7, 353 (1975).

1705 "The High-Energy Limb Event of January 17, 1974", Tousey, R., Bohlin, J. D., Moe, O. K., Purcell, J. D., and Sheeley, N. R., Jr., BAAS 7, 348 (1975).

1706 "Interpreting XUV Spectroheliograms in Terms of Coronal Magnetic Field Structures", Sheeley, N. R., Jr., Bohlin, J. D., Brueckner, G. E., Purcell, J. D., Scherrer, V. E., and Tousey, R., BAAS 7, 346 (1975).

1707 "Line Profiles of the Fe XXIV Emission at 192 Å and 255 Å in Solar Flares", Brueckner, G. E., Moe, O. K., and Van Hoosier, M. E., BAAS 7, 356 (1975).

1712 "The Superheating Instability as a Trigger for Solar Flares", Tidman, D. A., Spicer, D. S., and Davis, J., BAAS 7, 352 (1975).

1716 "The XUV Sun as Observed by ATM S082", Tousey, R., AIAA Bulletin 11, 344 (1974).

1718 "Classification of Flares and Flare-Like Events Observed by the ATM XUV Spectroheliograph S082A and Spectrograph S082B During the Skylab Missions", Scherrer, V. E. and Tousey, R., AIAA Bulletin 11, 345 (1974).

1726 "Structure and Temperature of Solar Flare Plasma", Scherrer, V. E. and Sandlin, G. D., BAPS 20, 659 (1974).

1750 "A Resistive Screw Instability Model of a Solar Flare", Spicer, D. S., BAAS 7, 397 (1975).

1751 "A Time Dependent Study of Conductive Heat Flow in a Flaring Arch", Kepple, P. C. and Spicer, D. S., BAAS 7, 397 (1975)

1752 "The Sun's Polar Caps as Coronal Holes; Their Sizes, Evolution, and Phenomenology During the Skylab Mission", Bohlin, J. D., Rubenstein, D. M., and Sheeley, N. R., Jr., BAAS 7, 457 (1975).

1753 "Energy Release and Thermal Structure in Solar Flares" Cheng, C. C. and Widing, K. G., BAAS 7, 424 (1975).

1754 "X-Ray Event of August 13-15, 1973", Scherrer, V. E., Sandlin, G. D., Sheeley, N. R., Jr., and Tousey, R., BAAS 7, 430 (1975).

1756 "Skylab/ATM Observations of Transient Events Having the GRF X-Ray and Microwave Character", Sheeley, N. R., Jr., Bohlin, J. D., Scherrer, V. E., and Tousey, R., BAAS 7, 429 (1975).

1757 "Measured Variation of the XUV Line Widths and Intensities Near the Solar Limb", Moe, O. K. and Nicolas, K. R., BAAS 7, 460 (1975).

1758 "Evolution of XUV Plasmas in Solar Flares", Widing, K. G. and Cheng, C. C., BAAS 7, 424 (1975).

1763 "Spectroscopic Study of Plasmas Preceding and During Solar Flares", Scherrer, V. E. and Sandlin, G. D., BAPS 10, 1325 (1975).

1768 "Solar Flare Collision Excitation Rate Coefficients", Tousey, R., Kepple, P. C., and Davis, J. BAAS 7, 398 (1975).

1769 "Plasma Heating and Flare X-Rays", Davis, J., Kepple, P., Strickland, D., and Brueckner, G., BAAS 7, 398 (1975).

1770 "Hydrodynamics of Electron Beam Deposition in Solar Flares", Bloomberg, H., Kepple, P. C., Davis, J., Boris, J., Brueckner, G., BAAS 7, 398 (1975).

1771 "Results from the NRL XUV Experiment on Skylab", Tousey, R., J. Opt. Soc. Am. 64, 523 (1974).

1772 "Maximum Efficiency of Ruled Concave Diffraction Gratings in the Ultraviolet", Mikes, T. L., J. Opt. Soc. Am. 64, 1371 (1974).

1776 "Time Dependent Ionization Equilibrium and Line Emission from Ionized Iron Under Flare-Like Conditions", Kepple, P. and Davis, J., EOS 56, 1183 (1974).

1777 "Transient Line Emission from Ionized Iron Under Flare-Like Conditions", Davis, J., Kepple, P., and Tousey, R., BAAS 7, 357 (1975).

1778 "Absolute Calibrated Solar UV Intensities 1700 - 2100 Å", Moe, O. K., J. Opt. Soc. 64, 1375 (1974).

1779 "The Source of Material Comprising a Mass Ejection Coronal Transient", Hildner, E., Gosling, J. T., Hansen, R. T., and Bohlin, J. D., BAAS 7, 473 (1975).

1781 "Evidence for Non-Hydrostatic Equilibrium Conditions in the Transition Region", Brueckner, G. E., Stanford Univ. Inst. for Plasma Res. Report No. 594 (1974).

1782 "Evidence for Magnetic Field Line Reconnection in the Lower Corona", Sheeley, N. R., Jr., EOS Transactions, Vol. 56, 1049.

1794 "Extreme Ultraviolet Spectroheliograph for Plasma Diagnostics," Scherrer, V. E., Purcell, J. D. and Sandlin, G. D. Frist Topical Conference on Diagnostics of High Temperature Plasmas, American Physical Society, 7-9 January 1976, Knoxville, Tennessee.

1796 "The Emission Line Spectrum Above the Limb of the Quiet Sun: 1175-1940 Angstroms," Doschek, G. A., Feldman, U., Van Hoosier, M. E. and Bartoe, J.-D. F. Astrophys. J. 206, 964 (1976).

1797 "The Emission Line Spectrum Above the Limb of a Solar Coronal Hole: 1175-1940 Angstroms," Feldman, U., Doschek, G. A., Van Hoosier, M. E. and Purcell, J. D. Astrophys. J. 206, 965 (1976).

1825 "Diagnostics for Plasma Temperatures in the Spectrum 171 - 630Å," Scherrer, Victor E. and Sandlin, G. D., 1976 Spring Meeting of APS, 26-29 April 1976, Washington, D. C., BAPS 21, 598 (1976).

1828 "High Spatial Resolution UV Spectra of the Sun: Observed Shifts of UV-Transition Zone Lines and Shockwaves," Kjeldseth Moe, O., Bartoe, J.-D. F., Brueckner, G. E., Nicolas, K. R. and Van Hoosier, M. E., XIX COSPAR Meeting, 8-19 June 1976, Philadelphia, PA.

1829 "High Spatial Resolution UV Spectra of the Sun: The Dynamics of the Transition Zone," Brueckner, G. E., Bartoe, J.-D. F., Kjeldseth Moe, O., Nicolas, K. R. and Van Hoosier, M. E., XIX COSPAR Meeting, 8-19 June 1976, Philadelphia, PA.

1830 "High Spatial Resolution UV Spectra of the Sun: Electron Densities and Emission Measures in the Solar Transition Zone," Nicolas, K. R., Bartoe, J.-D. F., Brueckner, G. E., Kjeldseth Moe, O., and Van Hoosier, M. E., XIX COSPAR Meeting, 8-19 June 1976, Philadelphia, PA.

1831 "Spectrophotometry of the Photospheric and Chromospheric Granulation in the UV Region 1240-1650Å," Bartoe, J.-D. F., Brueckner, G. E., Kjeldseth Moe, O., Nicolas, K. R. and Van Hoosier, M. E., XIX COSPAR Meeting, 8-19 June 1976, Philadelohia, PA.

1832 "High Spatial Resolution UV Spectra of the Sun: The Fine Structure of the Solar Atmosphere from the Temperature Minimum into the Corona," Van Hoosier, M. E., Bartoe, J.-D. F., Brueckner, G. E., Kjeldseth Moe, O. and Nicolas, K. R., XIX COSPAR Meeting, 8-19 June 1976, Philadelphia, PA.

1836 "Amplitude Instability and Stochastic Behavior During Magnetic Field Line Reconnection," Spicer, D. S., Solar Physics Div. of 148th A.A.A. Meeting, 21-24 June 1976, Haverford, PA., BAAS 8, 373 (1976).

1839 "Final Report on Coronagraph Feasibility Studies for an Out-of-Ecliptic Mission," Bohlin, J. D., Howard, R. A., Koomen, M. J., and Michels, D. J. 'Phase A Final Review of a Joine ESA/NASA Out-of-Ecliptic Mission,' ESA Headquarters, 6-7 April 1976, Paris, France.

1847 "Multiple Loop Activations and Continuous Energy Release in a Solar Flare," Widing, K. G., Solar Physics Div. of 148th A.A.S. Meeting, 21-24 June 1976, Haverford, PA., BAAS 8, 375 (1976).

1853 "Identification of Hα Macrospicules with EUV Macrospicules and with Flares in X-Ray Bright Points," Moore, R. L., Tang, F., Bohlin, J. D. and Golub, L., Solar Physics Div. of 148th A.A.S. Meeting, 21-24 June 1976, Haverford, PA., BAAS 8, 333 (1976).

1854 "Observation of a Kink Instability in a Solar Flare," Cheng, C. C., Solar Physics Div. of 148th A.A.S. Meeting, 21-24 June 1976, BAAS 8, 373 (1976).

1855 "Preliminary Analysis of NRL Skylab Spectroheliograms in Lines of He I and He II," Mango, S., Bohlin, J. D., Glackin, D. and Linsky, J., Solar Physics Div. of 148th A.A.S. Meeting, 21-24 June 1976, Haverford, PA., BAAS 8, 332 (1976).

1856 "Pre-flare Observations During the Evolutiion of McMath Region 12474 August 7-9, 1973," Scherrer, V., Brueckner, G., Sandlin, G. and Tousey, R., Solar Physics Div. of 148th A.A.S. Meeting, 21-24 June 1976, Haverford, PA., BAAS 8, 373 (1976).

1857 "Time Dependent Ionization and Radiation of a Gas Moving through the Solar Transition Zone," Kjeldseth Moe, O., Solar Physics Div. of 148th A.A.S. Meeting, 21-24 June 1976, Haverford, PA., BAAS 8, 331 (1976).

1858 "Coronal Lines in ATM Spectra 1100 - 3000 Å," Sandlin, G. D., Brueckner, G. E. and Tousey, R., Solar Physics Div. of 148th A.A.S. Meeting, 21-24 June 1976, Haverford, PA., BAAS 8, 339 (1976).

1859 "Spectrophotometry of the Photospheric and Chromospheric Granulation in the UV Region 1240-1650Å," Bartoe, J.-D. F., Brueckner, G. E., Kjeldseth Moe, O., Nicolas, K. R. and Van Hoosier, M. E., Solar Physics Div. of 148th A.A.S. Meeting, 21-24 June 1976, Haverford, PA., BAAS 8, 312 (1976).

1860 "The UV Spectrum of a Sunspot (1175 to 1700 Å) Observed with High Spatial and Spectral Resolution," Brueckner, G. E., Nicolas, K. R., Bartoe, J.-D. F. and Van Hoosier, M. E., Solar Physics Div. of 148th A.A.S. Meeting, 21-24 June 1976, Haverford, PA., BAAS 8, 345 (1976).

1861 "Densities in the Solar Chromosphere above the Quiet Sun and a Coronal Hole Derived from the Hydrogen Balmer Lines," Rosenberg, F. D., Feldman, U. and Doschek, G. A., Solar Physics Div. of 148th A.A.S. Meeting, 21-24 June 1976, Haverford, PA., BAAS 8, 338 (1976).

1865 "Preliminary Analysis of NRL Rocket Spectra of the Lα Line Wings," Basri, G., Bartoe, J.-D. F., Brueckner, G., Linsky, J. and Van Hoosier, M. E., Solar Physics Div. of 148th A.A.S. Meeting, 21-24 June 1976, Haverford, PA., BAAS 8, 331 (1976).

1891 "Multiple Loop Activations and Continuous Energy Release in a Solar Flare," Widing, K. G., XVI General Assembly, I.A.U., 24 August - 2 September 1976, Grenoble, France.

IV. PROFESSIONAL TALKS - INVITED

"The ATM Project", Tousey, R., Symp. on 'Calibration Methods in the UV and X-Ray Regions of the Spectrum', Institut fur extra-terrestrische Physik, Max Planck Institut fur Physik und Astrophysik, Munich, Germany, 27-30 May 1968.

1514 "Identifications in the Solar XUV Spectrum", Tousey, R., 14th Gen. Assembly IAU, Commission 44, University of Sussex, Brighton, England, 20 August 1970.

"Solar Astronomy, Some Highlights of the Past Year", Tousey, R., 14th Gen. Assembly IAU, IAU Commission 44, University of Sussex, Brighton, England, 20 August 1970.

1515 "Survey of New Solar Results", Tousey, R., IAU Symp. 41, 'New Techniques in Space Astronomy', Munich, Germany, 10-14 August 1970.

1518 "Solar Spectroscopy from Space Vehicles", Tousey, R., Tenth National Meeting of the Society for Applied Spectroscopy, St. Louis, Missouri, 18-22 October 1971.

1522 "High Angular Observations from Rockets: Solar XUV Observations", Tousey, R., COSPAR XII, Seattle, Washington, 17 June - 2 July 1971.

1565 "The Coronal Origin of a Solar Flare", Brueckner, G. E., COSPAR XV, Madrid, Spain, 10-24 May 1972.

Ibid., AAS, Solar Phys. Div., University of Maryland, College Park, Maryland, 4-6 April 1972.

1641 "The Extreme Ultraviolet Spectroheliograph and the Extreme Ultraviolet TV Monitor", Tousey, R., Bartoe, J.-D. F., Brueckner, G. E., and Purcell, J. D., Soc. Photo-Optical Instr. Eng., 'Instrumentation in Astronomy - II', Tucson, Arizona, 4-6 March 1974.

1642 "The Extreme Ultraviolet Spectrograph", Bartoe, J.-D. F., Brueckner, G. E., Purcell, J. D., and Tousey, R., Soc. Photo-Optical Instr. Eng., 'Instrumentation in Astronomy - II', Tucson, Arizona, 4-6 March 1974.

1651 "The Sun as Observed by the ATM XUV Spectroheliograph and Spectrograph, S082A and B", Tousey, R., COSPAR XVII, Sao Paulo, Brazil, 25 June - 1 July 1974.

1652 "Preliminary Results from the NRL/ATM Instruments from Skylab 2", Tousey, R., Bartoe, J.-D. F., Bohlin, J. D., Brueckner, G. E., Purcell, J. D., Scherrer, V. E., Schumacher, R. J., Sheeley, N. R., Jr., and Van Hoosier, M. E., IAU Symp. 57, 'Coronal Disturbances', Surfers Paradise, Queensland, Australia, 19 August - 11 September 1973.

1658 "Preliminary Results from the Extreme Ultraviolet Spectroheliograph and Ultraviolet Spectrograph on ATM", Tousey, R., AGU, 55th Annual Meeting, Washington, D. C., 8-12 April 1974.

"Results from the NRL Experiments on Skylab", Tousey, R., Opt. Soc. Am., Washington, D. C., 22 April 1974.

1662 "Some NRL/ATM Observations of a Coronal Hole at the Solar Limb", Sheeley, N. R., Jr., 3rd Solar Wind Conf., Asilomar, California, 25-29 March 1974.

1668 "Skylab Observations of the Sun (170-630 Å) with the NRL Objective Grating Spectroheliograph", Widing, K. G., Opt. Soc. Am., Houston, Texas, 15-18 October 1974.

1671 "Diffraction Gratings for the XUV - Conventional vs. Holographic" Hunter, W. R., Symp. on 'Diffraction Gratings and Grating Instruments', Tokyo, Japan, 31 August 1974.

1675 "Ultraviolet Emission Line Profiles of Flares and Active Regions", Brueckner, G. E., IAU/COSPAR Symp. 68, 'Solar Extreme UV, X and Radiation', Buenos Aires, Argentina, 11-14 June 1974.

1677 "Fe XXIV Emission in Solar Flares Observed with the NRL/ATM XUV Slitless Spectrograph", Widing, K. G., IAU/COSPAR Symp. 68, 'Solar Extreme UV, X and Radiation', Buenos Aires, Argentina, 11-14 June 1974.

1679 "XUV Observations of Coronal Magnetic Fields", Sheeley, N. R., Jr., Bohlin, J. D., Brueckner, G. E., Purcell, J. D., Scherrer, V. E., and Tousey, R., Conf. on 'Flare-Related Magnetic Field Dynamics', Boulder, Colorado, 23 September 1974.

1683 "Observations of the Hydrogen Ly-α (1216 Å) Emission Line of Comet Kohoutek (1973f) by the Skylab/ATM S082B Spectrograph", Keller, H. U., Bohlin, J. D., and Tousey, R., Comet Kohoutek Workshop, MSFC, Huntsville, Alabama, 13-14 June 1974.

1685 "ATM Observations on the XUV Emission from Flares", Brueckner, G. E., IAU Colloq. 27, 'Fourth Conf. on Ultraviolet and X-Ray Spectroscopy of Astrophysical and Laboratory Plasmas', Harvard University, Cambridge, Massachusetts, 9-11 September 1974.

Ibid., 'Solar Physics - Plasma Physics Workshop', Stanford University, Stanford, California, 17-20 September 1974.

1690 "Ultraviolet Observations of Solar Flares from Skylab", Brueckner, G. E., Royal Society Discussion Meeting 'The Physics of the Solar Atmosphere', London, England, 14-15 January 1975.

1691 "Eruptive Prominences Recorded by the XUV Spectroheliograph on Skylab", Tousey, R., Royal Society Discussion Meeting, 'The Physics of the Solar Atmosphere', London, England, 14-15 January 1975.

1715 "XUV Results from Skylab", Tousey, R., International Conf. on 'X-Rays in Space', University of Calgary, Calgary, Alberta, Canada, 14-21 August 1974.

1733 "XUV Emission from Above the West Limb Near 20:00 U.T., January 17, 1974", Tousey, R., IAU Colloq. 27, 'Fourth Conf. on Ultraviolet and X-Ray Spectroscopy of Astrophysical and Laboratory Plasmas', Cambridge, Massachusetts, 9-11 September 1974.

1734 "A Review of Skylab/ATM Observations and Analyses of Coronal Transients", Gosling, J. T., Bohlin, J. D., Krieger, A. S., Schmahl, E. J., Tandberg-Hanssen, E., COSPAR XVIII, Varna, Bulgaria, 29 May - 7 June 1975.

1748 "The Interpretation of Ultraviolet Solar Spectra", Moore-Sitterly, C. E., Twentieth Liege International Astrophysical Symp., Liege, Belgium, 17-20 June 1975.

1749 "Coronal Changes Associated With a Disappearing Filament", Sheeley, N. R., Jr., Bohlin, J. D., Brueckner, G. E., Purcell, J. D., Scherrer, V. E., Tousey, R., Smith, J. B., Jr., Speich, D. M., Tandberg-Hanssen, E., Wilson, R. M., de Loach, A. C., Hoover, R. B., and McGuire, J. P., Annual Meeting of HAO, SPO, KPNO, Santa Fe, New Mexico, 23 May 1975.

1760 "Absolute Solar Intensities 1750 Å - 2100 Å and Their Variations with Solar Activity", Brueckner, G. E., Bartoe, J.-D. F., Moe, O. K., Van Hoosier, M. E., 'Workshop on the Solar Constant and the Earth's Atmosphere', Big Bear Solar Observatory, Big Bear City, California, 19-21 May 1975.

1774 "First Results from Skylab", Tousey, R., AAS, Tucson, Arizona, 2-6 December 1973.

1778 "Absolute Calibrated Solar UV Intensities 1700 to 2100 Å", Moe, O. K., Opt. Soc. Am., Houston, Texas, 15-18 October 1974.

1781 "Evidence for Non-Hydrostatic Equilibrium Conditions in the Transition Region", Brueckner, G. E., 'Solar Physics - Plasma Physics Workshop', Stanford University, Stanford, California, 17-20 September 1974.

1784 "Spectroscopic Far Ultraviolet Observations of Active Regions Prior to and During Flares", Brueckner, G. E., Patterson, N. P., Scherrer, V. E., 'Flare Build-up Study Workshop', Falmouth, Cape Cod, Massachusetts, 8-11 September 1975.

1786 "Solar Research with Diffraction Gratings in the Far Ultraviolet", Brueckner, G. E., U. S.-Japan Seminar on Diffraction Gratings, Washington, D. C., 14-17 October 1975.

"Photospheric Magnetic Field and Its Coronal Extension", Sheeley, N. R., Jr., AAS, Solar Physics Div., 20 January 1975.

AD-A044 548 NAVAL RESEARCH LAB WASHINGTON D C F/G 3/2
NRL/ATM USER'S GUIDE TO EXPERIMENT S082A.(U)
FEB 77 I G PACKER, N P PATTERSON, S A MANGO NASA-S-60604-G
UNCLASSIFIED NRL-MR-3410 NL

2 OF 2
AD
A044548

END
DATE
FILMED
10-77
DDC

1838 "Mechanisms for Particle Acceleration in Solar Flares," Spicer, D. S., Goddard Space Flight Center/University of Maryland High Energy Astrophysics Seminar, 15 March 1976.

1840 "Resistive Kink Model of a Solar Flare," Spicer, D. S., Bartol Institute, Swarthmore, Pennsylvania, 17 February 1976.

1841 "The Morphology and Evolution of Coronal Holes," Bohlin, J. D., Coll. at Observatoire de Paris, Paris, France, 9 April 1976.

1862 "Spectroscopic Ultraviolet Observations of Flares from Skylab," Brueckner, G. E., U. S.-Japan Cooperative Seminar on "High Energy Phenomena in Solar Flares," 10-13 May 1976, Tokyo, Japan.

1863 "Skylab Spectroheliograph Observations of the Double Ribbon Flare of 1973 June 15," Widing, K. G., U. S.-Japan Cooperative Seminar on "High Energy Phenomena in Solar Flares," 10-13 May 1976, Tokyo, Japan.

1870 "The Physical Properties of Coronal Holes," Bohlin, J. D., AGU International Sym. on Solar-Terrestrial Physics, 7-18 June 1976, Boulder, Colorado.

1878 "The Thermal and Non-Thermal Flare: A Result of Non-Linear Threshold Phenomena," Spicer, D. S., I.A.U. Commission #14, 25 August 1976, Grenoble, France.

1895 "Analyses of Laboratory Spectra of Special Interest for the Interpretation of Ultraviolet Stellar Spectra," Moore-Sitterly, C. and Widing, K., I.A.U. Commission #14, 25 August 1976, Grenoble, France.

1907 "Detecting Ultraviolet Radiation from the through the Atmosphere," Prinz, D. K., 20th Annual Technical Symposium of the Society of Photo-Optical Instrumentation Engineers, 26 August 1976, San Diego, California. To be published in SPIE proceedings.

V. PROFESSIONAL TALKS - CONTRIBUTED

1420 "Some Recent XUV Spectroheliograms and Heliograms from Rockets," Purcell, J. D., Bartoe, J.-D. F., Snider, C. B., and Tousey, R., Second International Conf. on 'Vacuum Ultraviolet and X-Ray Spectroscopy of Laboratory and Astrophysical Plasmas', University of Maryland, 24-28 March 1968.

1469 "Radiation Light Sources for Stellar Telescope Calibration from 700 Å to 7000 Å," Hunter, W. R., Workshop on Optical Telescope Technology, MSFC, Huntsville, Alabama, May 1969.

1471 "Some Experiments on the Corona Surrounding a Spacecraft - Past, Planned and Proposed," Tousey, R., Opt. Soc. Am. Symp. on 'Optical Contamination in Space', Aspen, Colorado, 13-15 August 1969.

1479 "A Photographic Spectrum of a Flare in the XUV," Purcell, J. D. and Tousey, R., International Symp. on Solar Terrestrial Physics, Leningrad, U.S.S.R., 13 May 1970.

1481 "Observations of the Sun in the Extreme Ultraviolet," Tousey, R., Meeting of the Royal Society, London, England, 21-22 April 1970.

1499 "Observation of Stark-Effect in a Far UV Flare Spectrum," Brueckner, G. E., 14th Gen. Assembly IAU, University of Sussex, Brighton, England, 18-27 August 1970.

1509 "Absolute Intensity of the Continuum in the Ultraviolet Spectrum of the Sun Between 1650-1800 Å," Brueckner, G. E., Moe, O. K., Pitz, E., AAS, Solar Phys. Div., Huntsville, Alabama, 17 November 1970.

1510 "High Spectral and Spatial Resolution Ultraviolet Spectroscopy of the Sun in the Region 1170-1800 Å," Brueckner, G. E., AAS, Solar Phys. Div., Huntsville, Alabama, 17 November 1970.

1529 "On the Classification of Some Highly Ionized Iron and Nickel Lines in the 200-400 Å Region of the Solar Spectrum," Widing, K. G., Sandlin, G. D., and Cowan, R. D., Third Symp. on 'Ultraviolet and X-Ray Spectroscopy of Astrophysical and Laboratory Plasmas', Utrecht, The Netherlands, 24-26 August 1971.

1536 "XUV Television of a Solar Image from a Rocket," Tousey, R., Symp. on 'The Processing of Telescopic Images', Laval University, Quebec, Quebec, Canada, 1-2 October 1971.

1538 "Possibilities for Measuring Atmospheric Extinction and Absorption with the ATM Solar Experiments in Skylab," Tousey, R., Informal Conf. on 'The Uses of Astronomy in the Study of Air Pollution' Project, Seattle, Washington, 19 August 1971.

1544 "Extreme Ultraviolet Spectroheliograms of a Solar Flare," Purcell, J. D. and Tousey, R., AAS, 136th meeting, San Juan, Puerto Rico, 6-8 December 1971.

1545 "Preliminary Results of Identifications in the XUV Spectrum of a Solar Flare," Purcell, J. D., Tousey, R., and Widing, K. G., AAS, San Juan, Puerto Rico, 6-8 December 1971.

1572 "A Recalibration of Spectral Radiance of Mercury and Deuterium Arc Standard Lamps in the Near UV," Bartoe, J.-D. F. and Ott, W. R., Opt. Soc. Am., San Francisco, California, 17-20 October 1972.

1606 "The Increase in Transmittance of Unbacked Aluminum Filters Exposed to RF and DC Discharge in Oxygen," Hunter, W. R., Steele, G. N., and Gillette, R. B., Opt. Soc. Am., Rochester, New York, 9-12 October 1973.

1623 "The 1175 Å to 1900 Å Ultraviolet Spectrum of Solar Flares," Brueckner, G. E., Bohlin, J. D., Moe, O. K., Nicolas, K. R., Purcell, J. D., Scherrer, V. E., Sheeley, N. R., Jr., and Tousey, R., AAS, Solar Phys. Div., Honolulu, Hawaii, 9-11 January 1974.

1624 "Electron Density from Line Ratios in the XUV Spectrum of a Solar Flare," Widing, K. G., Purcell, J. D., and Tousey, R., AAS, Solar Phys. Div., Honolulu, Hawaii, 9-11 January 1974.

1625 "The Screw Pinch and the Solar Flare," Spi[illegible] D. S. and Cheng, C. C., AAS, Solar Phys. Div., 9[illegible]nuary 1974.

1626 "A Preliminary Study of Coronal Structures [illegible] Means of Time-Lapse Photography," Sheeley, N. R., Jr., Bohlin, J. D., Brueckner, G. E., Purcell, J. D., Scherrer, V. E., and Tousey, R., AAS, Solar Phys. Div., 9-11 January 1974.

1628 "Rocket Spectroheliogram Observations of the Heights of Formation and Sizes of Bright Features in the Transition Zone," Simon, G. W., Seagraves, P. H., and Tousey, R., AAS, Solar Phys. Div., Honolulu, Hawaii, 9-11 January 1974.

1629 "Cinematographic Observations for ATM and their Comparison with some ATM Results," Zirin, H., Holt, J., Brueckner, G. E., Bohlin, J. D., Purcell, J. D., Scherrer, V. E., Sheeley, N. R., Jr., and Tousey, R., AAS, Solar Phys. Div., Honolulu, Hawaii, 9-11 January 1974.

1637 "Studies of Atmospheric Extinction from Skylab," Brown, C. M., Tousey, R., Tilford, S. G., and Prinz, D. K., AGU, 55th Annual Meeting, Washington, D. C., 8-12 April 1974.

1640 "Coronal Extreme Ultraviolet Spectroheliograph and Chromospheric Extreme Ultraviolet Spectrograph," Tousey, R., AAS, Solar Phys. Div., Honolulu, Hawaii, 9-11 January 1974.

1643 "Oxygen Densities at Altitudes Between 70 and 129 km," Brueckner, G. E., Bartoe, J.-D. F., Brown, C. M., Prinz, D. K., Tilford, S. G., and Van Hoosier, M. E., COSPAR XVII, Sao Paulo, Brazil, 25 June - 1 July 1974.

1646 "Ultraviolet Emission Line Profiles of Flares and Flare-Like Events Observed from Skylab," Brueckner, G. E., Moe, O. K., and Nicolas, K. R., COSPAR XVII,, Sao Paulo, Brazil, 25 June - 1 July 1974.

1647 "On the Fe XXIV Emission in the Solar Flare of June 15, 1973," Widing, K. G. and Cheng, C. C., COSPAR XVII, Sao Paulo, Brazil, 25 June - 1 July 1974.

1650 "Structure of the Sun's Polar Cap in the Wavelengths 240-600 Å," Bohlin, J. D., Sheeley, N. R., Jr., and Tousey, R., COSPAR XVII, Sao Paulo, Brazil, 25 June - 1 July 1974.

1655 "Implications of NRL/ATM Solar Flare Observations on Flare Theories," Cheng, C. C. and Spicer, D. S., IAU/COSPAR Symp. 68, 'Solar Extreme UV, X and γ Radiation', Buenos Aires, Argentina, 11-14 June 1974.

1657 "Skylab Observation of the White Light Corona and the He II 304 Å Chromosphere During the Eruptive Prominence Event of August 21, 1973," Bohlin, J. D., Brueckner, G. E., Purcell, J. D., Scherrer, V. E., Sheeley, N. R., Jr., Tousey, R., and Poland, A. I., AGU, 55th Annual Meeting, Washington, D. C., 8-12 April 1974.

1657 "The Eruptive Prominence of August 21, 1973, Observed from Skylab in the White Light Corona and in the He II 304 Å Chromosphere," Poland, A. I., Bohlin, J. D., Brueckner, G. E., Purcell, J. D., Scherrer, V. E., Sheeley, N. R., Jr., and Tousey, R., AAS, Lincoln, Nebraska, 26-29 March 1974.

1666 "Some Reflections on the Use of Conventional and Holographic Diffraction Gratings in the Vacuum Ultraviolet Spectral Region," Hunter, W. R., IV International Conf. on Vacuum-Ultraviolet Radiation Physics, Hamburg, Germany, 22-26 July 1974.

1673 "Flare-Like Ultraviolet Spectra of Active Regions," Brueckner, G. E., IAU/COSPAR Symp. 68, 'Solar Extreme UV, X and γ Radiation', Buenos Aires, Argentina, 11-14 June 1974.

1678 "Flares Observed by the NRL/ATM Spectrograph and Spectroheliograph During the Skylab Missions," Scherrer, V. E. and Tousey, R., International Conf. on 'X-Rays in Space', University of Calgary, Calgary, Alberta, Canada, 14-21 August 1974.

1681 "The Impact of ATM/NRL Flare Data on Flare Theory," Spicer, D. S., Cheng, C. C., Widing, K. G., and Tousey, R., Second European Conf. on Cosmic Plasma Physics, Culham, England, 1 July 1974.

"Diffraction Gratings in Space Research - Problems and Accomplishments," Hunter, W. R., Informal meeting on Diffraction Gratings, Kyoto, Japan, 6 September 1974.

1684 "High Resolution Ly-α Observations of Comet Kohoutek by Skylab and Copernicus," Bohlin, J. D., Drake, J. F., Jenkins, E. B., and Keller, H. U., IAU Colloq. 25, Goddard Space Flight Center, Greenbelt, Maryland, 28 October - 1 November 1974.

1689 "Ultraviolet Solar Identifications Based on Extended Absorption Series Observed in the Laboratory Spectra of Si I," Moore, C. E., Tousey, R., Sandlin, G. D., Brown, C. M., Ginter, M. L., and Tilford, S. G., IAU Colloq. 27, 'Fourth Conf. on Ultraviolet and X-Ray Spectroscopy of Astrophysical and Laboratory Plasmas', Harvard University, Cambridge, Massachusetts, 9-11 September 1974.

1696 "A Catalog and Classification of Flares and Flare-Like Events Observed by the ATM XUV Spectrograph S082A and Spectroheliograph S082B," Scherrer, V. E., Tousey, R., and Sandlin, G. D., AAS, Solar Phys. Div., Boulder, Colorado, 20-22 January 1975.

1697 "Polar Plumes in XUV Emission-Line Corona," Bohlin, J. D., Purcell, J. D., Sheeley, N. R., Jr., and Tousey, R., AAS, Solar Phys. Div., Boulder, Colorado, 20-22 January 1975.

1698 "Macro-Spicules in He II 304 Å Over the Sun's Polar Cap," Bohlin, J. D., Vogel, S. N., Purcell, J. D., Sheeley, N. R., Jr., Tousey, R., and Van Hoosier, M. E., AAS, Solar Phys. Div., Boulder, Colorado, 20-22 January 1975.

1699 "Flare Mechanisms Based on the Current Limitation Concept," Spicer, D. S., AAS, Solar Phys. Div., Boulder, Colorado, 20-22 January 1975.

1700 "Absolute Solar UV Intensities 1680 Å to 2100 Å," Moe, O. K., Brueckner, G. E., Bartoe, J.-D. F., and Van Hoosier, M. E., AAS, Solar Phys. Div., Boulder, Colorado, 20-22 January 1975.

1701 "On the XUV Emissions in Solar Flares Observed with the ATM/NRL Spectroheliograph," Cheng, C. C. and Widing, K. G., AAS, Solar Phys. Div., Boulder, Colorado, 20-22 January 1975.

1703 "Observations from Skylab of the Density Dependent C III Multiplet at 1175 Å in Active and Quiet Regions and Above the Limb," Nicolas, K. and Brueckner, G. E., AAS, Solar Phys. Div., Boulder, Colorado, 20-22 January 1975.

1705 "The High-Energy Limb Event of January 17, 1974," Tousey, R., Bohlin, J. D., Moe, O. K., Purcell, J. D., and Sheeley, N. R., Jr., AAS, Solar Phys. Div., Boulder, Colorado, 20-22 January 1975.

1706 "Interpreting XUV Spectroheliograms in Terms of Coronal Magnetic Field Structures," Sheeley, N. R., Jr., Bohlin, J. D., Brueckner, G. E., Purcell, J. D., Scherrer, V. E., and Tousey, R., AAS, Solar Phys. Div., Boulder, Colorado, 20-22 January 1975.

1707 "Line Profiles of the Fe XXIV Emission at 192 Å and 255 Å in Solar Flares," Brueckner, G. E., Moe, O. K., and Van Hoosier, M. E., AAS, Solar Phys. Div., Boulder, Colorado, 20-22 January 1975.

1712 "The Super Heating Instability as a Trigger for Solar Flares," Tidman, D. A., Spicer, D. S., and Davis, J., AAS, Solar Phys. Div., Boulder, Colorado, 20-22 January 1975.

1714 "Forbidden Lines of Highly Ionized Iron in Solar Flare Spectra," Doschek, G. A., Sandlin, G. D., Brueckner, G. E., Van Hoosier, M. E., and Tousey, R., IAU Colloq. 27, 'Fourth Conf. on Ultraviolet and X-Ray Spectroscopy of Astrophysical and Laboratory Plasma', Harvard University, Cambridge, Massachusetts, 9-11 September 1974.

1716 "The XUV Sun as Observed by ATM S082," Tousey, R., AIAA/AGU Space Science Conf. on 'Scientific Experiments of Project Skylab', MSFC, Huntsville, Alabama, 30 October- 1 November 1974.

1718 "Classification of Flares and Flare-Like Events Observed by the ATM XUV Spectroheliograph S082A and Spectrograph S082B During the Skylab Missions," Scherrer, V. E. and Tousey, R., AIAA/AGU Space Science Conf. on 'Scientific Experiments of Project Skylab', MSFC, Huntsville, Alabama, 30 October-1 November 1974.

1726 "Structure and Temperature of Solar Flare Plasma," Scherrer, V. E. and Sandlin, G. D., Am. Phys. Soc., Washington, D. C., 28 April - 1 May 1975.

1731 "The Character and Temperature of a Coronal Transient: I. The Event of 25-27 August 1973," Bohlin, J. D., Hildner, E., and Hansen, R. T., COSPAR XVIII, Varna, Bulgaria, 29 May - 7 June 1975.

1738 "Experience with Schumann Type UV Film on Skylab," Van Hoosier, M. E., Bartoe, J.-D. F., Brueckner, G. E., Moe, O. K., Nicolas, K. R., and Tousey, R., Topical Meeting on 'Imaging in Astronomy', Harvard University, Cambridge, Massachusetts, 18-20 June 1975.

1739 "Limitations of Imaging Capabilities of Schumann Type UV Film," Bartoe, J.-D., Brueckner, G. E., and Van Hoosier, M. E., Topical Meeting on 'Imaging in Astronomy', Harvard University, Cambridge, Massachusetts, 18-20 June 1975.

1750 "A Resistive Screw Instability Model of a Solar Flare," Spicer, D. S., AAS, San Diego, California, 17-20 August 1975.

1752 "The Sun's Polar Caps as Coronal Holes; Their Sizes, Evolution, and Phenomenology During the Skylab Mission," Bohlin, J. D., Rubenstein, D. M., and Sheeley, N. R., Jr., AAS, San Diego, California, 17-20 August 1975.

1753 "Energy Release and Thermal Structure in Solar Flares," Cheng, C. C. and Widing, K. G., AAS, San Diego, California, 17-20 August 1975.

1754 "X-Ray Event of August 13-15, 1973," Scherrer, V. E., Sandlin, G. D., Sheeley, N. R., Jr., and Tousey, R., AAS, San Diego, California, 17-20 August 1975.

1756 "Skylab/ATM Observatins of Transient Events Having the GRF X-Ray and Microwave Character," Sheeley, N. R., Jr., Bohlin, J. D., Scherrer, V. E., and Tousey, R., AAS, San Diego, California, 17-20 August 1975.

1757 "Measured Variation of the XUV Line Widths and Intensities Near the Solar Limb," Moe, O. K. and Nicolas, K. R., AAS, San Diego, California, 17-20 August 1975.

1758 ""Evolution of XUV Plasmas in Solar Flares," Widing, K. G. and Cheng, C.C., AAS, San Diego, California, 17-20 August 1975.

1768 "Solar Flare Collisional Excitation Rate Coefficients," Tousey, R., Kepple, P. C., and Davis, J., AAS, San Diego, California, 17-20 August 1975.

1769 "Plasma Heating and Flare X-Rays," Davis, J., Kepple, P., Strickland, D., and Brueckner, G., AAS, San Diego, California, 17-20 August 1975.

1770 "Hydrodynamics of Electron Beam Deposition in Solar Flares," Bloomberg, H., Kepple, P. C., Davis, J., Boris, J. and Brueckner, G., AAS, San Diego, California, 17-20 August 1975.

1771 "Results from the NRL XUV Experiments on Skylab," Tousey, R., Opt. Soc. Am., Washington, D. C., 21-25 April 1974.

1772 "Maximum Efficiency of Ruled Concave Diffraction Gratings in the Ultraviolet," Mikes, T. L., Opt. Soc. Am., Houston, Texas, 15-18 October 1974.

1776 "Time Dependent Ionization Equilibrium and Line Emission from Ionized Iron Under Flare-Like Conditions," Kepple, P. and Davis, J., AGU, San Francisco, California, December 1974.

1777 "Transient Line Emission from Ionized Iron Under Flare-Like Conditions," Davis, J., Kepple, P., and Tousey, R., AAS, Solar Phys. Div., Boulder, Colorado, 20-22 January 1975.

1779 "The Source of Material Comprising a Mass Ejection Coronal Transient," Hildner, E., Gosling, J. T., Hansen, R. T., and Bohlin, J. D., AAS, San Diego, California, 17-20 August 1975.

1782 "Evidence for Magnetic Field Line Reconnection in the Lower Corona," Sheeley, N. R., Jr. 1975 Fall Annual Meeting of the American Geophys. Union, San Francisco, California, 8-12 Dec. 1975.

1789 "Energy Released by the Interaction of Coronal Magnetic Fields," Sheeley, N. R., Jr., 'Flare Build-up Study Workshop', Falmouth, Massachusetts, 8-11 September 1975.

1821 "The Locations, Sizes and Evolution of Coronal Holes," Bohlin, J. D., International Symp. on Solar-Terrestrial Physics, Boulder, Colorado, 7-18 June 1976.

1892 "Dynamics of the Solar Atmosphere from the Lower Chromosphere into the Corona," Brueckner, G. E. and Bartoe, J.-D. F. I.A.U. Colloquium No. 36, 6-10 September 1976, Nice, France.

1893 "Fine Structure of the Solar Atmosphere from the Temperature Minimum into the Corona," Brueckner, G. E. and Bartoe, J.-D. F. I.A.U. Colloquium No. 36, 6-10 September 1976, Nice, France.

VI. COLLOQUIA

1465 "Apollo Telescope Mount Project", Winter, T. C., National Bureau of Standards, Washington, D. C., 27 February 1969.

1635 "The Sun in Lyman-Alpha", Prinz, D. K., National Capitol Section of the Amateur Astronomers of America, 2 February 1974.

1661 "NRL/ATM Observations with the XUV Spectroheliograph", Sheeley, N. R., Jr., Sacramento Peak Observatory, Sunspot, New Mexico, 15 March 1974.

1708 "Observations of the Sun in XUV with ATM", Tousey, R., Goddard Space Flight Center, Greenbelt, Maryland, 6 December 1974.

"Observations of the Sun in XUV with ATM", Tousey, R., University of Michigan, Ann Arbor, Michigan, 12 February 1975.

1728 "Preliminary Results from the NRL XUV Spectroheliograph and Spectrograph", Bohlin, J. D., University of Maryland, College Park, Maryland, 26 February 1975.

1737 "Behavior of Coronal Magnetic Fields as Deduced from Skylab Observations", Sheeley, N. R., Jr. High Altitude Observatory, Boulder, Colorado, 14 March 1975.

1767 "Macrospicules, Polar Plumes, Coronal Holes, and Other Assorted Phenomena of the Sun's Polar Cap", Bohlin, J. D., National Capital Astronomers, Washington, D.C., 6 September 1975.

"The Structure and Development of Coronal Magnetic Fields as Deduced from Skylab Observations", Sheeley, N. R., Jr., Los Alamos Scientific Laboratory, Los Alamos, New Mexico, 21 March 1975.

VII. OTHER PUBLICATIONS

1438 "Effects of High-Energy Protons on Photographic Film", Winter, T. C., Jr. and Brueckner, G. E. 1969, NRL Report No. 6797.

1455 "DOD Solar Experiments in NASA Prototype Space Station", Winter, T. C., Jr. 1970, Military Review, February, p. 58.

1469 "Radiation Light Sources for Stellar Telescope Calibration from 700 Å to 7000 Å", Hunter, W.R. 1969, NRL Progress Report, September, p. 1.

1476 "Spectroscopy in the Space Science Division of the Naval Research Laboratory", Hunter, W. R. and Winter, T. C., Jr. 1969, ONR Reviews.

1500 "Schumann-Type Photographic Film: Preliminary Environment Test Results", Winter, T. C. and Van Hoosier, M. E. 1970, Report of NRL Progress, May.

1504 "Schumann-Type Photographic Film: Preliminary Environment Test Results", Winter, T. C. and Van Hoosier, M. E. 1970, NRL Report No. 7072.

1764 "The NRL Solar Experiments in the Apollo Telescope Mount of Skylab", Tousey, R. 1975, Report of NRL Progress, April, p. 1.

1823 "Electron Impact Excitation Rate Coefficients for Ions of Solar Interest", Kepple, P. C., Davis, J. and Blaha, M. 1975, NRL Memorandum Report 3171, Nov.

1890 "A Spectral Atlas of the Sun Between 1175Å and 2100Å," Kjeldseth Moe, O., Van Hoosier, M. E., Bartoe, J.-D. F. and Brueckner, G. E. 1976, NRL Report No. 8057.

1903 "An Unstable Arch Model of a Solar Flare," Spicer, D. S. 1976, NRL Report No. 8036.

1896 "Holes in the Coronal," Bohlin, J. D. 1976, Natural History 85, pp. 69-70.

VIII. *OTHER TALKS*

"The ATM Project", Tousey, R., After-dinner talk at Second International Conference on Vacuum Ultraviolet and X-Ray Spectroscopy of Laboratory and Astrophysical Plasmas, University of Maryland, College Park, Maryland, 25 March 1968.

"Spectroscopy from Space Vehicles", Tousey, R., Delaware Valley Section of the Society for Applied Spectroscopy, Philadelphia College of Textile Science, Philadelphia, Pennsylvania, 15 October 1968.

1442 "Highlights of the Naval Research Laboratory Solar Spectroscopy Program", Winter, T. C., Jr., Department of Aerospace Engineering, University of Connecticut, Storrs, Connecticut, 12 December 1967.

Ibid., Science and Engineering Council, Santa Barbara, California, 1 May 1968.

1436 "Observations of the Sun", Winter, T. C., Jr., Science Institute Thomas Jefferson High School, Alexandria, Virginia, 10 July 1968 and 27 June 1969.
Ibid., George Mason High School, Falls Church, Virginia, 28 October 1968.
Ibid., Washington Lee High School, Arlington, Virginia, 19 December 1968.
Ibid., Swanson Junior High School, Arlington, Virginia, 13 February 1969.
Ibid., Roosevelt High School, Seattle, Washington, 7 March 1969.
Ibid., Gonzaga High School, Science Club at the Naval Research Laboratory, Washington, D. C., 30 April 1969.

1486 "The NRL Solar Observing Program", Scherrer, V. E., Air Force Training Seminar, NRL, 1970-1975 (quarterly).

"NRL Skylab Experiments", Scherrer, V. E., NRL public presentations, 1970-1975 (bi-monthly).

1511 "Apollo Telescope Mount - The First Manned Orbiting Laboratory", Bohlin, J. D. , Hartford County Astronomical Society, Hartford Junior College, Maryland, 17 December 1970.

1568 "Skylab Scientific Acheivements", Schumacher, R.J., Teacher's Seminar, Alvernia College, Reading, Pennsylvania, 17 July 1972.

1659 "NRL's Solar Experiments on Skylab", Schumacher, R. J., Sertoma Club, Lancaster, Pennsylvania, 10 May 1974.

1775 "The Solar Experiments on Skylab", Tousey, R., Boise State College, Orlando, Florida, 13 May 1973.

1818 "Some Aspects of Skylab", Sitterly, Charlotte M., Eistophos Science Club, Washington, D. C., 9 Jan. 1976.

IX. MISCELLANEOUS APPEARANCES OF NRL MATERIAL

The New Sun, by Jack Eddy, to be published in NASA Skylab series.

The Amazing Universe, by Herbert Friedman, published by National Geographic Society.

National Geographic, "The Sun as Never Seen Before", Vol. 146, No. 4, p. 494, October 1974.
"Man's Conquest of Space", by William R. Shelton, p. 171.

Aviation Week and Space Technology
"Skylab Telescope Imagery Shown", p. 51, 11 June 1973.
"Skylab Instrument Reveals New Solar Details", Vol. 99, No. 6, p. 6 August 1973.
"Skylab Enriches Solar Data Hundredfold", Vol. 99, No. 22, p. 16, 26 November 1973.
"The Sun", Vol. 100, No. 2, p. 39, 14 January 1974.
"Apollo Telescope Shuttle Mission Studied", p. 14, 15 April 1974.
"Skylab ATM Imagery Shows Seething Sun", Vol. 101, No. 13, p. 24, 30 September 1974.

Scientific American, "Eruptive Prominence of August 21, 1973", p. 45, September 1975.

Christian Science Monitor, "Skylab - An Accounting: The Sun", p. F1, 7 February 1974.

Science News
"Peeking Beneath the Sun's Skirts", Vol. 104, No. 7/8, p. 120, 18/25 August 1973.
"The UV Sun Photographed from Skylab", Vol. 106, No. 5, p. 65, 3 August 1974.
"Cosmic Chroma", Vol. 106, No. 8/9, p. 122, 24/31 August 1974.
"The Inconstant Sun," cover, 6 March 1976.
"Mammoth Quakes Jostle the Sun", Vol. 110, No. 8, p. 113, 21 August 1976.

New Scientist,
"Helium goes up-with a kink-500,000 miles", p. 607, 29 November 1973.
"The Sun from Skylab", p. 738, 21 March 1974.
"New Science in The Solar System", Special Review, cover and pp. 7/8, 1975.

Sky and Telescope
"Some Results from Skylab Solar Experiments", Vol. 48, No. 1, July 1974.
"Giant Spicules on the Sun", Vol. 49, No. 4, p. 213, April 1975.
"Extreme Ultraviolet Coronal Observations", Vol. 50, No. 1, p. 11, July 1975.

Astronautics and Aeronautics
"Instruments, Systems, and Manned Operations of the Apollo Telescope Mount", p. 50, June 1971.
"Skylab II, Seeing the Sun in a Different Light", p. 36, February 1974.
Cover, May 1974.

Advances in the Astronautical Science, Vol. 31, 'The Skylab Results' (1975).
"A Discussion on the Development of the ATM Solar Instruments", p. 897.
"Skylab Apollo Telescope Mount Calibration Rocket Project", p. __.

Journal of the Astronomical Society of the Pacific, "A New Type of Solar Chromospheric Feature", Vol. 4, Sept./Oct., p. 26 (photo p. 27).

1975 Nature/Science Annual, "From Skylab: A Quirky Sun", p. 12, Time-Life Books (1974).

Popular Science, "Secrets of the Sun", Vol. 204, No. 5, p. 103, May 1974.

The British Journal of Photography, "Images from Space", cover, 3 May 1974.

Tages Anzeiger, "Die Sonne and wie wenig wir von ihr wissen", Vol. 19, No. 11, p. 34, May 1974.

Electro-Optical Systems Design,
"Optics in the Vacuum Ultraviolet", cover and p. 16, November 1973.
"Vacuum Ultraviolet Detectors and Sources", p. 24, 17 November 1973.

Mainliner, "Solar Power", Vol. 18, No. 12, p. 22, December 1974.

Heating/Piping/Air Conditioning, "Solar Energy in the 1970's", Vol. 47, No. 7, cover and p. 31, July 1975.

Analog/Science Fiction, Science Fact
"Skylab", Vol. LXXXIX, No. 1, p. 99, March 1972.
Ibid., No. 2, p. 95, April 1972.

New Horizons, NASA Publication, p. 36-37

Technology Review, cover, Jan. 1976

All Hands, "Lending a Hand in Exploring the Mysteries of Space", cover and p. 33, June 1974.

BBRC 1975 Appointment Calendar, "The Sun We Live By".
BBRC 1966 Appointment Calendar, "Incandescent Cascade".

NRL Labstracts
No. 35, 4 September 1972
No. 31, 30 July 1973.
No. 33, 13 August 1973.
No. 37, 10 September 1973.
No. 44, 29 October 1973.
No. 49, 3 December 1973.
No. 8, 25 February 1974.
No. 14, 8 April 1974.

Nation's Business, "Energy," cover, September 1976.

Forskning och Framsteg 6, "Solen jordens fusions-reaktor", cover and p. 11, 1974.

ODU Magazine, cover, Summer 1975.

NOAA Technical Report ERL 357-SEL 37, March 1976, NRL picture.

NRL Instruction Book No. 161, "Flare Atlas and Users Instruction Guide for NRL Flare Data, 15 June 5 and 7 September 1973," V. E. Scherrer and G. D. Sandlin, May 1976.

(This listing is incomplete, and includes only those publications referring to NRL ATM material that have been brought to our attention.)

APPENDIX B

S082A/ATM Documents at NRL

(1) NRL/ATM Exposure Catalog

Vol. I (Rev A)	Time Listing
Vol. II (Rev A)	Joint Observing Program Listing
Vol. III (Rev A)	Target Listing

These three volumes list the time, JOP, step and building block, the target, exposure time and wavelength band of each S082A (and S082B) exposure. They also include notes identifying special events, sequences and pointings.

(2) NRL/ATM Mission Engineering Data Book (Rev A)

This catalog (one volume for each of the six S082A cameras) lists: the opening and closing time of the camera shutter for each exposure, and the corresponding exact exposure time, wavelength band, and instrument operating mode; other instruments operating at the time, and their modes; and a verification of correct temperatures throughout the S082A instrument during the exposure.

For each exposure, the values are also given for the reconstructed ("correct") ATM roll position, ROLL or Γ_{RR}, the maximum excursion of any disturbance in the ATM pointing position during the exposure, the S082B BIAS, the beta angle of the Skylab orbit, the altitude of both the Skylab and its line of sight to the sun, and the orbit number.

This catalog also includes traceability charts for each film strip, the temperature and radiation histories of each camera, and transmission curves and pinhole maps for each aluminum filter.

(3) ATM Mission Operation Log (Vols. 1-5, and magnetic tape)

This catalog, prepared for S055, lists the time, pointing, operating modes and other information, for all observations by every ATM instrument (S052, S054, S055, S056, S082A, S082B and Hα1).

It should be noted that the ATM roll position values throughout

this catalog are not the reconstructed ("correct") values.

(4) <u>User's Guide for Reconstructed Roll Reference</u> (γ_{RR})

(5) <u>Reconstructed Roll Reference Data</u> (6 vols.)

(6) <u>Roll Reference Determination Summary Report</u>

(7) <u>Skylab Apollo Telescope Mount Pointing Reference Handbook</u>

The first three of these documents provide information from which a user can determine the correct value of the ATM roll position (Γ_{RR} = GAMMARR=EXP ROLL=ROLL), and ascertain its uncertainty (~ +40 arc-min). The roll value corresponds to the angle, in arc-min, between solar north and the UP pointing axis of the ATM (parallel to the axis of the S082B slit, and at right angles to the S055 raster lines). The error and uncertainty of the telemetered values developed as a result of the failure of the star-tracker roll reference during the mission.

The pointing bias required to coalign the center of the S082B slit with the ATM fine sun-sensor, and its variation over the mission is discussed in the fourth document.

(8) <u>ATM JOP Summary Sheets (with Shopping Lists), SL 1/2, SL-3, SL-4.</u>

This set of documents consists of copies of plastic sheets used by the astronaut operating the ATM control panel. These sheets, with guidelines for their use in each of the JOPs, provided explicit, self-contained, step-by-step instructions for pointing and operating the ATM experiments in unison. Photographic examples of solar features, and abbreviated descriptions of desired pointings are shown together with various combinations ("Building Blocks") of simultaneously operated instrument modes. Each sheet summarized all the information needed by Skylab crews and solar scientists to properly coordinate observations with the daily scientific objectives. A schedule was telemetered every morning to the crews, which gave suggestions for observations and operating modes, and guidelines for responding to flares and other interesting events.

The sheets evolved through an iterative process, during many months of practice on the ATM simulator, and much discussion in meetings between scientists representing the ATM experimenter groups. The sheets changed from one manned phase to the next. New JOPs were added, a few were dropped, and the operating strategies were made more efficient and flexible. JOP and step numberings are therefore not always the same from one mission to another. A **simplified listing of Joint Observing Programs for SL-3 follows:**

JOP 1 Chromospheric Network	JOP 10 Lunar Libration Clouds
JOP 2 Active Regions	JOP 11 Chromospheric Oscillations and Heating
JOP 3 Flares	JOP 12 Calibrations
JOP 4 Prominences	JOP 13 Night Sky Objects
JOP 5 Constant Latitude Studies	JOP 14 Eclipse (deleted for SL-3)
JOP 6 Synoptic Observations	JOP 15 Coronal Holes
JOP 7 Atmospheric Extinction	
JOP 8 Coronal Transients	JOP 16 Disk Transients
JOP 9 Solar Wind	JOP 17 Bright Points

Because of the formality of the NASA mission protocol which regulated the implementation of the JOP programs, a sheet of informal "Shopping List" items was included on each of the last two manned phases. These provided the astronaut with a list of pet projects for each of the experimenter groups, that he could conduct at his discretion when time was available.

(9) ATM Experiments Reference Book (SL 1/2, SL-3, SL-4)

This document is a copy of a book used as a training text and carried on board Skylab for crew reference during each manned phase. It provides a detailed discussion of the background , rationale and scientific objectives of each of the JOPs. Specific terms are defined, and photographs are given of features as they would appear in Hα and XUV emissions. Graphs and tables of filter transmissions, detector positions of XUV lines, and other information useful to the ATM operator are included. In addition, technical data is included on each of the ATM instruments and monitors, as well as teleprinter abbreviations, and ATM scheduling conventions.

(10) NOAA/Skylab Solar Data Books

Several dozen loose-leaf volumes containing copies of the solar photographs and data provided ATM experimenters by NOAA during the Skylab mission.

(11) Skylab ATM H-Alpha Atlas, and Atlas Guide (49 vols.)

Copies of photographs taken by the Hα telescope on ATM (Hα1). A print is included with a scale of 2 arc-min per inch, for the beginning and end of each orbit, for each significant ATM pointing change, and, when no pointing change occurred, at 15 minute intervals, for the entire Skylab mission.

(12) NRL Science Console Execution Log Books

Roughly two dozen loose-leaf volumes containing information pertinent to the operation of NRL's two instruments on the ATM, logged in real-time by NRL representatives who manned consoles in the mission control center round-the-clock. These logs contain summary charts of the orbits in which the ATM was operated, and the as-flown schedule of ATM operations relative to orbital sun-rise and sun-set. Of particular value to users of S082A data, are notes of crew-reported solar events, operating errors, and special observations with the S082A instrument.

(13) Skylab Astronaut-Ground Voice Transcripts

This is a complete set of all voice communication between the Skylab astronauts and the ground, of both live conversations and comments taped on an onboard recorder and dumped. In addition, a set of transcripts is available edited for ATM-related communications.

(14) Skylab Operational Handbook, (Vol. I and II)

Detailed diagrams of ATM instruments, as well as the ATM, and the checklists of their operating procedures.

Appendix C*

Camera No A1 SL 1/2

Log Sequence

ATM No.	Film Roll Strip Cut	Dev Run	ATM No.	Film Roll Strip Cut	Dev Run	ATM No.	Film Roll Strip Cut	Dev Run	ATM No.	Film Roll Strip Cut	Dev Run
1A001	19-17	1									
1A002	19-16										
1A003	19-14										
1A004	19-13										
1A005	19-12										
1A006	19-11										
1A007	19-10										
1A008	19-9										
1A009	19-8										
1A010	19-7										
1A011	19-6										
1A012	19-5										
1A013	20-91										
1A014	20-90										
1A015	20-89										
1A016	20-88										
1A017	20-87										
1A018	20-86										
1A019	20-85	1									
1A020	19-18	2									
1A021	18-20	2									

Film Data	
Roll No.	Film Type
18	104-06-05
19	104-06-05
20	104-06-05

*Appendix C compiled at NRL by Warren H. Funk.

Camera No A2 SL 1/2

Sequence Log

ATM No	Film Roll-Strip Cut	Dev Run	ATM No	Film Roll-Strip Cut	Dev Run	ATM No	Film Roll-Strip Cut	Dev Run	ATM No	Film Roll-Strip Cut	Dev Run
1A201	14-9	A	1A253	15-51	2	1A305	14-28	5	1A357	14-85	4
1A202	14-8	1	1A254	15-50		1A306	14-29		1A358	14-86	
1A203	14-7		1A255	15-49		1A307	14-30		1A359	14-87	
1A204	14-6		1A256	15-48		1A308	14-31		1A360	14-88	
1A205	14-5		1A257	15-46		1A309	14-32		1A361	14-89	
1A206	15-102		1A258	15-45		1A310	14-33		1A362	14-90	
1A207	15-101		1A259	15-44		1A311	14-34		1A363	12-5	
1A208	15-100		1A260	15-43		1A312	14-35		1A364	12-6	
1A208	15-99		1A261	15-42		1A313	14-37		1A365	12-7	
1A210	15-98		1A262	15-41		1A314	14-38		1A366	12-8	
1A211	15-97		1A263	15-40		1A315	14-39		1A367	12-9	
1A212	15-96		1A264	15-39		1A316	14-40		1A368	12-10	
1A213	15-95		1A265	15-38		1A317	14-41		1A369	12-11	
1A214	15-94		1A266	15-36		1A318	14-42		1A370	12-12	
1A215	15-93		1A267	15-35		1A319	14-43		1A371	12-13	
1A216	15-91		1A268	15-34		1A320	14-44		1A372	12-14	
1A217	15-90		1A269	15-33		1A321	14-45		1A373	12-16	
1A218	15-89		1A270	15-32		1A322	14-46		1A374	12-17	
1A219	15-88		1A271	15-31		1A323	14-48		1A375	12-18	
1A220	15-87		1A272	15-30		1A324	14-49		1A376	12-19	
1A221	15-86		1A273	15-29		1A325	14-50		1A377	12-20	
1A222	15-85		1A274	15-28		1A326	14-51		1A378	12-21	
1A223	15-84		1A275	15-27		1A327	14-52		1A379	12-22	
1A224	15-83		1A276	15-26		1A328	14-53		1A380	12-23	
1A225	15-82		1A277	15-24		1A329	14-54		1A381	12-24	4
1A226	15-80		1A278	15-23		1A330	14-55		1A382	12-25	3
1A227	15-79		1A279	15-22		1A331	14-56		1A383	12-27	
1A228	15-78		1A280	15-21		1A332	14-57		1A384	12-28	
1A229	15-77		1A281	15-20	2	1A333	14-59		1A385	12-29	
1A230	15-76		1A282	15-19	3	1A334	14-60		1A386	12-30	
1A231	15-75		1A283	15-18		1A335	14-61		1A387	12-31	
1A232	15-74		1A284	15-17		1A336	14-62		1A388	12-32	
1A233	15-73		1A285	15-16		1A337	14-63		1A389	12-33	
1A234	15-72		1A286	15-14		1A338	14-64		1A390	12-34	
1A235	15-71		1A287	15-13		1A339	14-65		1A391	12-35	
1A236	15-69		1A288	15-12		1A340	14-66		1A392	12-36	
1A237	15-68		1A289	15-11		1A341	14-67	5	1A393	12-38	
1A238	15-67		1A290	15-10		1A342	14-68	4	1A394	12-39	
1A239	15-66		1A291	15-9		1A343	14-70		1A395	12-45	
1A240	15-65		1A292	15-8		1A344	14-71		1A396	12-46	
1A241	15-64	1	1A293	15-7		1A345	14-72		1A397	14-15	
1A242	15-63	2	1A294	15-6		1A346	14-73		1A398	14-14	
1A243	15-62		1A295	15-5		1A347	14-74		1A399	14-13	
1A244	15-61		1A296	14-17		1A348	14-75		1A400	14-12	
1A245	15-60		1A297	14-18		1A349	14-76		1A401	14-11	
1A246	15-58		1A298	14-19		1A350	14-77		1A402	14-22	3
1A247	15-57		1A299	14-20		1A351	14-78		1A403	14-10	A
1A248	15-56		1A300	14-21	3	1A352	14-79				
1A249	15-55		1A301	14-23	5	1A353	14-81				
1A250	15-54		1A302	14-24		1A354	14-82				
1A251	15-53		1A303	14-25		1A355	14-83				
1A252	15-52		1A304	14-27		1A356	14-84				

Film Data

Roll No.	Film Type
12	104-06-05
14	104-06-05
15	104-06-05

Camera No A2* SL-3

Sequence Log

ATM No.	Film Roll Strip Cut	Dev Run	ATM No.	Film Roll Strip Cut	Dev Run	ATM No.	Film Roll Strip Cut	Dev Run	ATM No	Film Roll Strip Cut	Dev Run
2A001	8-7	3	2A051	7-51		2A101	8-23	3	2A151	8-78	
2A002	8-6	1	2A052	7-50		2A102	8-24	3	2A152	8-79	
2A003	8-5	A	2A053	7-49		2A103	8-25	5	2A153	8-80	
2A004	7-102	1	2A054	7-47		2A104	8-27		2A154	9-5	
2A005	7-101		2A055	7-46		2A105	8-28		2A155	9-6	
2A006	7-100		2A056	7-45		2A106	8-29		2A156	9-7	
2A007	7-99		2A057	7-44		2A107	8-30		2A157	9-8	
2A008	7-98		2A058	7-43		2A108	8-31		2A158	9-9	
2A009	7-97		2A059	7-42		2A109	8-32		2A159	9-10	
2A010	7-96		2A060	7-41		2A110	8-33		2A160	9-11	
2A011	7-95		2A061	7-40		2A111	8-34		2A161	9-12	
2A012	7-94		2A062	7-39		2A112	8-35		2A162	9-13	
2A013	7-93		2A063	7-38		2A113	8-36		2A163	9-14	
2A014	7-91		2A064	7-37		2A114	8-38		2A164	9-16	
2A015	7-90		2A065	7-35		2A115	8-39		2A165	9-17	
2A016	7-89		2A066	7-34		2A116	8-40		2A166	9-18	
2A017	7-88		2A067	7-33		2A117	8-41		2A167	9-19	
2A018	7-87		2A068	7-32		2A118	8-42		2A168	9-20	
2A019	7-86		2A069	7-31		2A119	8-43		2A169	9-21	
2A020	7-85		2A070	7-30		2A120	8-44		2A170	9-22	
2A021	7-84		2A071	7-29		2A121	8-45		2A171	9-23	
2A022	7-83		2A072	7-28		2A122	8-46		2A172	9-24	
2A023	7-82		2A073	7-27		2A123	8-47		2A173	9-25	
2A024	7-80		2A074	7-25		2A124	8-49		2A174	9-27	
2A025	7-79		2A075	7-24		2A125	8-50		2A175	9-28	
2A026	7-78		2A076	7-23		2A126	8-51		2A176	9-29	
2A027	7-77		2A077	7-22		2A127	8-52		2A177	9-30	
2A028	7-76		2A078	7-21		2A128	8-53		2A178	9-31	
2A029	7-75		2A079	7-20		2A129	8-54		2A179	9-32	
2A030	7-74		2A080	7-19	2	2A130	8-55		2A180	9-33	
2A031	7-73		2A081	7-18	3	2A131	8-56		2A181	9-34	
2A032	7-72		2A082	7-17		2A132	8-57		2A182	9-35	
2A033	7-71		2A083	7-16		2A133	8-58		2A183	9-36	
2A034	7-69		2A084	7-14		2A134	8-60		2A184	9-38	
2A035	7-68		2A085	7-13		2A135	8-61		2A185	9-39	4
2A036	7-67		2A086	7-12		2A136	8-62		2A186	9-40	3
2A037	7-66		2A087	7-11		2A137	8-63		2A187	9-41	
2A038	7-65		2A088	7-10		2A138	8-64		2A188	9-42	
2A039	7-64		2A089	7-09		2A139	8-65		2A189	9-43	
2A040	7-63	1	2A090	7-08		2A140	8-66		2A190	9-44	
2A041	7-62	2	2A091	7-7		2A141	8-67		2A191	9-45	
2A042	7-61		2A092	7-6		2A142	8-68		2A192	9-46	
2A043	7-60		2A093	7-5		2A143	8-69		2A193	9-47	
2A044	7-58		2A094	8-16		2A144	8-71		2A194	9-48	
2A045	7-57		2A095	8-17		2A145	8-72	5	2A195	9-49	
2A046	7-56		2A096	8-18		2A146	8-73	4	2A196	8-14	
2A047	7-55		2A097	8-19		2A147	8-74		2A197	8-13	
2A048	7-54		2A098	8-20		2A148	8-75		2A198	8-12	
2A049	7-53		2A097	8-21		2A149	8-76		2A199	8-11	
2A050	7-52		2A100	8-22	3	2A150	8-77		2A200	8-10	
									2A201	8-9	
									2A202	8-8	3

Film Data	
Roll No.	Film Type
7	104-06-07
8	104-06-07
9	104-06-07

Camera No. A3 SL-3

Sequence Log

ATM No.	Film Roll - Strip Cut	Dev Run
2A301	4-109	1
2A302	4-108	A
2A303	4-107	1
2A304	4-106	
2A305	4-105	
2A306	4-104	
2A307	4-102	
2A308	4-101	
2A309	4-100	
2A310	4-99	
2A311	4-98	
2A312	4-97	
2A313	4-96	
2A314	4-95	
2A315	4-94	
2A316	4-93	
2A317	4-91	
2A318	4-90	
2A319	4-89	
2A320	4-88	
2A321	4-87	
2A322	4-86	
2A323	4-85	
2A324	4-84	
2A325	4-83	
2A326	4-82	
2A327	4-80	
2A328	4-79	
2A329	4-78	
2A330	4-77	
2A331	4-76	
2A332	4-75	
2A333	4-74	
2A334	4-73	
2A335	4-72	
2A336	4-71	
2A337	4-69	
2A338	4-68	
2A339	4-67	
2A340	4-66	1
2A341	4-65	2
2A342	4-64	
2A343	4-63	
2A344	4-62	
2A345	4-61	
2A346	4-60	
2A347	4-58	
2A348	4-57	
2A349	4-56	
2A350	4-55	

ATM No.	Film Roll - Strip Cut	Dev Run
2A351	4-54	
2A352	4-53	
2A353	4-52	
2A354	4-51	
2A355	4-50	
2A356	4-49	
2A357	4-47	
2A358	4-46	
2A359	4-45	
2A360	4-44	
2A361	4-43	
2A362	4-42	
2A363	4-41	
2A364	4-40	
2A365	4-39	
2A366	4-38	
2A367	4-36	
2A368	4-35	
2A369	4-34	
2A370	4-33	
2A371	4-32	
2A372	4-31	
2A373	4-30	
2A374	4-29	
2A375	4-28	
2A376	4-27	
2A377	4-25	
2A378	4-24	
2A379	4-23	
2A380	4-22	2
2A381	4-21	3
2A382	4-20	
2A383	4-19	
2A384	4-18	
2A385	4-17	
2A386	4-16	
2A387	4-14	
2A388	4-13	
2A389	4-12	
2A390	4-11	
2A391	4-10	
2A392	4-9	
2A393	4-8	
2A394	4-7	
2A395	4-6	
2A396	4-5	
2A397	4-115	
2A398	4-116	
2A399	4-117	
2A400	4-118	

ATM No.	Film Roll - Strip Cut	Dev Run
2A401	4-119	3
2A402	4-120	5
2A403	4-121	
2A404	4-122	
2A405	4-123	
2A406	6-5	
2A407	6-6	
2A408	6-7	
2A409	6-8	
2A410	6-9	
2A411	6-10	
2A412	6-11	
2A413	6-12	
2A414	6-13	
2A415	6-14	
2A416	6-16	
2A417	6-17	
2A418	6-18	
2A419	6-19	
2A420	6-20	
2A421	6-21	
2A422	6-22	
2A423	6-23	
2A424	6-24	
2A425	6-25	
2A426	6-27	
2A427	6-28	
2A428	6-29	
2A429	6-30	
2A430	6-31	
2A431	6-32	
2A432	6-33	
2A433	6-34	
2A434	6-35	
2A435	6-36	
2A436	6-38	
2A437	6-39	
2A438	6-40	
2A439	6-41	
2A440	6-42	5
2A441	6-43	4
2A442	6-44	
2A443	6-45	
2A444	6-46	
2A445	6-47	
2A446	6-49	
2A447	6-50	
2A448	6-51	
2A449	6-52	
2A450	6-53	

ATM No.	Film Roll - Strip Cut	Dev Run
2A461	6-54	
2A452	6-55	
2A453	6-56	
2A454	6-57	
2A455	6-59	
2A456	6-60	
2A457	6-61	
2A458	6-62	
2A459	6-63	
2A460	6-64	
2A461	6-65	
2A462	6-66	
2A463	6-67	
2A464	6-68	
2A465	6-69	
2A466	6-71	
2A467	6-72	
2A468	6-73	
2A469	6-74	
2A470	6-75	
2A471	6-76	
2A472	6-77	
2A473	6-78	
2A474	6-79	
2A475	6-80	
2A476	6-82	
2A477	6-83	
2A478	6-84	
2A479	6-85	
2A480	6-86	4
2A481	6-87	3
2A482	6-88	
2A483	6-89	
2A484	6-90	
2A485	6-91	
2A486	6-93	
2A487	6-94	
2A488	6-95	
2A489	6-96	
2A490	6-97	
2A491	6-98	
2A492	6-99	
2A493	6-100	
2A494	6-101	
2A495	6-102	
2A496	6-103	
2A497	6-104	
2A498	6-105	
2A499	6-111	
2A600	4-113	
2A601	4-112	
2A602	4-111	
2A503	4-110	3

Film Data	
Roll No.	Film Type
4	104-06-06
6	104-06-06

Camera No A 4
Sequence Log

ATM No.	Film Roll Strip Cut	Dev Run	ATM No.	Film Roll Strip Cut	Dev Run	ATM No.	Film Roll Strip Cut	Dev Run	ATM No.	Film Roll Strip Cut	Dev Run
3A001	6A-5	2	3A051	1A-27		3A101	6A-73	2	3A151	6B-52	
3A002	1A-80		3A052	1A-25		3A102	6A-74		3A152	6B-53	
3A003	1A-79		3A053	1A-24		3A103	6A-75		3A153	6B-54	
3A004	1A-78		3A054	1A-23		3A104	6A-76		3A154	6B-55	
3A005	1A-77		3A055	1A-22		3A105	6A-77		3A155	6B-56	
3A006	1A-76		3A056	1A-21		3A106	6A-78		3A156	6B-57	
3A007	1A-75		3A057	1A-20		3A107	6A-79		3A157	6B-58	
3A008	1A-74		3A058	1A-19		3A108	6B-5		3A158	6B-60	
3A009	1A-73		3A059	1A-18		3A109	6B-6		3A159	6B-61	
3A010	1A-72		3A060	1A-17		3A110	6B-7	2	3A160	6B-62	
3A011	1A-71		3A061	1A-16		3A111	6B-8	3	3A161	6B-63	
3A012	1A-69		3A062	1A-14		3A112	6B-9		3A162	6B-64	
3A013	1A-68		3A063	1A-13		3A113	6B-10		3A163	6B-65	
3A014	1A-67		3A064	1A-12		3A114	6B-11		3A164	6B-66	
3A015	1A-66		3A065	1A-11		3A115	6B-12		3A165	6B-67	
3A016	1A-65		3A066	1A-10		3A116	6B-13		3A166	6B-68	
3A017	1A-64		3A067	1A-9		3A117	6B-15		3A167	6B-69	
3A018	1A-63		3A068	1A-8		3A118	6B-16		3A168	6B-71	
3A019	1A-62		3A069	1A-7		3A119	6B-17		3A169	6A-84	
3A020	1A-61		3A070	1A-6	1	3A120	6B-18		3A170	6A-85	
3A021	1A-60		3A071	6A-38	3	3A121	6B-19		3A171	6A-86	
3A022	1A-58		3A072	6A-39		3A122	6B-20		3A172	6A-87	5
3A023	1A-57		3A073	6A-40		3A123	6B-21		3A173	6A-88	4
3A024	1A-56		3A074	6A-41		3A124	6B-22		3A174	6A-33	
3A025	1A-55		3A075	6A-42		3A125	6B-23		3A175	6A-32	
3A026	1A-54		3A076	6A-43		3A126	6B-24		3A176	6A-31	
3A027	1A-53		3A077	6A-44		3A127	6B-25		3A177	6A-30	
3A028	1A-52		3A078	6A-45		3A128	6B-27		3A178	6A-29	
3A029	1A-51		3A079	6A-46		3A129	6B-28		3A179	6A-28	
3A030	1A-50	2	3A080	6A-48		3A130	6B-29		3A180	6A-27	
3A031	1A-49	1	3A081	6A-49		3A131	6B-30	3	3A181	3-1	
3A032	1A-47		3A082	6A-50		3A132	6B-31	5	3A182	6A-26	
3A033	1A-46		3A083	6A-51		3A133	6B-32		3A183	6A-24	
3A034	1A-45		3A084	6A-52		3A134	6B-33		3A184	6A-23	
3A035	1A-44		3A085	6A-53		3A135	6B-34		3A185	6A-22	
3A036	1A-43		3A086	6A-54		3A136	6B-35		3A186	6A-21	
3A037	1A-42		3A087	6A-55		3A137	6B-36		3A187	6A-20	
3A038	1A-41		3A088	6A-56		3A138	6B-38		3A188	6A-19	
3A039	1A-40		3A089	6A-57		3A139	6B-39		3A189	6A-18	
3A040	1A-39		3A090	6A-59	3	3A140	6B-40		3A190	6A-17	
3A041	1A-38		3A091	6A-60	4	3A141	6B-41		3A191	6A-16	
3A042	1A-36		3A092	6A-61		3A142	6B-42		3A192	6A-14	
3A043	1A-35		3A093	6A-62		3A143	6B-43		3A193	6A-13	
3A044	1A-34		3A094	6A-63		3A144	6B-44		3A194	9-5	
3A045	1A-33		3A095	6A-64		3A145	6B-45		3A195	9-6	
3A046	1A-32		3A096	6A-67		3A146	6B-46		3A196	9-7	
3A047	1A-31		3A097	6A-68		3A147	6B-47		3A197	9-8	
3A048	1A-30		3A098	6A-70		3A148	6B-49		3A198	6A-10	
3A049	1A-29		3A099	6A-71		3A149	6B-50		3A199	6A-9	
3A050	1A-28		3A100	6A-7[illegible]	4	3A150	6B-51		3A200	6A-8	
									3A201	6A-7	
									3A202	6A-6	4

Film Data	
Roll No.	Film Type
1A	104-06-04
6A	104-06-04
6B	104-06-04
9	104-06-08
3	101-06-06

Camera No A5 SL4
Sequence Log

ATM No.	Film Roll Strip Cut	Dev Run	ATM No.	Film Roll Strip Cut	Dev Run	ATM No.	Film Roll Strip Cut	Dev Run	ATM No.	Film Roll Strip Cut	Dev Run
3A301	16-12	8	3A351	15-68		3A401	16-18	5	3A451	16-73	
3A302	16-11	3	3A352	15-67		3A402	16-19	1	3A452	16-74	
3A303	16-10		3A353	15-66		3A403	16-20	3	3A453	16-75	
3A304	16-9		3A354	15-65		3A404	16-21		3A454	16-76	
3A305	16-8		3A355	15-64		3A405	16-22		3A455	16-78	
3A306	16-7		3A356	15-63		3A406	16-23		3A456	16-79	
3A307	5-9		3A357	15-62		3A407	16-24		3A457	16-80	
3A308	5-8		3A358	15-61		3A408	16-25		3A458	16-81	
3A309	5-7		3A359	15-56		3A409	16-27		3A459	16-88	
3A310	5-6		3A360	15-55		3A410	16-28		3A460	16-84	
3A311	5-5		3A361	15-54	4	3A411	16-29		3A461	16-85	
3A312	15-115		3A362	15-53	5	3A412	16-30		3A462	16-86	
3A313	15-114		3A363	15-52		3A413	16-31		3A463	16-87	
3A314	15-113		3A364	15-51		3A414	16-32		3A464	16-88	2
3A315	15-112		3A365	15-50		3A415	16-33		3A465	16-89	1
3A316	15-111		3A366	15-49		3A416	16-34		3A466	16-90	
3A317	15-110		3A367	15-47		3A417	16-35		3A467	16-91	
3A318	15-109		3A368	15-45		3A418	16-36		3A468	16-92	
3A319	15-107		3A369	15-43		3A419	16-38		3A469	17-5	
3A320	15-106		3A370	15-41		3A420	16-39		3A470	17-6	
3A321	15-105	3	3A371	15-37		3A421	16-40		3A471	17-7	
3A322	15-104	4	3A372	15-36		3A422	16-41		3A472	17-8	
3A323	15-103		3A373	15-35		3A423	16-42		3A473	17-9	
3A324	15-102		3A374	15-34		3A424	16-43	3	3A474	17-10	
3A325	15-101		3A375	15-33		3A425	16-44	2	3A475	17-11	
3A326	15-100		3A376	15-31		3A426	16-45		3A476	17-12	
3A327	15-99		3A377	15-30		3A427	16-46		3A477	17-13	
3A328	15-98		3A378	15-28		3A428	16-47		3A478	17-14	
3A329	15-94		3A379	15-25		3A429	16-49		3A479	17-16	
3A330	15-93		3A380	15-24		3A430	16-50		3A480	17-17	
3A331	15-92		3A381	15-23		3A431	16-51		3A481	17-18	
3A332	15-91		3A382	15-22		3A432	16-52		3A482	17-19	
3A333	15-90		3A383	15-21		3A433	16-53		3A483	17-20	
3A334	15-89		3A384	15-20		3A434	16-54		3A484	17-21	
3A335	15-88		3A385	15-19		3A435	16-55		3A485	17-22	
3A336	15-87		3A386	15-18		3A436	16-56		3A486	17-23	
3A337	15-86		3A387	15-17		3A437	16-57		3A487	17-24	
3A338	15-85		3A388	15-16		3A438	16-58		3A488	17-25	
3A339	15-83		3A389	15-14		3A439	16-60		3A489	17-27	
3A340	15-82		3A390	15-13		3A440	16-61		3A490	17-28	
3A341	15-81		3A391	15-12		3A441	16-62		3A491	17-29	
3A342	15-80		3A392	15-11		3A442	16-63		3A492	17-30	
3A343	15-79		3A393	15-10		3A443	16-64		3A493	17-31	
3A344	15-78		3A394	15-9		3A444	16-65		3A494	17-33	
3A345	15-77		3A395	15-8		3A445	16-66		3A495	17-34	
3A346	15-76		3A396	15-7		3A446	16-67		3A496	17-36	
3A347	15-75		3A397	15-6		3A447	16-68		3A497	17-36	
3A348	15-74		3A398	15-5		3A448	16-69		3A498	17-37	
3A349	15-70		3A399	16-16		3A449	16-71		3A499	17-39	
3A350	15-69		3A400	16-17		3A450	16-72		3A500	17-40	
									3A501	16-14	1
									3A502	16-13	A

Film Data	
Roll No	Film Type
15	104-06-07
16	104-06-07
17	104-06-07
5	101-06-10

ATM/SKYLAB S082A SPECTROHELIOGRAPH

SHORT-WAVE BAND

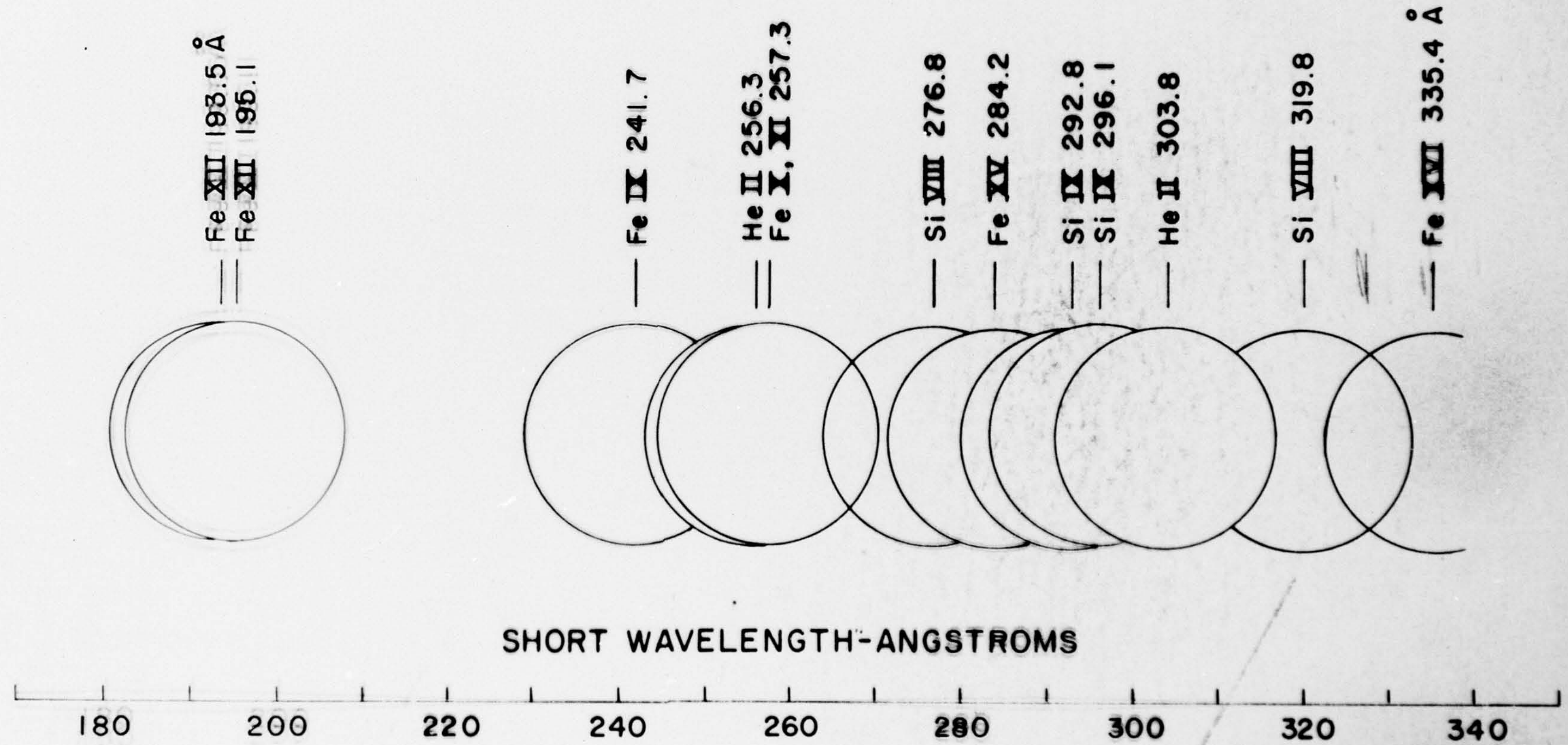

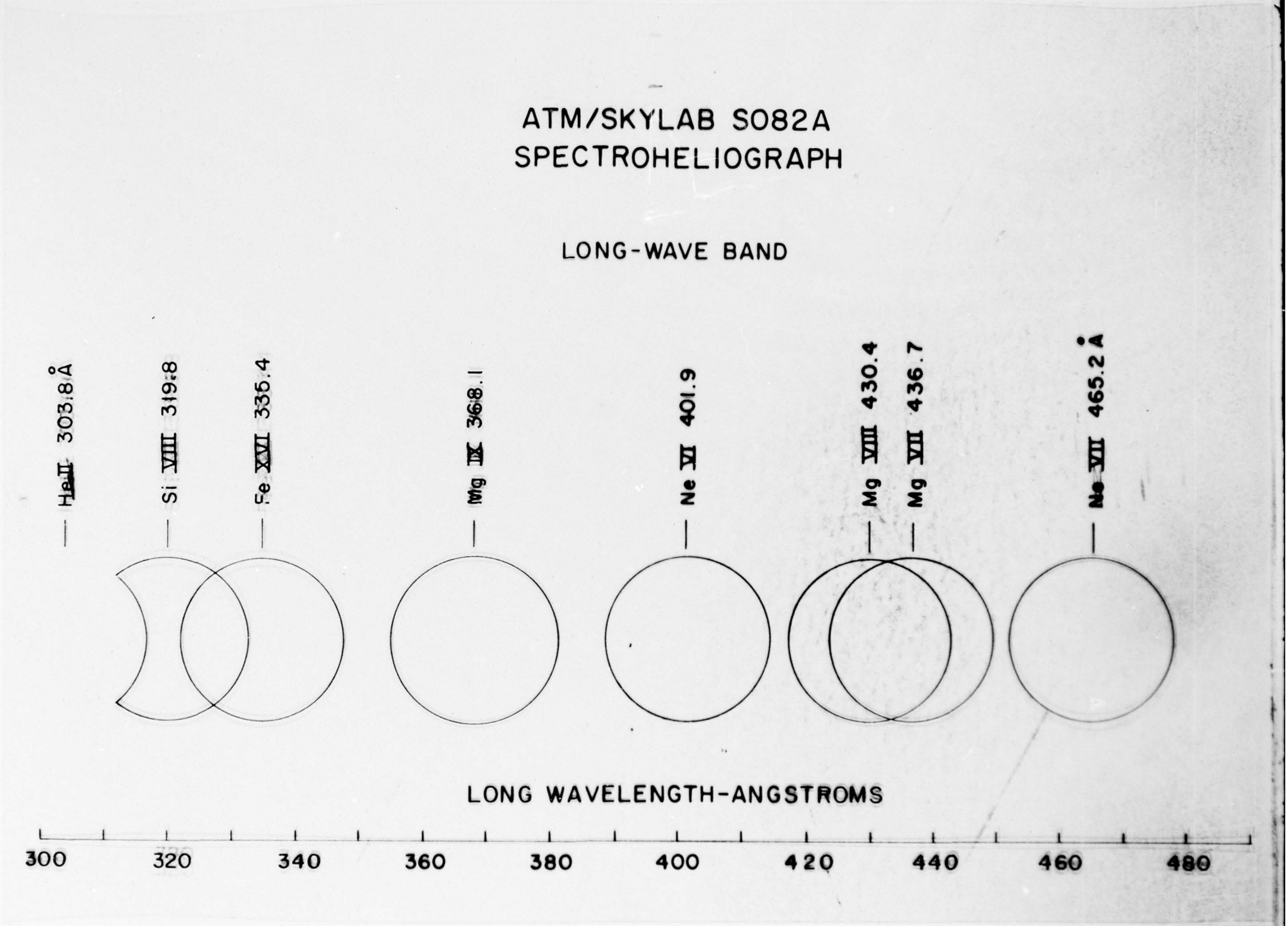
ATM/SKYLAB S082A
SPECTROHELIOGRAPH
LONG-WAVE BAND
He II 303.8 Å
Si VIII 319.8
Fe XVI 335.4
Mg IX 368.1
Ne VI 401.9
Mg VIII 430.4
Mg VII 436.7
Ne VII 465.2 Å
LONG WAVELENGTH-ANGSTROMS
300
320
340
360
380
400
420
440
460
480

ATM/SKYLAB S082A
SPECTROHELIOGRAPH

LONG-WAVE BAND